AD A039370

NAVAL POSTGRADUATE SCHOOL
Monterey, California

THESIS

A Photographic Reconnaissance of the Microrelief in the Monterey and Carmel Submarine Canyons, California

by

John Alexander Jensen

December 1976

Thesis Advisor: S. P. Tucker
R. S. Andrews

Approved for public release; distribution unlimited.

AD No.
DDC FILE COPY

DDC
RECEIVED
MAY 13 1977
D

UNCLASSIFIED

SECURITY CLASSIFICATION OF THIS PAGE (When Data Entered)

REPORT DOCUMENTATION PAGE	READ INSTRUCTIONS BEFORE COMPLETING FORM
1. REPORT NUMBER	2. GOVT ACCESSION NO. 3. RECIPIENT'S CATALOG NUMBER (9)
4. TITLE (and Subtitle) (6) A Photographic Reconnaissance of the Microrelief in the Monterey and Carmel Submarine Canyons, California,	5. TYPE OF REPORT & PERIOD COVERED Master's Thesis; December 1976
	6. PERFORMING ORG. REPORT NUMBER
7. AUTHOR(s) (10) John Alexander Jensen	8. CONTRACT OR GRANT NUMBER(s)
9. PERFORMING ORGANIZATION NAME AND ADDRESS Naval Postgraduate School Monterey, CA 93940	10. PROGRAM ELEMENT, PROJECT, TASK AREA & WORK UNIT NUMBERS
11. CONTROLLING OFFICE NAME AND ADDRESS Naval Postgraduate School Monterey, CA 93940 (11)	12. REPORT DATE December 1976
	13. NUMBER OF PAGES 142
14. MONITORING AGENCY NAME & ADDRESS(if different from Controlling Office) Naval Postgraduate School Monterey, CA 93940 (12) 140p.	15. SECURITY CLASS. (of this report) Unclassified
	15a. DECLASSIFICATION/DOWNGRADING SCHEDULE

16. DISTRIBUTION STATEMENT (of this Report)

Approved for public release; distribution unlimited.

17. DISTRIBUTION STATEMENT (of the abstract entered in Block 20, if different from Report)

18. SUPPLEMENTARY NOTES

19. KEY WORDS (Continue on reverse side if necessary and identify by block number)

Sea Bottom Photography
Submarine Microrelief
Monterey Submarine Canyon
Carmel Submarine Canyon

20. ABSTRACT (Continue on reverse side if necessary and identify by block number)

Over 500 underwater photographs were taken in the Monterey and Carmel submarine canyons for the purpose of studying their microrelief. The pictures indicated that a variety of biological and physical differences exist not only within each canyon but also between the two nearby canyons. → next page

DD FORM 1 JAN 73 1473 (Page 1)

EDITION OF 1 NOV 65 IS OBSOLETE
S/N 0102-014-6601

UNCLASSIFIED

SECURITY CLASSIFICATION OF THIS PAGE (When Data Entered)

251 450

LB

20. Abstract (continued)

In Monterey Canyon are to be found fine grain sediments which have been very actively churned by benthic organisms. Few rock outcrops were noted, and definitive evidence of current activity in the form of ripple marks was observed in only one region. Carmel Canyon included generally coarser grain material than Monterey Canyon and showed a marked absence of active burrowing. A large number of rock outcrops was observed and there appeared to be extensive current activity throughout most of the canyon.

A Photographic Reconnaissance of the Microrelief in the Monterey and Carmel Submarine Canyons, California

by

John Alexander Jensen
Lieutenant, United States Navy
B.S., United States Naval Academy, 1971

Submitted in partial fulfillment of the
requirements for the degree of

MASTER OF SCIENCE IN OCEANOGRAPHY

from the

NAVAL POSTGRADUATE SCHOOL
December 1976

Author John A. Jensen

Approved by: Robert L. Anderson
Thesis Co-Advisor

Steven P. Tucker
Thesis Co-Advisor

Lee F. Leibee
Chairman, Department of Oceanography

Robert R. Brown
Dean of Science and Engineering

ACCESSION for
NTIS White Section
DDC Buff Section
UNANNOUNCED
JUSTIFICATION
BY
DISTRIBUTION/AVAILABILITY CODES
Dist. AVAIL. and/or SPECIAL
A

DDC
RECEIVED
MAY 13 1977
D

ABSTRACT

Over 500 underwater photographs were taken in the Monterey and Carmel submarine canyons for the purpose of studying their microrelief. The pictures indicated that a variety of biological and physical differences exist not only within each canyon but also between the two nearby canyons.

In Monterey Canyon are to be found fine grain sediments which have been very actively churned by benthic organisms. Few rock outcrops were noted, and definitive evidence of current activity in the form of ripple marks was observed in only one region. Carmel Canyon included generally coarser grain material than Monterey Canyon and showed a marked absence of active burrowing. A large number of rock outcrops was observed and there appeared to be extensive current activity throughout most of the canyon.

TABLE OF CONTENTS

I. INTRODUCTION ---------- 12

A. PURPOSE ---------- 12

B. MONTEREY SUBMARINE CANYON ---------- 12

C. CARMEL SUBMARINE CANYON ---------- 13

D. PREVIOUS INVESTIGATIONS ---------- 14

II. EQUIPMENT AND PROCEDURE ---------- 15

A. UNDERWATER PHOTOGRAPHIC SYSTEM ---------- 15

B. MODE OF OPERATION ---------- 17

C. PROCEDURES ---------- 17

D. CALIBRATION ---------- 19

III. DATA ANALYSIS ---------- 21

A. DEFINITION OF MICRORELIEF ---------- 21

B. ORIGIN AND OCCURRENCE OF MICRORELIEF ---------- 21

1. Physical Properties ---------- 21

2. Benthic Organisms ---------- 23

C. DATA PRESENTATION AND ANALYSIS ---------- 25

1. General ---------- 25

2. Monterey Canyon ---------- 26

a. Legs VW-1, VW-2, VW-3 ---------- 26

b. Legs CD-2, CD-3, UV-1 ---------- 28

c. Leg EF-2 ---------- 32

d. Leg GH ---------- 34

e. Leg IJ ---------- 36

3. Carmel Canyon ---------- 38
a. Leg TU ---------- 38
b. Legs ST-1, ST-2, ST-3 ---------- 41
c. Legs QR-1 and QR-2 ---------- 43
d. Legs KL-1, KL-2, KL-3 ---------- 43
e. Leg MN ---------- 45
IV. DISCUSSION AND CONCLUSION ---------- 47
V. SUGGESTIONS FOR FURTHER STUDIES ---------- 53
REFERENCES CITED ----------138
INITIAL DISTRIBUTION LIST ----------140

LIST OF FIGURES

1. Monterey and Carmel Canyons ---------- 54

2. Location of Photographic Runs in Monterey Canyon --- 55

3. Location of Photographic Runs in Carmel Canyon ----- 57

4. Axial Relationship of Units in Standard Mounting Arrangement ---------- 58

5. Launching Camera Rig from R/V ACANIA ---------- 59

6. Monitoring the Camera-to-Bottom Distance with the UGR ---------- 60

7. Example of Typical Camera Operation ---------- 61

8. Design of Underwater Trip Switch ---------- 62

9. UGR Output Showing Direct and Bottom Reflected Pulses ---------- 63

10. Sea Floor Topographic Features ---------- 64

11. Spectrum Range of the Sea Floor Roughness ---------- 65

12. Current Velocities Required for Erosion, Transportation and Deposition ---------- 66

13. Minimum Current Velocities Required for Erosion of the Principal Deep-sea Sediments ---------- 67

14a. Bathymetric Profile of Leg VW-1 ---------- 68

14b. Bathymetric Profile of Leg VW-2 ---------- 69

14c. Bathymetric Profile of Leg VW-3 ---------- 70

15. Bathymetric Profile of Leg CD-2 ---------- 71

16. Bottom Photograph Leg CD-2, 1109.5 hr, 203 m ------- 72

17. Bottom Photograph Leg CD-2, 1103.3 hr, 200 m ------- 73

18. Bottom Photograph Leg CD-2, 1120.6 hr, 220 m ------- 74

19. Bottom Photograph Leg CD-2, 1116.7 hr, 210 m ------- 75

20. Bottom Photograph Leg CD-2, 1118 hr, 214 m --------- 76

21. Bottom Photograph Leg CD-2, 1118.6 hr, 215 m ------- 77
22. Bottom Photograph Leg CD-2, 1118.9 hr, 215 m ------- 78
23. Bottom Photograph Leg CD-2, 1122.5 hr, 220 m ------- 79
24. Bottom Photograph Leg CD-2, 1122.3 hr, 220 m ------- 80
25. Bathymetric Profile of Leg UV-1 ------------------- 81
26. Bottom Photograph Leg UV-1, 1039.25 hr, 330 m ------ 82
27. Bottom Photograph Leg UV-1, 1049.1 hr, 340 m ------- 83
28. Bottom Photograph Leg UV-1, 1107.8 hr, 400 m ------- 84
29. Bottom Photograph Leg CD-3, 0946.4 hr, 360 m ------- 85
30. Bathymetric Profile of Leg EF-2 ------------------- 86
31. Bottom Photograph Leg EF-2, 1430.4 hr, 420 m ------- 87
32. Bottom Photograph Leg EF-2, 1429.8 hr, 420 m ------- 88
33. Bottom Photograph Leg EF-2, 1433.9 hr, 420 m ------- 89
34. Bottom Photograph Leg EF-2, 1434.5 hr, 415 m ------- 90
35. Bathymetric Profile of Leg GH --------------------- 91
36. Bottom Photograph Leg GH, 0922.2 hr, 624 m --------- 92
37. Bottom Photograph Leg GH, 0931.1 hr, 650 m --------- 93
38. Bottom Photograph Leg GH, 0921.25 hr, 622 m -------- 94
39. Bathymetric Profile of Leg IJ --------------------- 95
40. Bottom Photograph Leg IJ, 1213.25 hr, 740 m -------- 96
41. Bottom Photograph Leg IJ, 1209.8 hr, 745 m --------- 97
42. Bottom Photograph Leg IJ, 1217.4 hr, 735 m --------- 98
43. Bottom Photograph Leg IJ, 1203.75 hr, 750 m -------- 99
44. Bottom Photograph Leg IJ, 1215.7 hr, 735 m --------- 100
45. Bottom Photograph Leg IJ, 1219.8 hr, 737 m --------- 101
46. Bathymetric Profile of Leg TU --------------------- 102

47. Bottom Photograph Leg TU, 1403 hr, 200 m ---------- 103
48. Bottom Photograph Leg TU, 1341.9 hr, 70 m ---------- 104
49. Bottom Photograph Leg TU, 1350.8 hr, 240 m --------- 105
50. Bottom Photograph Leg TU, 1401.7 hr, 219 m --------- 106
51. Bottom Photograph Leg TU, 1400.9 hr, 221 m --------- 107
52. Bottom Photograph Leg TU, 1326.3 hr, 217 m --------- 108
53. Bottom Photograph Leg TU, 1329.8 hr, 256 m --------- 109
54. Bottom Photograph Leg TU, 1338 hr, 254 m ---------- 110
55. Bottom Photograph Leg TU, 1344.7 hr, 245 m --------- 111
56. Bottom Photograph Leg TU, 1358.5 hr, 230 m --------- 112
57. Bathymetric Profile of Leg ST-1 ------------------- 113
58. Bathymetric Profile of Leg ST-2 ------------------- 114
59. Bathymetric Profile of Leg ST-3 ------------------- 115
60. Bottom Photograph Leg ST-1, 0958.5 hr, 230 m ------- 116
61. Bottom Photograph Leg ST-3, 1140.75 hr, 256 m ------ 117
62. Bottom Photograph Leg ST-2, 1041.4 hr, 146 m ------- 118
63. Bottom Photograph Leg ST-2, 1043.2 hr, 142 m ------- 119
64. Bottom Photograph Leg ST-2, 1050.25 hr, 120 m ------ 120
65. Bottom Photograph Leg QR-1, 0958.6 hr, 270 m ------- 121
66. Bottom Photograph Leg QR-1, 1006.6 hr, 260 m ------- 122
67. Bottom Photograph Leg KL-1, 0930.7 hr, 528 m ------- 123
68. Bottom Photograph Leg KL-1, 0933.6 hr, 528 m ------- 124
69. Bottom Photograph Leg KL-1, 0934.3 hr, 528 m ------- 125
70. Bottom Photograph Leg KL-1, 0936.2 hr, 528 m ------- 126
71. Bottom Photograph Leg KL-1, 0941.2 hr, 520 m ------- 127
72. Bottom Photograph Leg KL-3, 1228 hr, 480 m --------- 128

73. Bottom Photograph Leg KL-3, 1235.5 hr, 478 m ------- 129

74. Bottom Photograph Leg KL-2, 1043.2 hr, 400 m ------- 130

75. Bottom Photograph Leg KL-2, 1044.5 hr, 400 m ------- 131

76. Bottom Photograph Leg MN, 1340.9 hr, 660 m --------- 132

77. Bottom Photograph Leg MN, 1346.3 hr, 660 m --------- 133

78. Bottom Photograph Leg MN, 1350.2 hr, 660 m --------- 134

79. Bottom Photograph Leg MN, 1352.2 hr, 660 m --------- 135

80. Orientation of Ripple Mark Crests in Monterey Canyon ---------- 136

81. Orientation of Ripple Mark Crests in Carmel Canyon ---------- 137

ACKNOWLEDGMENT

The author gratefully acknowledges Professors Robert S. Andrews and Stevens P. Tucker, co-advisors, for their support and advice; the Captain and crew of the R/V ACANIA for their professional and enthusiastic assistance, in particular boatswain Charles Bowen whose expertise and personal initiative on at least one occasion prevented the loss of the camera rig; the men of the NPS oceanography electronics repair facility for their technical assistance; PH3 Alan Goode and the men of the Fleet Air Photo Lab, NAS Moffett for their excellent photographic work; Professor Eugene C. Haderlie and Mr. Eric Anderson for their assistance in identifying the biological features observed.

The author wishes to express his sincere appreciation to his wife, Susan, without whose encouragement and assistance this project would not have been completed. To my mother and father I express my unspoken thanks for their years of patience, trust and guidance.

I. INTRODUCTION

A. PURPOSE

Small scale roughness of the sea floor is an important consideration when discussing the reflectivity processes of sound propagation. Diminutive features, ranging from centimeters to tens of meters in size, are of the same order of magnitude as acoustic wavelengths (Akal, 1974). These small features: ripples, boulders, mounds and rock outcrops, can not be detected or measured by standard echo sounding techniques. The best present day means available to measure small scale roughness is the underwater camera.

The purpose of this study is to investigate the very small bottom relief features found at different depths in a particular topographic feature, submarine canyons. Of primary interest was the identification and mapping of current activity. Over 500 bottom photographs at pre-selected locations in the Monterey and Carmel Submarine Canyons off the central coast of California were taken to accomplish this objective (Fig. 1, 2 and 3).

B. MONTEREY SUBMARINE CANYON

Monterey Canyon is not the longest, but perhaps possesses the greatest vertical relief of any known submarine canyon. The head of the canyon is near Moss Landing, California, and initially cuts through unconsolidated sediment. Proceeding

from its head, it cuts through Pliocene and Miocene sedimentary rocks out to about 12.8 km from the shore, where its walls are found to be made up of Cretaceous granodiorite beneath a depth of about 640 m. The canyon is V-shaped, with very steep, high walls containing rock outcrops.

The gradient of the floor in the upper portion is on the order of 125 m/km, decreasing to 40 m/km at a depth of 91 m. The gradient remains fairly constant to a depth of approximately 1200 m (Shepard and Dill, 1966). Significant relief (10-100 m) in the shape of steep peaks and deep depressions is common throughout the length of the canyon. Beyond about the 2,000 m isobath, the canyon yields its narrow V-shaped walls to a broader, trough-like bathymetry. However, steep walls continue to exist out to a depth of about 2,900 m.

C. CARMEL SUBMARINE CANYON

Carmel Submarine Canyon is possible the only canyon on the west coast of the United States heading into a bay which might be a drowned river valley (Shepard and Dill, 1966, p. 88). The canyon head begins offshore from the San Jose Creek, and its precipitous walls are Cretaceous granodiorite, unlike most canyons which are cut in sedimentary rock. The rim of the canyon is defined by a break occurring at a depth of about 60 ft (18.3 m) and the canyon floor seaward of its head is about 275 ft (75 m) wide.

The gradient at the head of the canyon is on the order of 300 m/km, and the axial slope, continuous in a seaward direction, possesses an average incline of 73 m/km (Shepard and Dill, 1966). Several minor tributaries enter the canyon before it intersects the Monterey Canyon several miles out to sea (Fig. 1).

D. PREVIOUS INVESTIGATIONS

Underwater photography has been used frequently by oceanographers to investigate many regions of the ocean. Despite their considerable interest and the significant amount of oceanographic work which has been conducted in Monterey and Carmel Canyons, a search of the literature failed to produce any reference to previous deep underwater photographic surveys. There have been several studies which employed shallow scuba dives down into the head of Carmel Canyon. A thesis written by Wallin (1966), incorporated underwater pictures taken with a handheld Rollieflex underwater camera at a depth of 100 ft (30.5 m) in the Carmel Canyon.

The geology of these canyons has been described by Martin and Emery (1967) and the geology of Monterey Bay is presently being studied by Greene (in preparation).

II. EQUIPMENT AND PROCEDURE

A. UNDERWATER PHOTOGRAPHIC SYSTEM

The EG&G automatic camera system model CA-9 (deep water unit) and associated light source LS-9 is a self-contained instrument package capable of operating to a depth of 37,000 ft (11,000 m).

The camera and the light source are each housed in a hardened stainless steel, watertight cylindrical case approximately 6 inches (15.24 cm) in diameter and 25 inches (63.5 cm) long weighing nearly 50 lb (22.68 kg) in the air [34 lb (15.42 kg) in water].

The camera is electrically driven and can take up to 500 separate exposures on a standard 100 foot (30.5 m) roll of 35-mm film. While a picture of the bottom is taken through the conical plexiglass window, a photograph of an internal data chamber is simultaneously taken at the other end of the chassis. This data chamber exposure, nine frames removed from its associated subject frame, shows a clock and various notations on a data card. It is an aid in identifying photographs and in maintaining records.

The Wollensak f/11 lens is a special three-element lens designed to correct for the distortion created when light passes from the water through the window to the air inside the camera. The lens has a fixed focus at 6 ft (1.83 m) in water, providing a depth of field of 3.5 to 20 ft (1.07 to 6.1 m).

If desired, the focal length can be adjusted for greater distances or close-ups. A shutter was fitted to the camera to permit shallow water operations where ambient light might be sufficient to cause fogging of the film.

The light source, a 100-wsec electronic flash unit, is synchronized to the shutter. The light output has essentially the same color spectrum as sunlight.

Power is derived from a 6-V, four-cell, wet, rechargeable silver-zinc battery. The 21 amp-hr battery is housed in the light-source case and when fully charged, can deliver a minimum of 500 flashes in a period of about 100 min.

The two cases are arranged on the MT-8 mounting rack with the camera at one end of the rack looking straight down. The light source is mounted at the other end of the rack at an angle such that the axis of the light beam intersects the axis of the camera when the rack is about 5 ft (1.52 m) above the bottom (Fig. 4). The angled light source, separated from the camera, prevents "flare back" and provides better shadow detail. The MT-8 rack is attached to 3/16 inch (0.48 cm) standard hydrographic wire with a ball bearing swivel to prevent kinks in the wire.

The need to position the camera equipment near the bottom required the placement of a sonar type device (EG&G type SP-9 thumper) on the rack. All associated electronic equipment and power source (silver-zinc battery), were encased in a stainless steel cylinder identical to those used for the

camera and light. The thumper operates at a frequency of 12 kHz, with a ping rate of 1 sec^{-1}.

B. MODE OF OPERATION

There are two basic modes of operation associated with the camera: automatic triggering and remote triggering.

The camera-light source combination is normally wired to operate automatically, taking a picture approximately every 12 sec. A delay timer can be set up to 120 min to allow positioning of the camera. When the switch closes, a timing motor in the light source case begins to rotate a cam which in turn closes a relay once every revolution. The closed relay causes the shutter to open, tripping the electronic strobe. Once the relay opens, the film advances one frame. The operation can only be stopped if the delay timer is reset or the power source disconnected.

A minor wiring change must be made to accomplish remote triggering. In this mode of operation the timing motor is disconnected and actuation by an external switch will cause the camera to operate. The sequence of shutter-strobe operation is the same as the automatic mode.

C. PROCEDURES

The EG&G camera system was tethered from the R/V ACANIA, (Fig. 5), which does not have the capability to maintain a fixed position; consequently, the ship was adrift during all camera runs. The effects of wind, seas and currents produced

an average drift of 0.5 kt (25.4 cm/sec) for most of the traverses. The predominant factor controlling the set and drift of the ship was the wind.

In order to monitor the camera-bottom distance, the ship's Universal Graphic Recorder (UGR) plotted the direct and bottom reflected sonar pulses (Fig. 6). The camera's height above the bottom could be determined by measuring the distance between the leading edge of the two pulses. The pulse from the EG&G SP-9 thumper was received by utilizing the hull-mounted receiving transducer, part of the shipboard AN/UQN 1B (EDO model 185) fathometer, and associated electronics. Figure 7 depicts a typical acoustic method for positioning an underwater camera.

Initially the camera was configured to operate in the automatic trigger mode. After several attempts it became obvious that the maximum permissible height above the bottom was 7-8 ft (2.1-2.4 m), with optimum heights of 4-6 ft (1.2-1.8 m). Simultaneously, it was discovered that the resolution of the UGR in the operational depths of the canyons was insufficient to distinguish the two traces at camera-bottom distances less than 8 ft (2.4 m). As a result it was not possible to know when the camera was dragging on the bottom, out of focus by being too close, or at the correct distance.

The remote triggering mode was selected to alleviate the problem of subjecting the camera to unnecessary abuse and to increase the number of acceptable pictures. A spring-loaded

waterproof switch was designed (Fig. 8) to trigger the shutter when the suspended weight touched the bottom. A tensiometer was installed on the winch sheave to sense the camera rig's contact with the sea floor. After each exposure taken at the correct camera-bottom distance, the camera was then raised a safe distance above the bottom. A UGR trace of a typical pick-up and put down operation is shown in Fig. 9.

A compass was suspended 3.5 ft (1.1 m) below the camera in order to determine the orientation of observed lineaments and provided a means of estimating their size.

Radar ranges and visual bearings were the modes of navigation utilized, depending on the visibility and location. In the Monterey Canyon a combination of both methods was used with an estimated accuracy of approximately 150-200 yards (137-182 m). Visual bearings were used exclusively in Carmel Canyon with an estimated accuracy of 100 yards (91.5 m).

A bathymetric profile was recorded for each photographic run using an average sound speed of 4,800 ft/sec (1,463 m/sec).

D. CALIBRATION

A calibration of underwater cameras is necessary for determining the size of objects in a photograph. Precision calibration was neglected because this underwater photography was conducted for interpretation and gross metrical purposes. A bottom-mounted target with measurement marks of known

separation was photographed in a tank in a laboratory at selected heights above the bottom. For a camera-bottom distance of 4.5 ft (1.03 m), an area 28 x 44 inches (71 x 111.75 cm) is covered by a full frame negative. A distance of 5.25 ft (1.6 m) covers a 32 x 50 inch (91.3 x 127 cm) area and a distance of 6.0 ft (1.8 m) a 40 x 60 inch (101.6 x 152.4 cm) area.

III. DATA ANALYSIS

A. DEFINITION OF MICRORELIEF

The sea floor topographic relief can be divided into three categories based on vertical and horizontal dimensions (Fig. 10). The large earth features such as abyssal plains, plateaus, trenches, mountain ranges and continental slopes characterize major relief. Canyons, submarine fan valleys, terraces and basins are a few examples of intermediate relief. Microrelief, very small surficial topographic features, are superimposed on both major and intermediate relief and are distinguishable by examination of bottom photographs (Fig. 11). Vertical heights and horizontal lengths normally measure from 1 mm to 50 m (Shipek, 1966).

B. ORIGIN AND OCCURRENCE OF MICRORELIEF

1. Physical Properties

The surface of the sea floor is affected by many physical processes which alter the structure of the bottom sediments. Common forces are storm waves, tsunamis, tidal oscillations, gravity slumping, turbidity currents and bottom currents.

Large areas of the bottom may be under the influence of a continuous circulation which is often too weak to produce recognizable results. Current lineations are frequently temporal and it is often difficult to assess whether sediment transport has indeed taken place. The

absence, deformation or partial destruction of burrows, mounds and tracks can be an indicator of current activity. Deflected parts of organisms attached to the bottom or scour pits around bottom obstructions can also be positive evidence. Quite often no dominant features are present, yet a photograph may give a subtle general impression of oriented lineation.

Ripples, scour marks and current lineations are dependent primarily on the strength of the bottom current and the coherence of the sediments. Local variation in currents, sediment composition, and topography result in a diversity of wave-length, crest-length, amplitude and symmetry in a given area. Symmetrical ripple marks indicate oscillatory water motion, while asymmetrical ones imply unidirectional motion.

Relationships between particle size and current velocity are shown in the graph in Fig. 12. A nearly linear correlation appears to exist for grain sizes larger than about 1.0 mm (very coarse sand), while an inverse relation is indicated for silt and clay (0.0024 - 0.0625 mm). This inverse relation is in part due to an increase in cohesion between particles as the grain size decreases and a relatively hydrodynamically smooth surface. In order to initiate sediment motion currents of greater magnitude are required. These relationships are general, and meaningful data is difficult to extract. The nature of the sediment can affect the erosional ability of a current. For example,

the current velocity necessary to erode a bottom material such as red clay and globigerina ooze mixture may differ from that for some other aggregate of similar grain size (Fig. 13).

Ripples begin to form when the current velocity reaches the transportational limits for the sediment. Using theoretical and experimental results, the criterion $V_c=57\ [D(\rho-1)^2]^{0.2}$ cm/sec was derived by Laughton (1963, p. 456) to determine the critical velocity (V_c) as a function of grain density(ρ) and particle diameter (D) in the cgs system for the initiation of ripples. This indicates currents on the order of 30 cm/sec are necessary to form ripples in sediments of particle size 0.2 mm and density 1.5 g/cm^3 (approximate values of globigerina sand). When the velocities exceed the transportational limits, erosion takes place, destroying the ripple marks.

2. Benthic Organisms

Benthic organisms living on or beneath the bottom sediments are generally too small to be seen in photographs. Those that can be observed are often unidentifiable due to their small size. Organisms existing in this region can be divided into three main groups: free swimmers, bottom crawlers and burrowers. The composition and abundance of each type is primarily a function of the amount of organic material on the sea floor and in suspension immediately above it. The free swimmers are perhaps the least observed of the three groups. Rat tails, ray fins, eels and octopi

form the chief population of the deeper regions and are suited for either plucking their prey off the surface of the sea floor or rooting in the sediment for them.

The vast majority of photographs show footprints, plow marks, excrement, holes and mounds. Discrete footprints, tracks and trails are formed principally by echinoderms, arthropods and chordates. The arthropod has small sharp feet and creates distinctive footprints. Large, prominant tracks and trails are often the work of echinoderms such as the brittle star (orphiuroids) pulling himself across the bottom leaving a feathery trail. The asteroids, on the other hand, walk on their tubed feet leaving blunt footprints. The holothurian, a principal bottom crawler, generally produces straight or slightly curved four-row and two-row trails, or a path of holes. However, at other times this organism plows its way along the bottom leaving furrowed paths.

Small grooves, gouges and ridges are created by roving creatures which creep and crawl on or just below the soft surface. Echinoderms are the predominant plowers, but close examination may reveal a worm or snail at the end of plow marks. The abrupt beginning or termination of marks may be due to the fact that the producer swam off, burrowed or was carried away. Fish, eels and octopi rooting for food also deface the sea floor.

Due to the large quantities of sediment injested to sustain life, fecal deposits in the form of random piles,

loops, coils and gentle spirals are a common feature. A catalog of organisms and their associated feces would be an aid in determining the inhabitants of a region.

Holes, mounds and depressions are the common characteristics of the bottom but the sculptors: mollusks, worms, crustaceans, urchins and fish, are seldom seen. Protruding organisms such as sea pens, worm extensions and sponges are often observed searching the water for nourishment.

C. DATA PRESENTATION AND ANALYSIS

1. General

The most difficult problem encountered in interpreting the photographs was determining the size of bottom features. Leg CD-2 in the Monterey Canyon was the only run to successfully utilize the automatic triggering mode. The UGR trace was the sole means available for establishing physical dimensions. The time of a particular picture was correlated with the UGR record and the height above the bottom computed. By placing the photographic negative over the appropriate calibration frame for that height, a distinctive feature could be measured. Since this was the least accurate means utilized, an asterisk (*) was placed beside the size scale for example, see Fig. 17. The remaining runs were configured for the remote triggering method with the trip weight positioned for a specific camera-bottom distance. All other lineaments were measured by employing the method of superimposing negatives for the

given trip distance, or by using the dimensions of the compass when possible. In a few instances, accurate size estimates could not be made; consequently no scale was placed on the picture for example, see Fig. 21.

Identification of benthic organisms and their telltale traces was accomplished with the assistance of E. Anderson of Moss Landing Marine Laboratories, Moss Landing, Ca. and E.C. Haderlie of the Naval Postgraduate School.

2. Monterey Canyon

a. Legs VW-1, VW-2, VW-3

The head of Monterey Canyon was photographed extensively (legs VW-1, VW-2, VW-3) at depths of 91 to 146 m (Fig. 14a, 14b and 14c). The ship drifted up the canyon axis at an approximate rate of 30 cm/sec, repositioning twice to remain in the desired area. Out of 100 photographs taken at an average height of 1.6 m above the canyon floor, it was not possible to distinguish the bottom, although the compass was visible 1.1 m below the camera. From pictures taken in other parts of the canyon using the compass as a reference background it is apparent that this is a region of high turbidity.

Reduced visibility at the head of Monterey Canyon was experienced by H.G. Greene of the U.S. Geological Survey Office on September 15, 1970, while diving in the submersible NEKTON BETA (personal communication). He reported near-zero visibility in an uncharted, anomalous depression apparently blocked at the seaward end by a

slumped feature. It was his belief that trapped sediment was easily disturbed by the submersible touching the bottom, creating a large, dense sediment cloud. It might then be assumed that each time the camera rack touched the bottom a sediment cloud was produced. The camera traveling at 18 m/min and touching the bottom only after a picture is taken does not seem the likely cause of such extensive turbidity. Leg VW-2 was on the side of the canyon, not in the deeper central axis area, yet no difference in turbidity was noted. This condition was not experienced during any of the other runs in the canyon.

A more probable source of the turbidity might be due to longshore transport carrying sediments into the head of the canyon. Bottom current measurements have been conducted in this region by Gatje and Pizinger (1965), Dooley (1968), and Njus (1968). Gatje and Pizinger recorded currents in 130 m of water shoreward of the subject area, 4.8 m above the bottom. Currents varied between 0 and 41 cm/sec, with a mean speed of 10 cm/sec following the canyon axis. Dooley, measuring in the same vicinity, reported similar results. Njus investigated currents 12 m above the bottom in the same area as the camera runs and reported flows of 0 to 50 cm/sec with a mean velocity of 33 cm/sec. This is considerably higher than for the other two studies and appears excessive. In all three studies the current was found to be bimodal, up and down the canyon axis, reaching maximum velocities during the rise and fall

of the tide. Results of other measurements (Shepard, Marshall and McLoughlin, 1974) taken 3 m above the bottom, at a depth of 155 m, indicated an average flow of 9 to 10 cm/sec reaching maximum values of 24 to 32 cm/sec. The direction of flow was predominantly up- and downcanyon and appeared to be tidally influenced.

In a study of the sediments of Monterey Bay, Galliher (1932) describes the grain size in this part of the canyon as very find sand (0.0625-0.125 mm), generally greenish gray. A partially successful grab sample indicated a layer of sand about 1.3 cm thick overlying a firmer silty mud. The maximum velocities reported above are of sufficient magnitude to maintain in suspension material of this size (Fig. 12).

b. Legs CD-2, CD-3, UV-1

These three legs are located within close proximity of each other. Leg CD-2 consisted of 40 pictures taken at depths of 210 to 260 m (Fig. 15) while the ship drifted up-canyon at an average rate of 30 cm/sec.

Active biological churning, evidenced by holes, exists in 40% of the pictures and is probably the work of clam siphons and tube and tubeless worms (Fig. 16). Larger, rimless depressions, possibly the product of burrowing urchins and protruding sea pens (Alcyonacea), are observed in many of the photos (Fig. 17 and 18). Plow marks, tracks and large, free swimmers were not common, but several brittle star impressions could be seen.

Three pictures show good examples of rock outcrops (Fig. 19, 20, and 21). The first (Fig. 19) appears to be a piece of layered sedimentary rock, possibly Miocene Monterey shale. The rock may be out of place due to slumping which is common along the walls of the Monterey Submarine Canyon (H.G. Greene, personal communication). Sediment with ripple marks indicate current activity, and a fish appears to be resting in a depression. Due to an excessive camera-bottom distance, the canyon floor could not be seen in the next four frames, creating roughly an 18-m gap in the coverage. The first picture after Fig. 19 shows 30 to 40 angular rock fragments ranging in size from less than 2.5 cm to about 20 cm, resting on a sloped surface (Fig. 20). These rocks have the same general appearance as the exposed layered rock, and from their angularity one might speculate they are shale. The rocks, free of sediment, suggest an erosional process exists, and the eel grass (Zostera) debris, partially buried in the sediment, is evidence of transport from shallower regions. The rock outcrop in Fig. 21 is important because its surface is virtually free of sediments. Of particular interest is the crack which contains no depositional material, thus indicating active scouring.

The picture immediately following Fig. 21, about 4 m removed in space, depicts mud clumps similar to those found in biologically active regions, and borders a smoothed-over bottom (Fig. 22). Apparently, a short abrupt transition zone exists between a sloping rocky wall and a relatively

flat bottom exposed to current activity. Indeed, the last 14 pictures, representing about 35% of the run, show varying degrees of current lineations. Distinct ripple marks with crest-to-crest distances of 16 to 18 cm appear in several photos (Fig. 23). Since the compass was not shown in any of the frames, the orientation of the crests could not be determined. Debrís, consisting of eel grass lying on top of faintly rippled sediment about 5 m removed from Fig. 23, further supports the existence of currents (Fig. 24).

Caster (1969) observed current speeds of 0 to 25 cm/sec which were primarily bimodal up and down the canyon axis. A mean speed of 10.8 cm/sec was computed, and a relationship with the semidiurnal tide was evident. This association of current and tidal fluctuations is consistent with other studies conducted near the head of the canyon. The velocities recorded are sufficient to transport the silt and clay (0.005 - 0.0625 mm) sediment reported in this region.

A bathymetric profile of UV-1 (Fig. 25) indicates that the photographed area is relatively flat with an average depth regime from 320 to 350 m. A total of 55 pictures were taken as the ship drifted down the canyon at an average rate of 25 cm/sec.

The first 120 m of the run revealed a biologically disturbed bottom similar to that of leg CD-2, except that the density of small holes was considerably less. The poorly defined current lineations seen in the negatives

were difficult to reproduce on a print. Immediately following this region, an area of well-developed ripple marks occurred with the crests oriented in a WNW - ESE direction and an average crest-to-crest distance of 10 cm (Fig. 26). The distance traveled between adjacent pictures was about 1.5 m, slightly more than the field of vision for a single frame, and no overlapping coverage was noted. Since there was no gap in the data except the normal 1 min firing rate, it is reasonable to conclude that a well defined region exists where current activity is of sufficient magnitude and duration to hinder burrowing organisms from establishing their holes. The peripheral region apparently experiences velocities which create sediment ripples less frequently. As a result, the holes and rimless craters can be produced and maintained for a period of time. E.C. Haderlie (personal communication) indicated that destroyed holes can be restored within several hours.

A region of alternating biological activity and current lineations followed, covering about 135 m of the run. The surface of the bottom eventually yielded to a smooth appearance (Fig. 27 and 28) for the remainder of the traverse with a noticeable absence of small holes. Initially it was believed that the camera-to-bottom distance might have been too great to clearly see these smaller features. After comparing the pictures from this and other runs of equal height, it seems more reasonable to conclude that the holes do not exist. It may be that the area had been recently

scoured and evidence of burrowers not yet reestablished. On the other hand water velocities may be sufficient to either prevent or destroy biologically produced features, yet insufficient to create current lineations. The rock in the lower left corner of Fig. 27 appears to have sediment nearly covering the upper right side while a depression exists exposing more of the rock on the lower left side. This might be interpreted as a scour pit indicating sediment transport from the upper right to lower left of the picture.

Upon completion of leg CD-3, in an average depth of 310 m, it was discovered that only four pictures had been taken. Ripple marks oriented in a W-E direction with an average crest-to-crest distance of 14 cm were observed in all four photos (Fig. 29). Although bathymetric charts are not sufficiently detailed, there is evidence of a deep tributary tending to the NE which intersects the canyon axis in this area. H.G. Greene (personal communication) believes that a current exists in this extension. He further speculates that the tributary extends closer to shore and intercepts longshore sediment transport that would otherwise reach the head of Monterey Canyon at Moss Landing. No known direct current measurements or sediment transport studies have been conducted in this tributary.

c. Leg EF-2

This photographic run crossed over a gently sloping hill, possessing a vertical relief of about 30 m at a mean speed of 41 cm/sec (Fig. 30). Over 60 pictures

were acquired covering a depth regime from 433 to 405 m.

The bottom sediments had been extensively churned by burrowers and surface feeders with no appreciable difference during the entire traverse. E. Anderson (personal communication) reported that dredging in this area often produces small clams and worm tubes, some as long as 12 cm. The coiled fecal deposits (Fig. 31) had an average density of about 8 to 10 per frame and are nearly 1.2 cm in diameter. The fact that there is no trail originating or terminating at the feces tends to indicate a burrower as the producer. Similar excretions known to be produced by burrowing worms have been recorded in tidal mud flats by Russell and Young (1963, plate 18). If these feces had been produced by surface organisms, the added weight of the material prior to deposition would generally tend to create a deeper than normal furrowed trail, which would be easily detectable.

The thin, narrow plow marks are primarily the result of gastropods creeping along the bottom, and close examination occasionally reveals a small snail at the end of a trail (Fig. 32). These gastropods are about 1.3 cm in size and had an average density of about 12 to 36 per frame, the highest for all the Monterey Canyon runs. Their presence in significant numbers would seem to indicate an organically rich sediment.

Throughout the entire leg there was no evidence of active bottom scouring. Gastropods and intact feces were not observed in regions of current activity; thus their

presence tends to support the idea of little or no water motion. Fecal deposits can, however, be very resistive and remain intact when under the influence of currents. Small burrowed holes in the sediment are not a reliable indicator, because they begin to reappear shortly after scouring occurs. The absence of the sea pen, which seeks suspended material for nourishment, might indicate that the water circulation is insufficient to carry new supplies of nutrients into the area.

Although it was not possible to identify the creators of the larger rimless craters, the eel pout (Fig. 33) and the heart urchin are the probable modelers. The heart urchin can exist in both current swept and tranquil environments and feeds by using its podia to pass sediment by its mouth and then over the top of the body. They can not go backwards but must burrow forward into the bottom, and Fig. 34 may show one at work.

It is virtually impossible to distinguish different grain size and texture from underwater photographs except when looking at very coarse sand compared to ooze. However, a general impression exists that the sediment here is finer than the shoreward area. Although no sampling station was located near line EF-2, Galliher (1932) has classified the sediments in this area as silt and clay (0.062 - 0.005 mm).

d. Leg GH

The ship was positioned on the north wall of the

canyon and initially carried away from the side, then more parallel to it, at an average speed of 61 cm/sec. The depth increased from 616 m down to 658 m (Fig. 35), and after 16 pictures a broken connection to the camera's shutter prevented further operation.

Each frame contains at least one or two starfish (Astropecten), measuring about 10 cm from tip to tip (Fig. 36 and 37). Two rows of holes in Fig. 36 may be the tracks of a large holothurian, while the narrow plow marks are the product of the gastropod which can be seen at the end of several of the furrows (Fig. 37). The density of gastropods is greatly reduced from that of leg EF-2, averaging less than 12 in any given picture. The sea pen is not generally present except in the lower center of Fig. 38, where a feather-like extension is plainly visible. The lower number of small holes and the lack of feces distinguishes this sloping bottom from that in leg EF-2, perhaps suggesting a more active water environment.

The decrease in biological activity may be in part due to the increase in depth which may not be favorable to certain types of organisms. This is probably not true of the burrowing worm, although partially successful bottom grab samples produced smaller and fewer worm tubes from this area of the canyon. It would seem that there is nutrient-enriched sediment due to the presence of a large organism, the starfish. The single, most probable, reason for what appears is the steepness of the bottom. No current

lineations were observed, yet the bottom looks on the basis of the almost washboard appearance of the sediment as if it may be under some type of stress. Perhaps during periods of strong cross-canyon winds, storm waves and/or earthquakes in Monterey Bay, small gravity slumps are triggered. Other initiating mechanisms such as seiches, tidal fluctuations and simple sediment overburdening may initiate sediment motion down the sides. Frequent slumping would create a hostile environment for most small surface crawlers and would disturb burrowing organisms.

Observing how the ballast weight of the compass sinks into the bottom, producing only a small sediment cloud, one concludes that the bottom material is cohesive (Fig. 36 and 37). This is not unexpected, since noncohesive sediment such as fine sand would probably be unable to maintain its position on a steep slope. A general mapping of this region by Galliher (1932) indicates coarse sediment about 4 cm thick overlying silt and clay, but examination of the pictures does not support his findings.

e. Leg IJ

The ship was positioned to drift up the axis of the canyon in depths of 831 m, but a shift in the wind resulted in a southeasterly set at about 51 cm/sec. This caused the camera to travel up the south wall of the canyon to a final depth of 658 m (Fig. 39), during which time a total of 40 pictures was taken.

Large mud clumps varying in size and shape

distinguished this region from the other areas. Sea pens, no less than 12 per frame, dominated the first 38% of the run in the deeper flatter region. Small burrowing holes were least noticeable in this photographic series, and rimless craters were much less pronounced. Considering the slope of the bottom, if the camera rack were oriented with the trip weight on the upslope side and the camera on the downslope, a greater camera-bottom distance would result. Thus, the ability to detect smaller features would be reduced and a study of the photos seemed to suggest that this was the case.

The first noticeable change occurred with the appearance of small shell fragments lying on and partially buried in the surface of the sediment (Fig. 40). These shells were probably transported down the wall of the canyon from shallower depths, though it is conceivable that they were displaced during some type of downslope sediment slump. Simultaneously, a marked decrease in the number of sea pens was observed. The first picture taken, after approximately 91 m of no coverage, revealed a bottom heavily populated by buried brittle stars (Fig. 41). The reasons for these changes are not known, however changing environmental conditions are undoubtedly involved.

Three photos during the traverse clearly show distinct ridges in the sediments, their origin and orientation unknown. Similar ridges previously photographed and described by Heezen and Hollister (1971) have been

attributed to erosional currents carrying away sediment leaving a differential in height (Fig. 42 and 43). The third picture (Fig. 44) differs from the other two in that several ridges similar to aged ripple marks cover the area. One explanation could be that sediment slumping down the walls of the canyon scours the slopes and perhaps piles up in the flatter areas, forming several ridges. Flows down a canyon wall could be the result of cross-canyon currents, which have been reported by Shepard (Shepard et al., 1974) and Hollister (1975). Hollister measured a maximum cross-canyon velocity of 12.5 cm/sec and a mean of 2.01 cm/sec, 30 m above the bottom in the vicinity of leg EF-2. It is reasonable then to assume that similar cross currents exist in other areas of the canyon. The exposed shell fragments and ridges certainly tend to indicate the existence of some type of sediment movement.

The last picture of the run (Fig. 45) shows a biologically encrusted group of rocks containing sea anemones and soft coral (Anthomastus Ritter), one with polyps extended and the other with them retracted. A build-up of sediment on one side of the rocks and a deficit on the other suggest sediment movement from the top to the bottom of the picture.

3. Carmel Canyon

a. Leg TU

Drifting up the head of the Carmel Canyon at almost 30.5 cm/sec permitted the taking of 59 pictures. Initially the camera, on the side of the canyon, descended

to 260 m and then slowly followed the slope upward toward shore to a final depth of 128 m (Fig. 46).

Biological life, primarily the crab (Galatheid) and the shrimp (Pandalus platyceros), abound, while rock outcrops and ripple marks appear throughout the entire traverse (Fig. 47 and 48). The crab is observed periodically throughout the run, always associated with rock outcrops, which they seem to use as hiding places (Fig. 49 and 50). The shrimp, on the other hand, were photographed in the open, walking on a smooth sandy-looking bottom (Fig. 51). These two crustaceans dominated 26% of the pictures, with the shrimp being the most numerous. Carmel Canyon is a known commerical shrimp bed, and such a high density is not unexpected.

The ship drifted near the base of the canyon's southern wall, and periodically the camera passed over associated rock formations. Rock outcrops, present in 12% of the photos and ranging over the entire length of the line, were covered by biological growth as well as sediment (Fig. 47, 49, 50, and 52). This contrasts with the few rocks seen in Monterey Canyon, which for the most part were free of sediment and biologics.

Current lineations were observed over most of the area, being more prominant at the seaward end of the leg (Fig. 53). In the nearshore part of the canyon the current lineations were less noticeable. This may be due to higher current velocities which have smoothed out the

sediment. The crests of the ripple marks oriented in a N-S direction had an average crest-to-crest distance of about 11 cm. This would be the proper alignment for a current traveling along the axis of the canyon. Large quantities of nearshore debris (Fig. 54 and 55) can be seen at the seaward portion of the leg but not at the shallower end. This supports the concept that the current slows as it travels seaward, allowing deposition of material. Currents measured under stormy conditions, 3 m above the bottom, at a depth of 205 m had an average speed of 12 to 14 cm/sec with maximum surges between 28 and 31 cm/sec (Shepard et al., 1974). The surges are of sufficient magnitude to transport the sediment in this region.

In general the surface sediments look grainy, perhaps being fine sand (Fig. 47, 51, and 53). The size and density of the sediment clouds produced by the compass striking the bottom (Fig. 56) indicate that the sediment is noncohesive. Attempts have been made to relate the apparent size and density of a sediment cloud to the average grain size of the surface sediment (Athearn, 1967). Sediments with higher silt and clay content tend to create denser, smaller clouds, whereas a greater amount of sand content produces a less dense cloud. Athearn (1967) concluded that the determination of grain size by comparing sediment clouds is limited to distinguishing finer and coarser sediments in a particular area. A bottom sample collected by Carter (1971) indicates that the surface sediment at that time

consisted of 55% sand, 39% silt and 5.5% clay for a mean grain size of 0.065 mm (very fine sand). This analysis appears consistent with the overall general appearance of the bottom sediments.

The very tiny holes in straight lines are the footprints of the shrimp or crab, while the plow marks are probably created by bottom fish resting on the bottom or worms and holothurians crawling along the surface (Fig. 48 and 51). The uniform lack of holes and the absence of feces indicate a low population of burrowing organisms. Coarse sediment, which might not provide the environmental requirements of burrowers, and frequent scouring may be the reasons for the sparsity of these features.

b. Legs ST-1, ST-2, ST-3

The bottom profiles of this region just seaward of leg TU are quite different for each line (Fig. 57, 58, and 59). A total of 50 pictures was obtained as the camera traveled at about 25 cm/sec during legs ST-1 and ST-2 and slightly slower, about 17 cm/sec, during leg ST-3.

The bathymetric profile of ST-1 (Fig. 57) indicates that the camera followed the side of the canyon wall from 329 m up to 219 m. One might expect mostly rock outcrops, primarily because during leg TU, when near the base of the wall, rocks were present. Only four pictures, however, revealed rock outcrops, presumably granite, known to be the dominant rock structure in the canyon (Fig. 60). The presence of the sediment and the lack of scour pits

suggest little active transport in this region.

The remaining 11 pictures of leg ST-1 and the 16 pictures of leg ST-3 depict a bottom potmarked with half-moon shaped depressions (Fig. 61). Virtually no small holes exist, and the sea pen is rarely seen. Surface crawlers and free swimmers are completely absent. This is undoubtedly the most biologically barren area photographed in Carmel Canyon.

A general impression of current lineation in Fig. 61 possessing a crest-to-crest distance of slightly less than 11 cm and oriented in a NNW - SSE direction, indicates an axial current flow. The apparent ripple marks are probably not recently formed, considering the number of depressions and short track marks present. Average current velocities of 15 to 18 cm/sec were measured 3 m above the bottom at this depth under stormy conditions (Shepard et al., 1974). Maximum surges of 30 to 36 cm/sec are well above transportational limits. A 49% sand, 46% silt and 5.3% clay sediment composition with a mean grain size of 0.060 mm (very fine sand) is reported by Carter (1971), which is a slight decrease in the sand size compared to leg TU. This is not unexpected, since under normal conditions the velocity of a current tends to decrease as it travels seaward, which in turn means that the particle size it can transport also decreases.

Leg ST-2 was located on a shallower shelf (Fig. 58) and was markedly different than ST-1 and ST-3. The general impression one has after examining the photos is

that the pictures were taken on a sloping surface, which is consistent with the bathymetric bottom trace. The slope is heavily sediment laden, and small scale slumping appears to have taken place (Fig. 62, 63 and 64). Exposed worm tubes sticking out of the sediment, shell fragments and general arrangement of the bottom material are supportive evidence. Sources for activity may be associated with water motion over the side of the canyon from longshore currents, storm waves and periodic discharges from the Carmel River.

c. Legs QR-1 and QR-2

Rocks covered with biological growth dominated over 80% of the 50 pictures taken during this run (Fig. 65 and 66), and no current activity was noted. The drift rate was excessive, almost 50 cm/sec, and apparently at the beginning of the run the camera hit the bottom breaking an O-ring seal. As a result, all of the pictures were either partially or totally distorted by a small amount of water on the inside of the camera window.

d. Legs KL-1, KL-2, KL-3

During legs KL-1 and KL-3 the ship crossed the canyon normal to the axis at an average speed of 41 cm/sec and 36 cm/sec, respectively. The depths, 530 m and 480 m respectively, remained reasonably constant for the two legs, and no bathymetric profiles were recorded.

The 28 pictures taken during leg KL-1 all revealed evidence of current activity in the form of well-developed asymmetrical ripple marks (Fig. 67, 68 and 69).

The average crest-to-crest distance was 13 cm with an orientation of WNW - ESE. In most of these pictures coarse sediment can be seen in the troughs of the ripple waves, which indicates substantial current velocities. In Fig. 70 a pebble approximately 1.9 cm in size along with gravel and shell fragments can be plainly observed. Because of the near absence of ripple marks and the size of the sediments, it is probable that the current in this area exceeded transportational limits and began eroding the previously formed ripple crests. Studies indicate that velocities in excess of 50 cm/sec are necessary to erode these grain sizes (Fig. 12). Finer looking sediment, perhaps medium and fine sand, and a few small holes appear in the pictures taken after Fig. 70, indicating slower water motion (Fig. 71). The poorly defined remnant ripples might indicate that the current velocity was just beginning to initiate ripple development or was sufficient to smooth out the sediment. Most probably leg KL-1 passed across the axial current flow of the canyon at the point of greatest velocity.

Leg KL-3 photographed south of the canyon axis in relatively the same area as the latter part of leg KL-1 but about 0.6 km shoreward. The bottom throughout looked similar to that at the end of leg KL-1 having poorly defined ripple marks and a sparse number of small holes (Fig. 72 and 73).

Leg KL-2 located on the northern wall of the canyon followed a sloped surface upward from 415 m to 385 m.

No evidence of current activity was noted, but there was evidence of burrowing activity in the form of small holes and larger rimless depressions. In several photos piles of feces and plow marks were present (Fig. 74 and 75), and the overall appearance suggests relative stability.

e. Leg MN

The bottom remained basically flat with an average depth of 700 m as the ship drifted shoreward at about 39 cm/sec parallel to the canyon axis. The bathymetric profile taken by traversing the camera line after the photographic run was in sharp contrast with the recorded camera wire lengths. Therefore, the profile, indicating a large vertical relief, was not included in the report.

This region of the canyon does not appear to be strongly influenced by current activity, and on the average each of the 36 pictures contained between 100 and 150 gastropods per frame feeding on the surface sediments (Fig. 76 and 77). Occasionally the gastropods, about 1.27 cm in size, gather in a group of about 24 (Fig. 76) or gravitate to a certain area (Fig. 78). The high density of these organisms indicates an organically rich bottom material, and the small, thick sediment cloud (Fig. 77) suggests fine sediments. Assuming that the gastropod requires a certain grain size in order to be able to injest it, a silt and clay (0.062 - 0.005 mm) sediment might be inferred. Starfish, averaging 1.7 cm and occasionally less, and shallow rimless depressions common to many of the pictures in Monterey Canyon

appeared in a few pictures (Fig. 79).

Although there is no direct evidence of current activity, water motion from shallower regions may exist, since surf grass is present in Fig. 78.

IV. DISCUSSION AND CONCLUSION

The Monterey and Carmel Canyons have significantly different microreliefs. This is in part due to the different topography and geology of the two canyons.

The broad opening of Monterey Bay and the relatively wide and shallow shelf northeast and south of Monterey Canyon exposes the canyon to a wide spectrum of sea and swell and sediment sources. The main source of sediment in the canyon is probably longshore littoral transport from the north with the Pajaro River seasonally infusing significant quantities of material into the system. The sediments are continuously sorted as they move down the coast, the smaller grain sizes reaching the head of the canyon. The sluggish outflow of Elkhorn Slough and sediment carried across the shallow shelf by storm waves also contribute to the mud and silt found along most of the walls and bottom of the canyon. The fine nutrient enriched sea floor offers favorable environment for many burrowing organisms accounting for the large number of holes and rimless craters observed throughout the canyon.

Carmel Canyon, on the other hand, is situated in a small and narrow bay about 5.6 km wide on the seaward side. There is a very narrow shelf, and the transition from deep to shallow water is rapid. Sedimentary material is supplied principally by the Carmel River and San Jose Creek combined

with the erosion and weathering of the shoreline. Littoral transport of sediments into the bay is effectively blocked by the geographical configuration of the coastline (Carter, 1971). Carmel Canyon appears to be the only means of sediment movement out of the bay, and, as a consequence of the shorter traver distance, the sediment found in the canyon is not as well sorted, composed generally of medium and fine sand. The grainier bottom may not contain adequate nutritional material to support large populations of burrowing and surface organisms. This may account for the significant reduction of visible biological activity in Carmel Canyon as compared to Monterey Canyon.

The topography and geology of the two canyons undoubtedly contributed to the difference in the distribution of benthic organisms. Monterey Canyon is cut through Miocene and Upper Pliocene sedimentary rock, while Carmel Canyon is carved entirely in Cretaceous granite. As a result, the former is longer, wider and possesses a more gentle gradient. The finer sediment in Monterey Canyon is better able to maintain its position on the steep walls than the coarser sediment in Carmel Canyon. Shepard and Dill (1966) report that at the head of Carmel Canyon, the steep granite walls are covered with sand held in place by burrowing worm tubes. Pictures taken along the walls in Carmel Canyon reveal many exposed worm tubes suggesting sediment slumping. Similar coverage in Monterey Canyon indicates more extensive areas of undisturbed burrowing activity.

The steepness of the walls, the type of rock formations of the canyons and the degree of sediment deposition were probably the main reasons for the difference in the number of rock outcrops seen in the two canyons. Exposed rocks were observed in Monterey Canyon only along line CD-2. The rate of sedimentation on the walls of this canyon probably exceeds that for erosion. The coarser sediment on the steeper Carmel Canyon walls, however, more easily carried away, leaving an increased amount of exposed rock. Most of the pictures of rock outcrops in Carmel Canyon indicate some sediment cover, but primarily a thick biological incrustation.

The principal area of interest in this survey was the region of current activity along the lengths of the canyons. By plotting the location and orientation of ripple marks, the current axis and the thalweg of each canyon could then be located. It is reasonable to assume that, like a river, the turbulent flow near the bottom follows the deepest part of the canyon. The starting point for each traverse was picked to take the ship across the canyon, but wind and sea conditions often altered the set from the desired direction.

In Monterey Canyon the only region where current lineations were observed was in the vicinity of lines CD-2, CD-3 and UV-1. The primary reason for this is that the other legs were located on the sides of the canyon, not down in the deep axis where the current is expected to exist. The exposed rock adjacent to the ripple marks in leg CD-2 give the general impression that the current is next to a wall and

the pile of rocks on the sloped bottom is similar to a river bank. Since the canyon axis is curved at this point, it is probable that the current is undercutting the north side of the wall as it sweeps around. A plot of the location of the ripple marks (Fig. 80) reflects the bend in the canyon and the orientation of the crests suggests axial flow.

The Carmel Canyon traverses crossed the axis of the canyon more frequently and as a result there was greater coverage in the areas of interest. There is little doubt that line KL-1, which showed pebbles and coarse sand accompanied by well developed ripple formations, photographed the axis of the current. The other lines where current activity was detected (Fig. 81) most likely did not photograph the axial flow, otherwise the presence of coarse material similar to that seen in KL-1 would have been expected.

In both canyons on either side of the prominent ripples were regions of less distinctive current lineations, indicating the presence of thalwegs along which swifter currents travel, while lower velocities influence the peripheral regions. This is analogous to a river with a swift current following the deeper channel and slower currents elsewhere. Ripple marks yielding to a region of current-starved ripples and evidence of burrowing activity constitute the general character of line CD-2 and KL-1 and provides further evidence for the presence of thalwegs.

Bottom currents in a canyon are influenced by the physical characteristics of the canyon as well as external

forces. Divergence of water motion by small local topographic features such as rock outcrops can change the orientation and shape of ripple marks. Observations of such features might provide inaccurate information as to the net direction of flow. In regions of constricted passages and steep gradients, currents of higher velocities may result due to a Venturi effect. Carmel Canyon possesses a narrow bottom and a gradient much greater than that for Monterey Canyon, reaching the 900 m isobath in 8 km from its head, as compared to a distance of 16 km for the Monterey Canyon to reach this depth. It's relative narrowness and steeper bottom slope may account for the slightly higher average net downcanyon flow measured in the Carmel Canyon.

Periodic up- and downcanyon flow of 10 to 15 cm/sec occasionally surging to speeds of 25 to 50 cm/sec appear to be common in some canyons. A comparison of bottom currents and tidal fluctuations in canyons suggests that these normal near-bottom currents are caused by the progression of internal tidal waves along the canyon (Shepard et al., 1974). Occasionally excessive downcanyon velocities are observed and may be the result of storm waves, but little data has been collected under such conditions.

High winds nearly normal to a canyon axis appear to be a reason for crosscanyon currents recorded such as those reported by Hollister (1975) in Monterey Canyon. Cross-canyon flow noted near a bend in the Carmel Canyon was

probably not due to high winds, but suggests that a sharp curve might cause the current to shift across the axis to the other side (Shepard et al., 1974).

The currents measured in the Monterey and Carmel Canyons are sufficient to transport fine sediment in suspension and along the bottom. It is the movement of sediment, whether by induced currents or simple gravity flow, that is important because of its ability to erode and change the topography of the canyon. The mechanism is slow, yet effective, and by examining the variety of microrelief present one can better understand the dynamic processes influencing the bottom.

The purpose of this study was to examine the small scale features of the sea floor and to explain in part why they appeared. There seems to be sufficient evidence to indicate that distinct differences in the biological and physical features exist not only between the two different canyons studied but also within each one.

Additional photographic surveying in each canyon is necessary to further our understanding of the processes affecting and creating their microrelief.

V. SUGGESTIONS FOR FURTHER STUDIES

To more fully understand the marine and geological environments of the canyons the following studies would be useful:

1. Simultaneous current measurements and photographic coverage in the deep axis of the canyon. The current record should be at least 31 days to record a complete tidal cycle. Photography should be conducted at different stages of the tidal cycle.

2. Coordinated current, light scattering or beam transmission measurements and photography in the head of the Monterey Canyon to determine the extent of turbidity in the water.

3. A grab sample at each photographic site should be obtained in order to conduct a detailed sediment analysis and to recover and identify the benthic organisms dwelling in a given area.

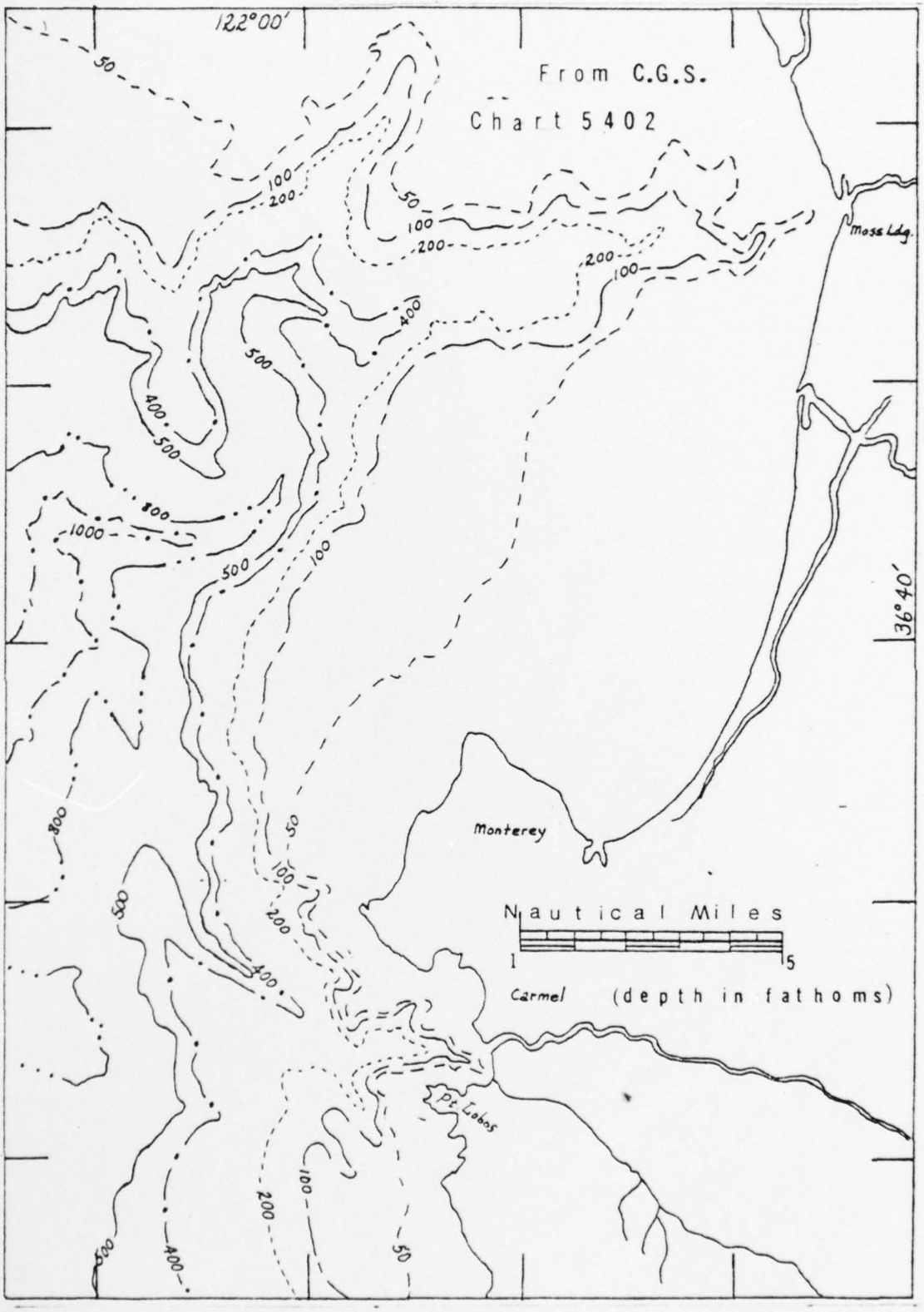


Fig. 1. Monterey and Carmel Canyons

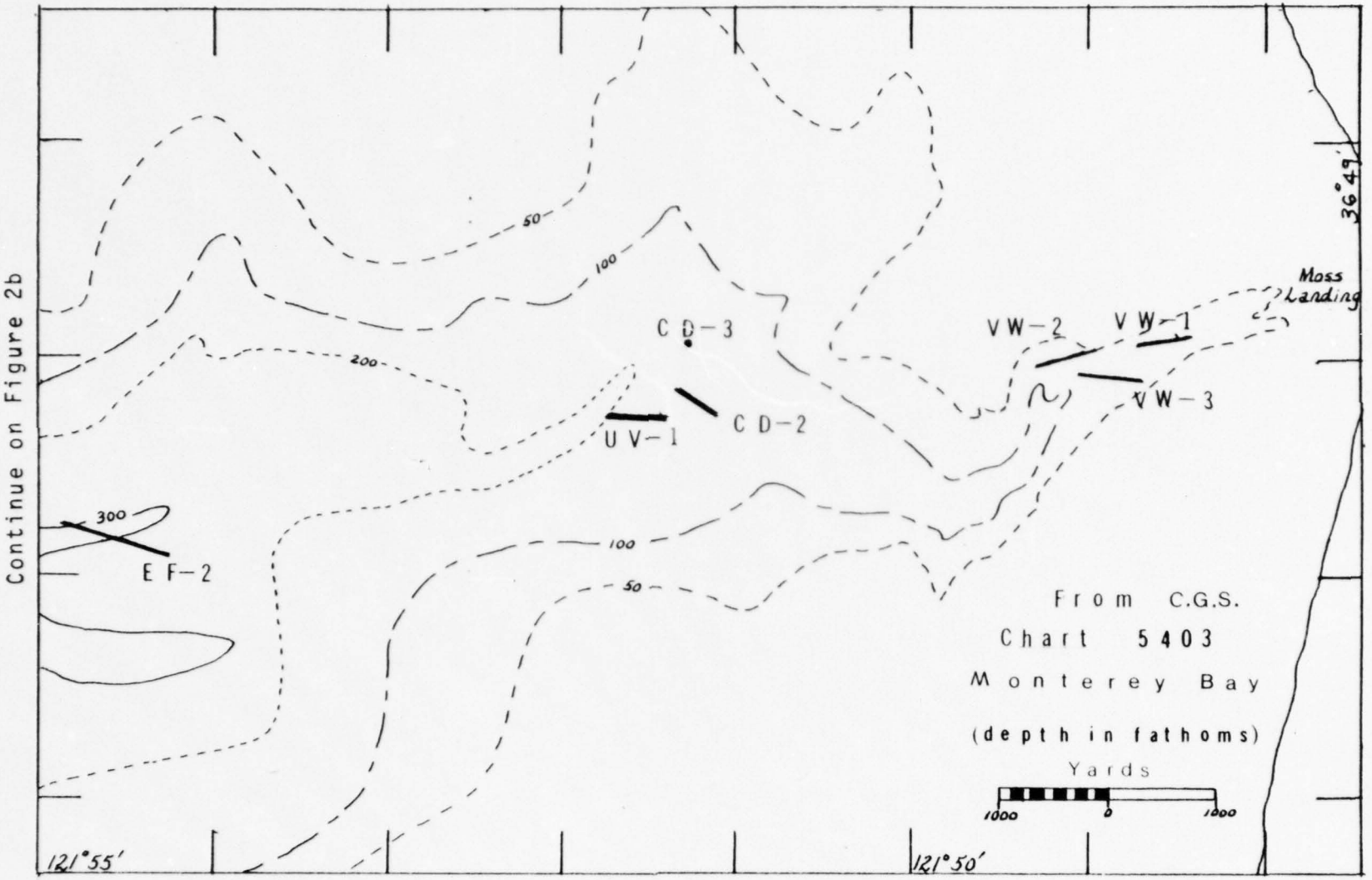
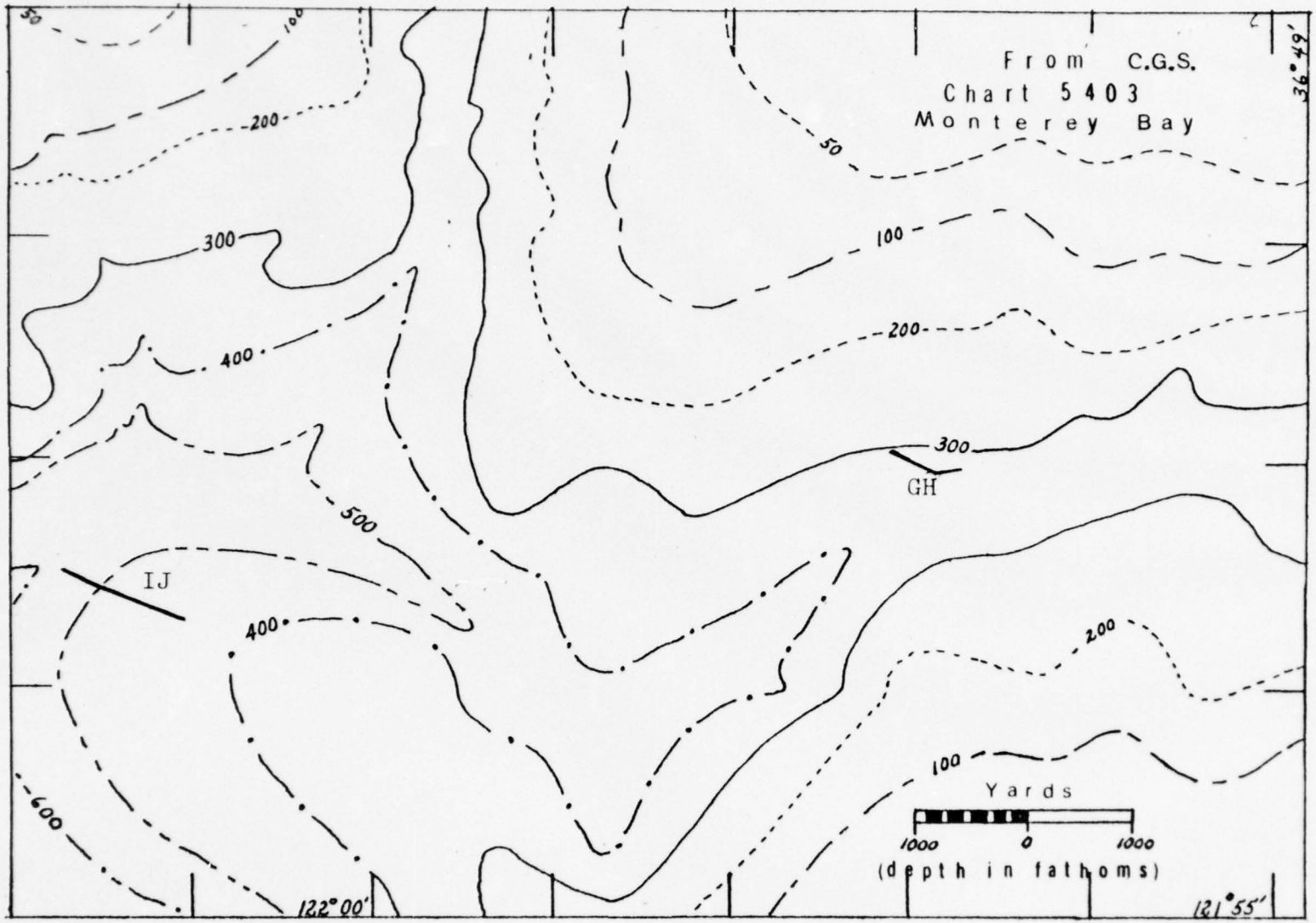


Fig. 2a. Location of Photographic Runs in Monterey Canyon



Continued from Figure 2a

Fig. 2b. Location of Photographic Runs in Monterey Canyon (cont.)

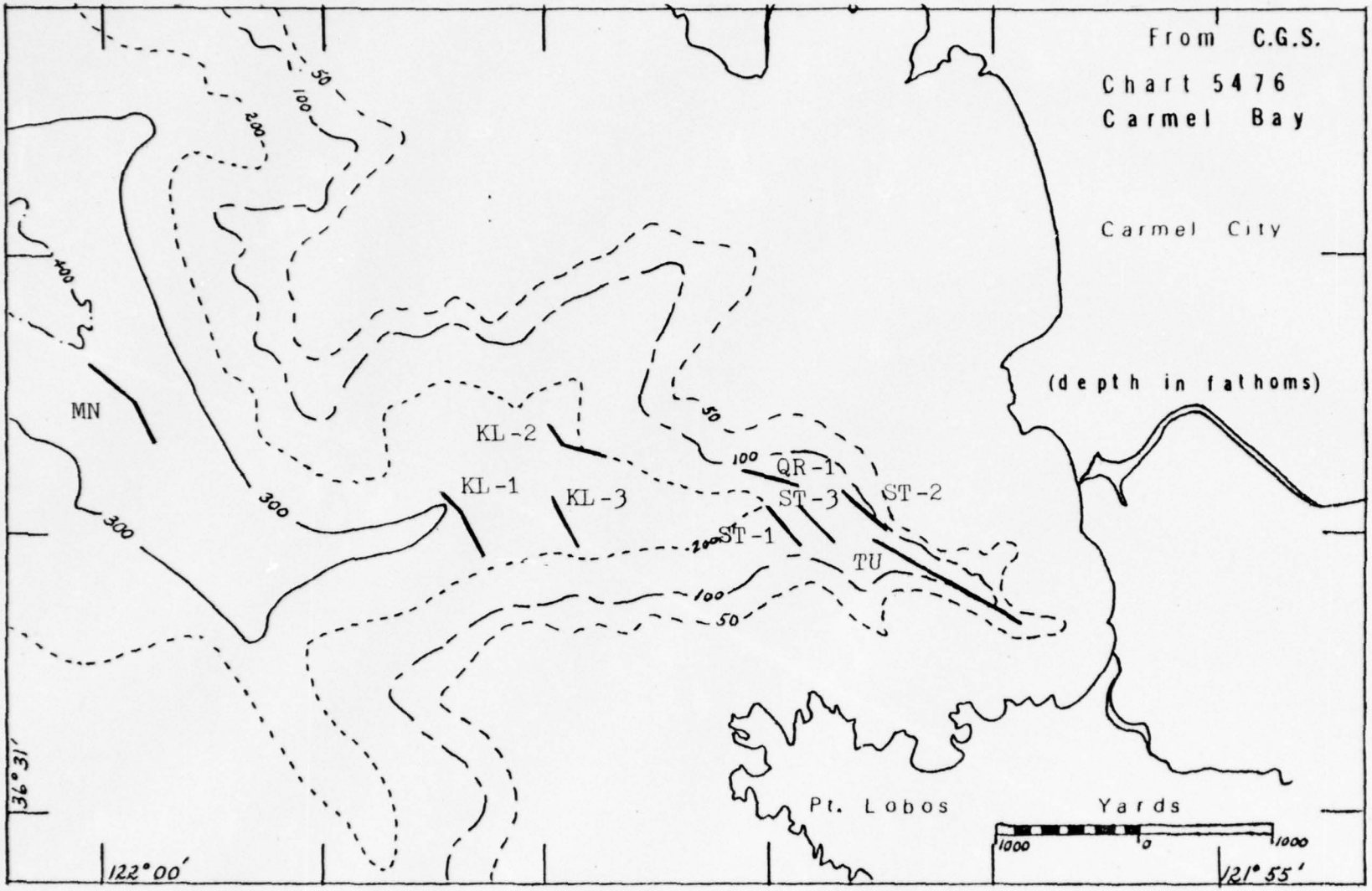


Fig. 3. Location of Photographic Runs in Carmel Canyon

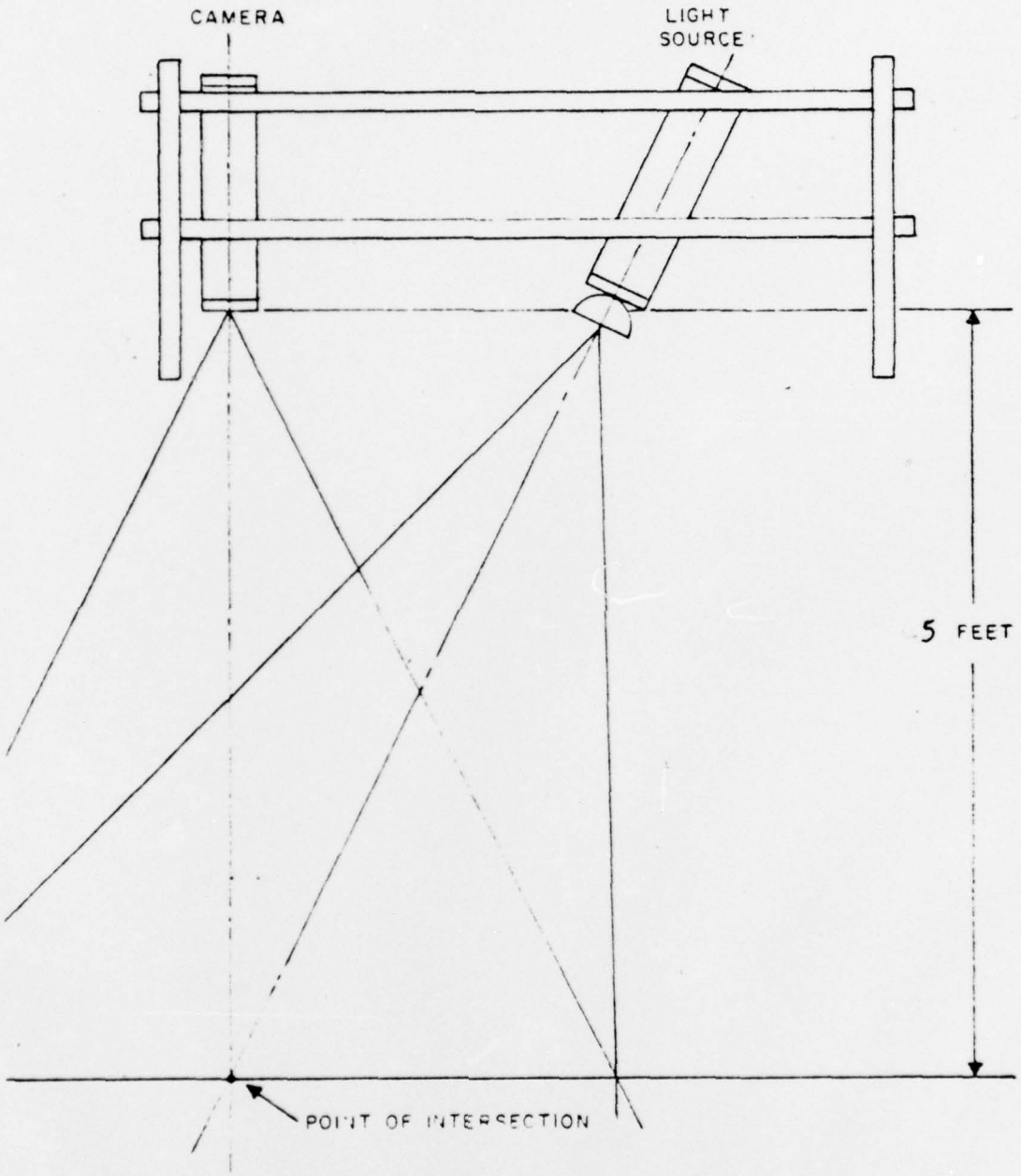


Fig. 4. Axial Relationship of Units in Standard Mounting Arrangement (From EG&G, 1960)

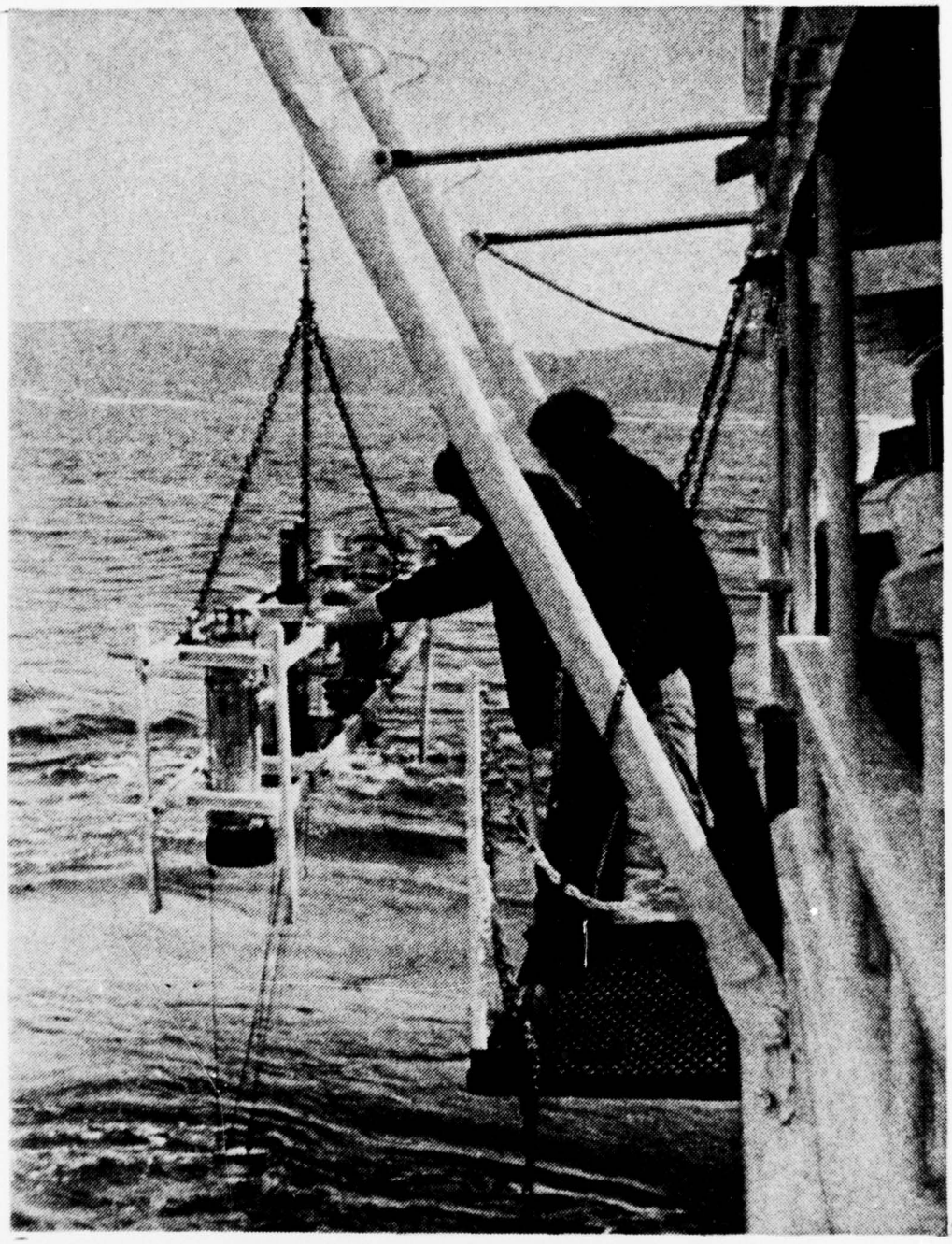


Fig. 5. Launching Camera Rig from R/V ACANIA
(Photo by PH3 Goode)

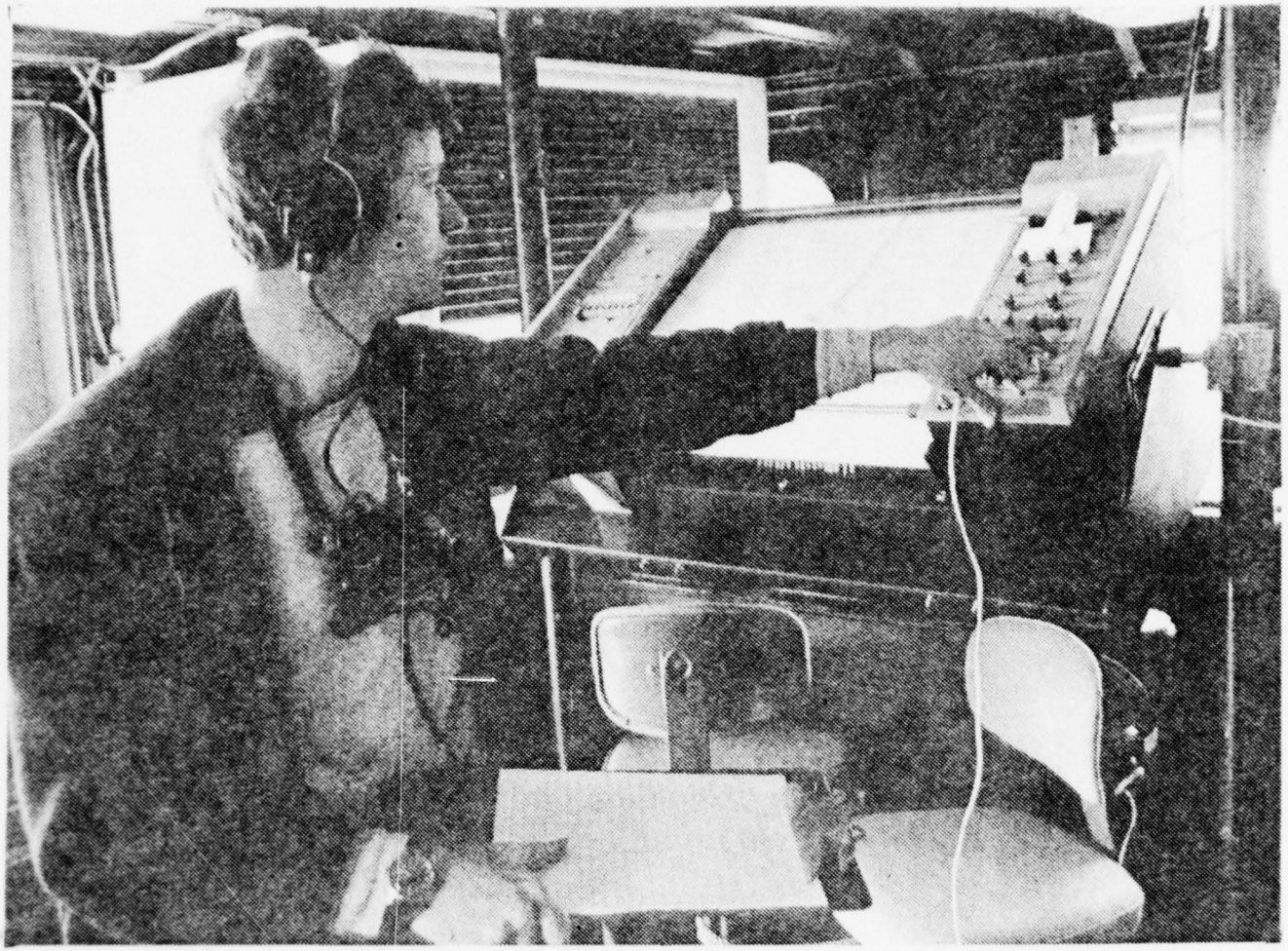


Fig. 6. Monitoring the Camera-to-Bottom Distance with the UGR (Photo by PH3 Goode)

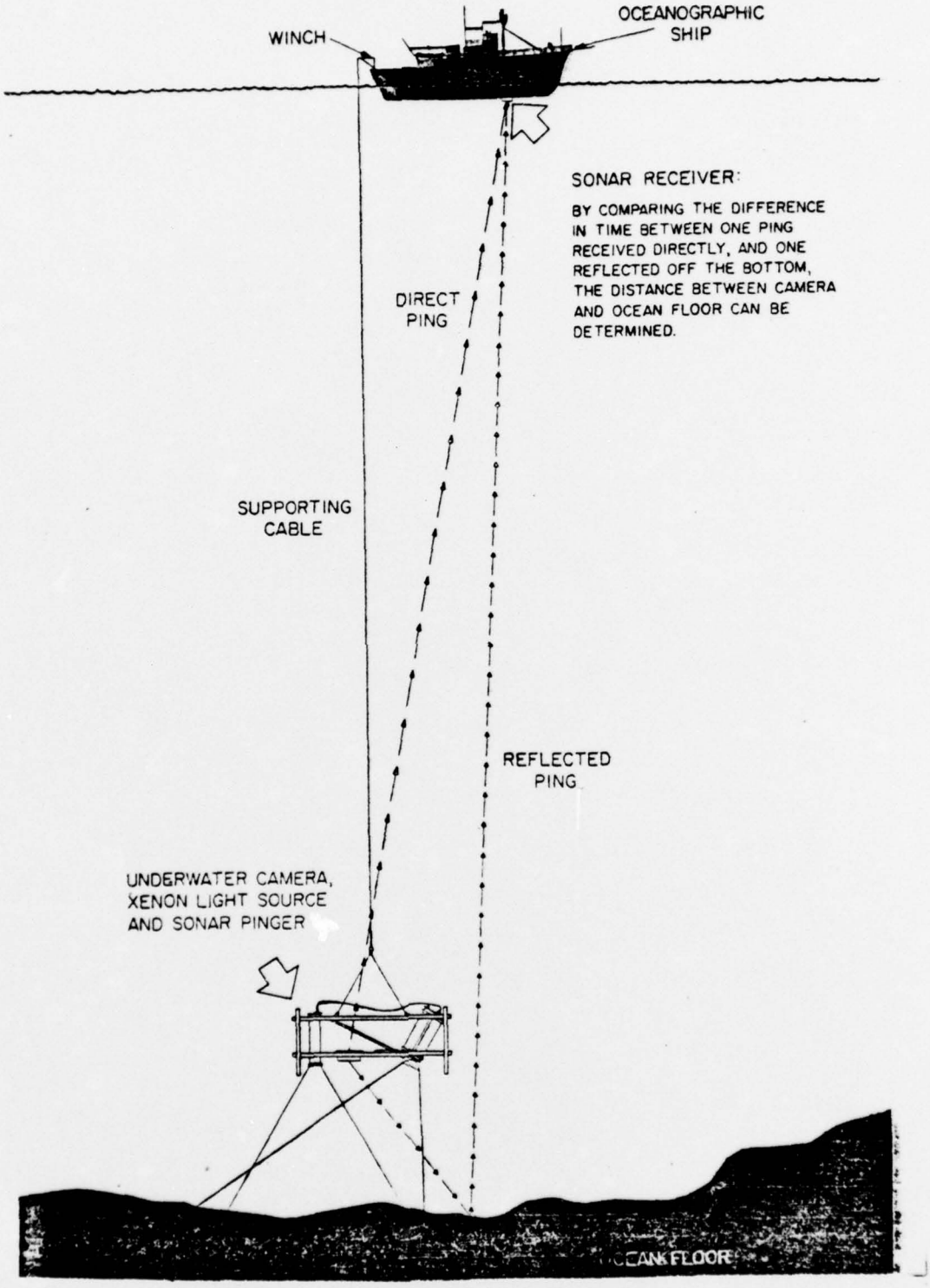


Fig. 7. Example of Typical Camera Operation (From EG&G, 1960)

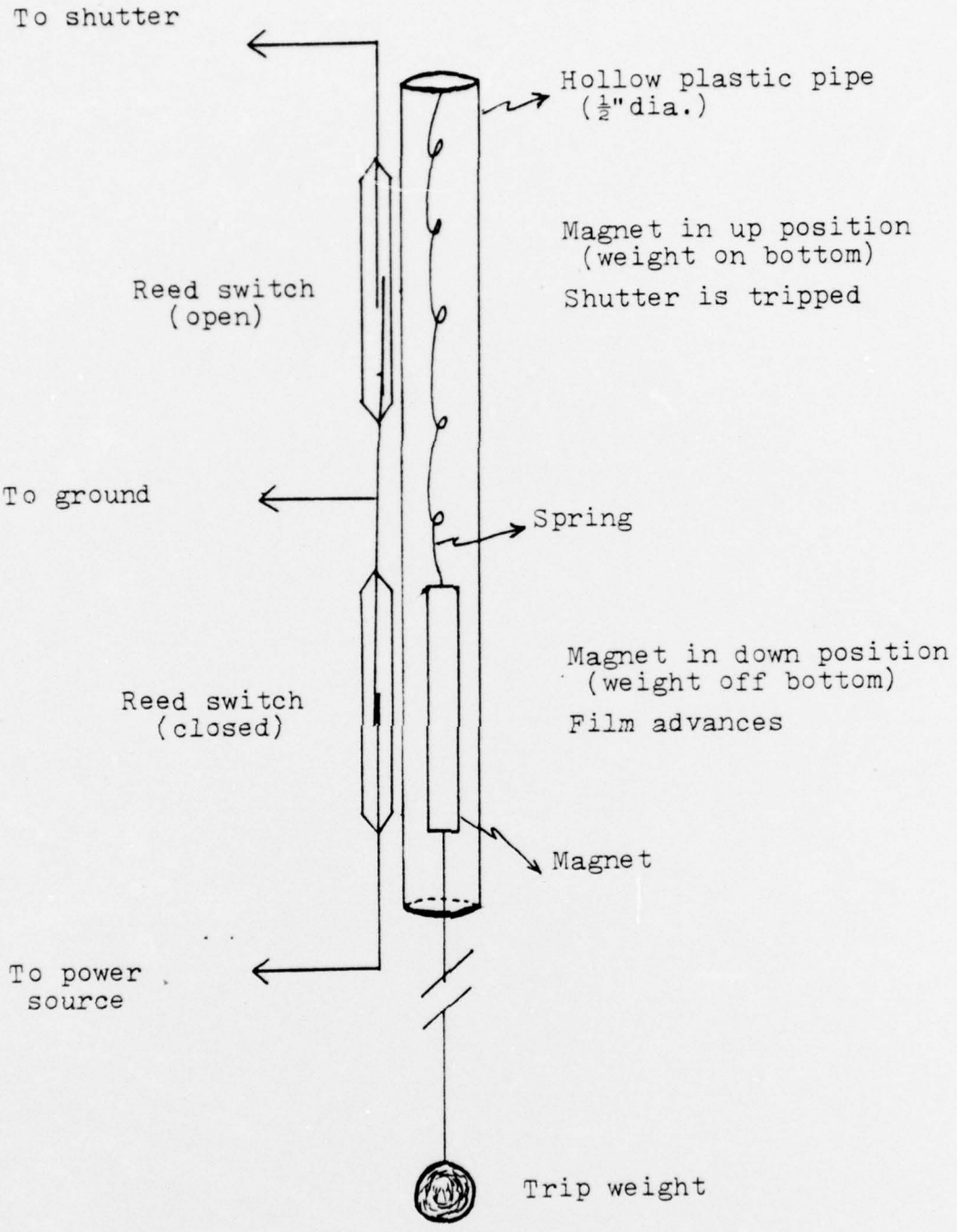


Fig. 8. Design of Underwater Trip Switch

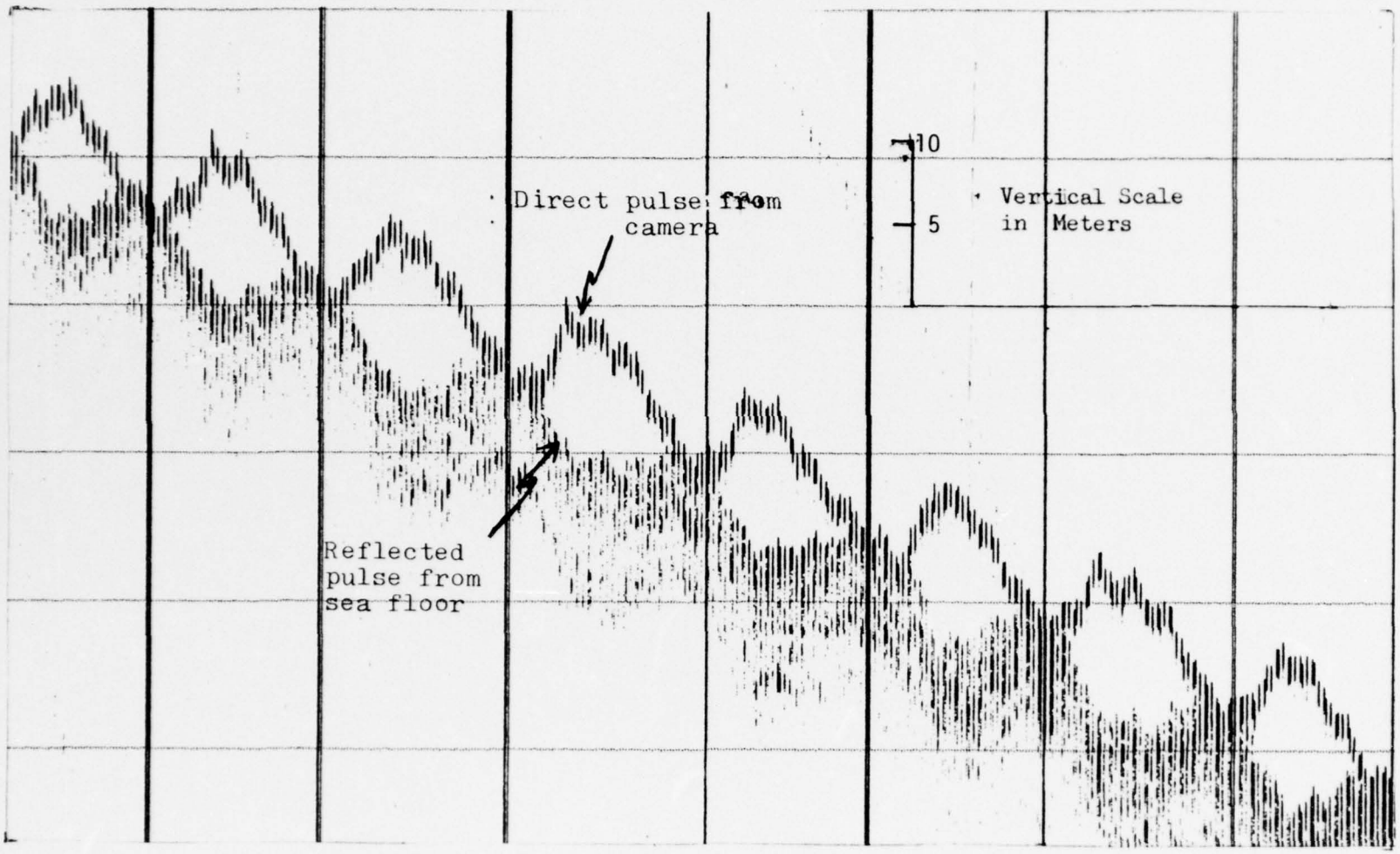


Fig. 9. UGR Output Showing Direct and Bottom Reflected Pulses

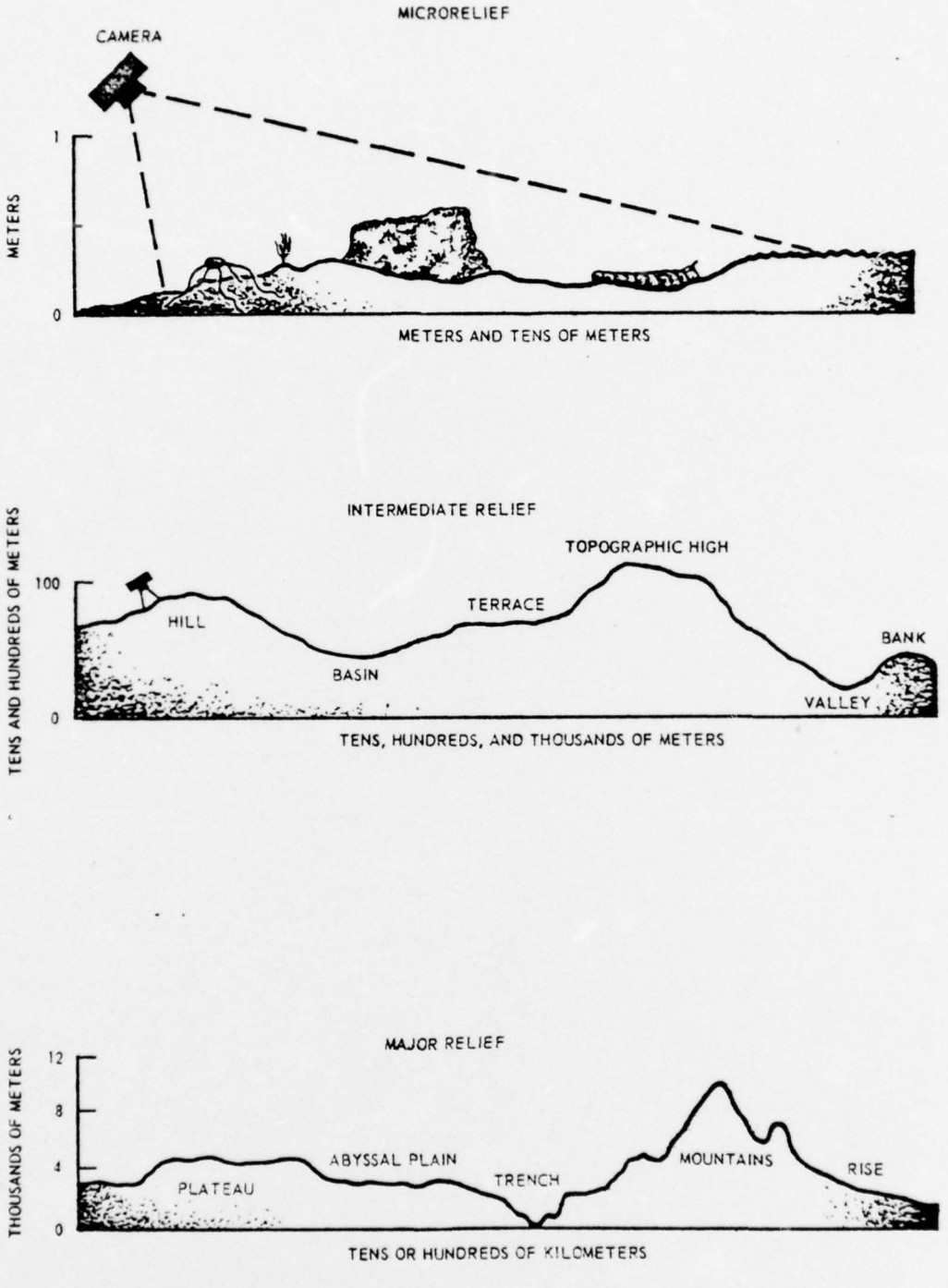
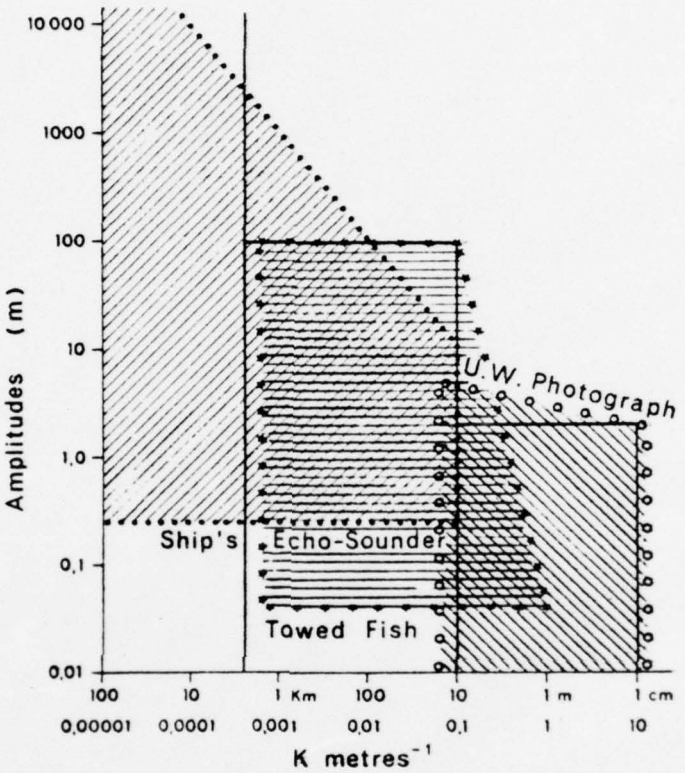


Fig. 10. Sea Floor Topographic Features
(From Shipek, 1966)



GROSS FEATURES	INTERMEDIATE FEATURES	SMALL FEATURES
RIDGES	BANKS	RIPPLES
ABYSSAL PLAINS	VALLEYS	BOULDERS
TRENCHES	HILLS	MOUNDS
ETC.	ETC.	ROCK OUTCROPS
		ETC.

Fig. 11. Spectrum Range of the Sea Floor Roughness (From Akal, 1974)

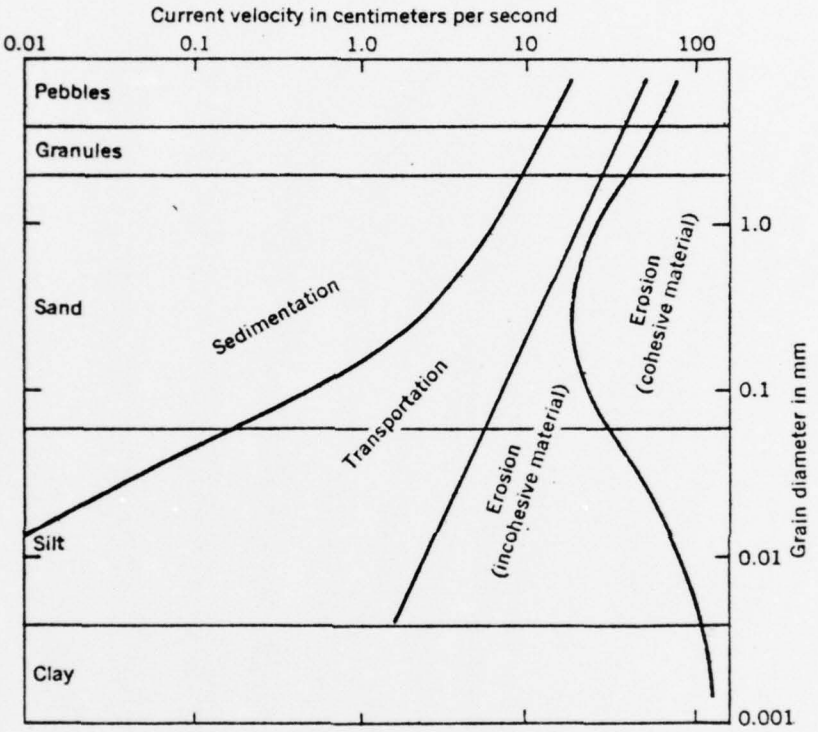


Fig. 12. Current Velocities Required for Erosion, Transportation and Deposition (From Heezen and Hollister, 1971)

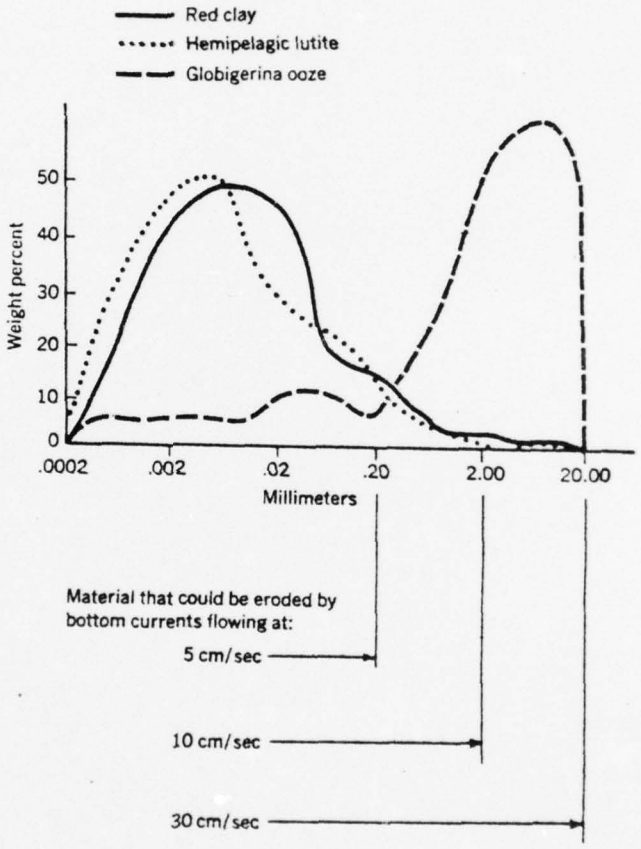


Fig. 13. Minimum Current Velocities Required for Erosion of the Principal Deep-sea Sediments (From Heezen and Hollister, 1971)

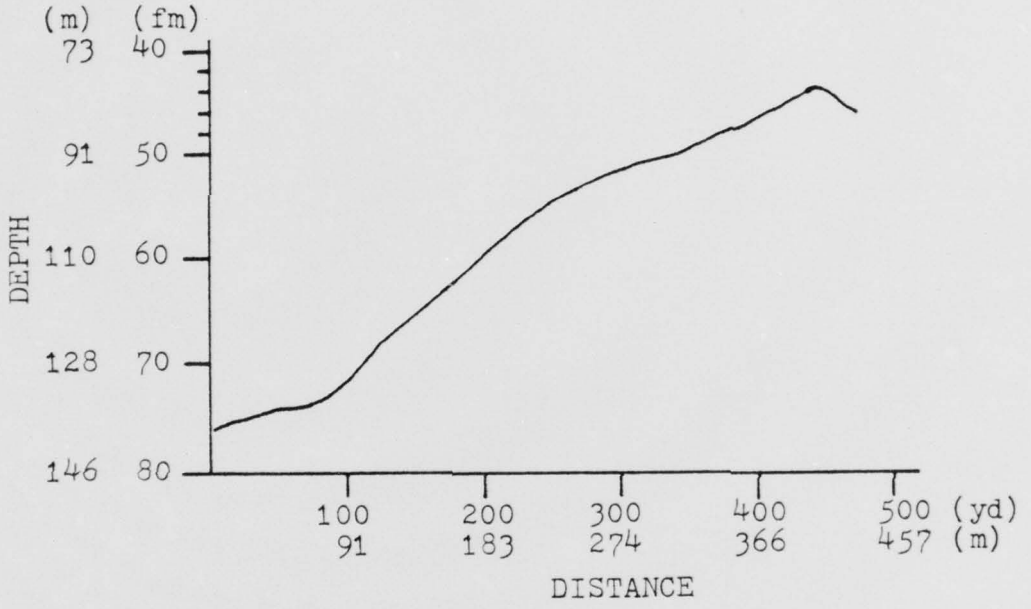


Fig. 14a. Bathymetric Profile of Leg VW-1

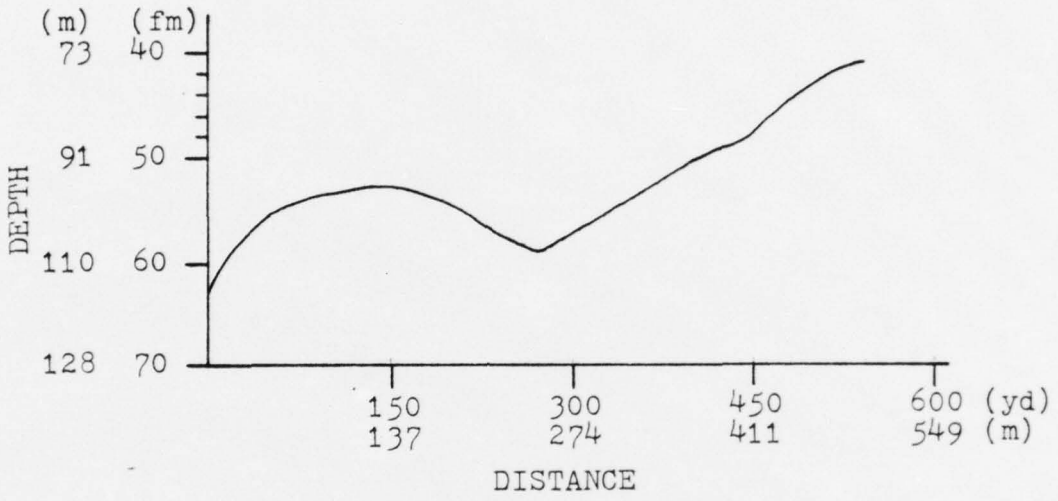


Fig. 14b. Bathymetric Profile of Leg VW-2

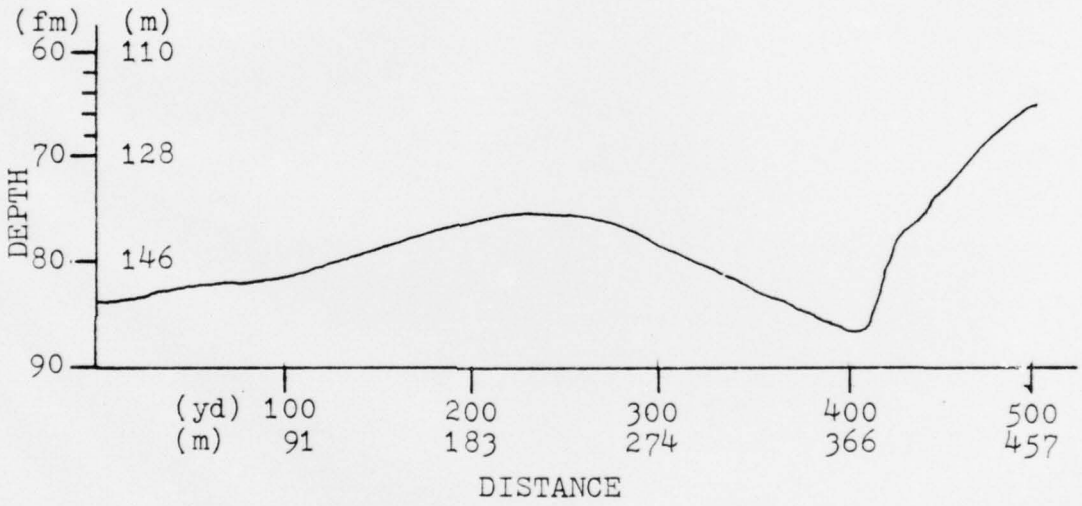


Fig. 14c. Bathymetric Profile of Leg VW-3

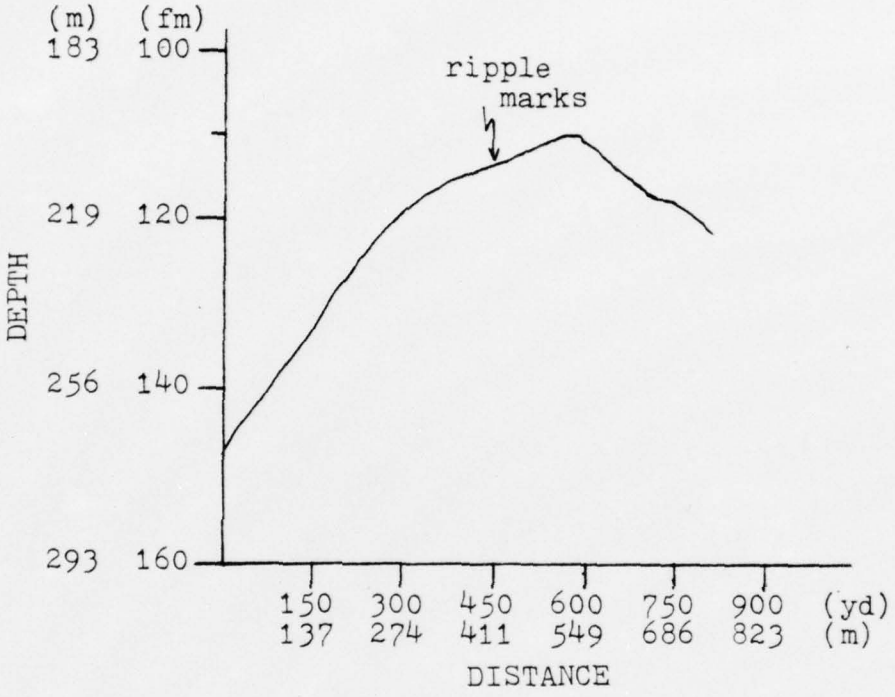


Fig. 15. Bathymetric Profile of Leg CD-2

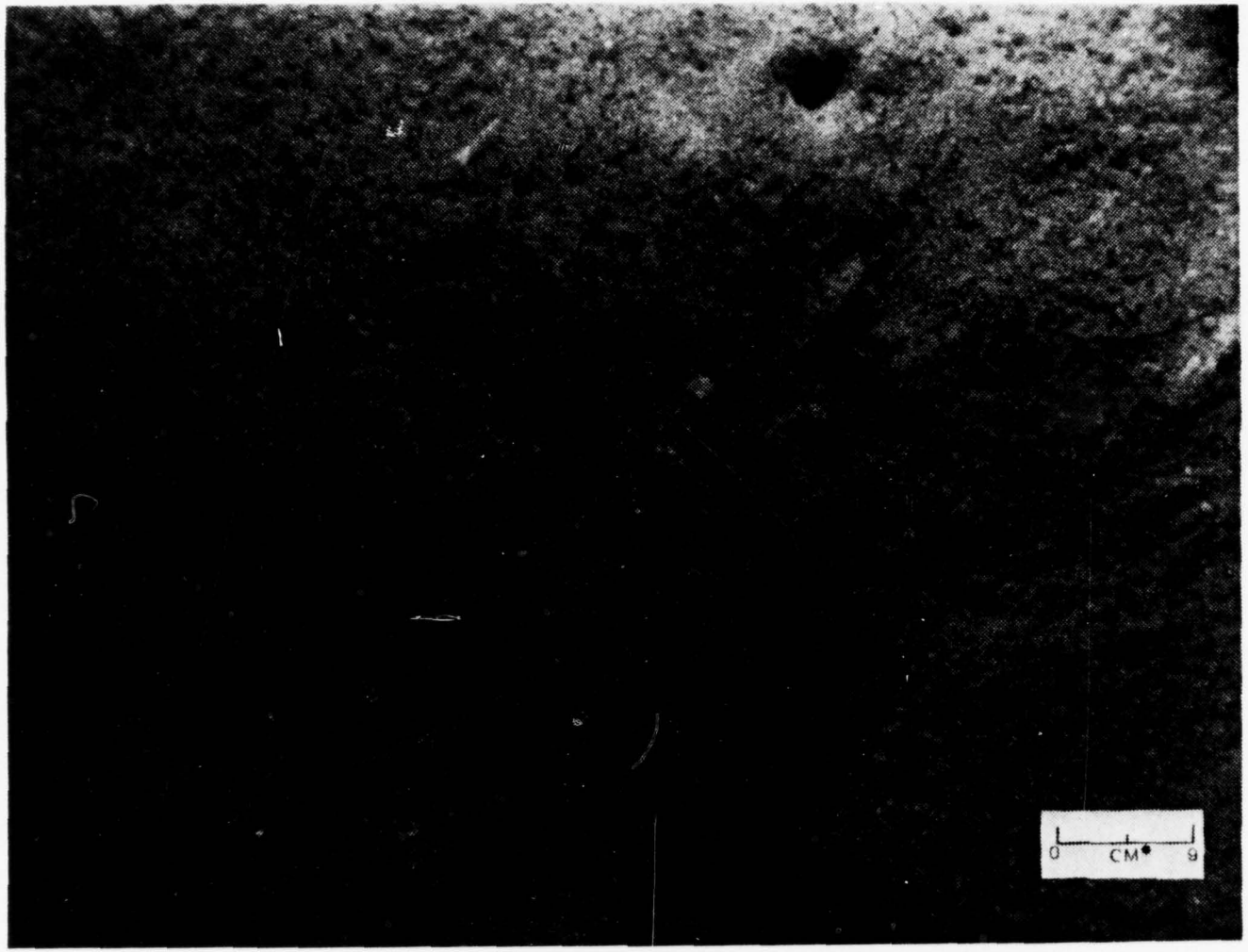


Fig. 16. Bottom Photograph Leg CD-2, 1109.5 hr, 203 m, Small holes probably the work of burrowing organisms, brittle star depressions.

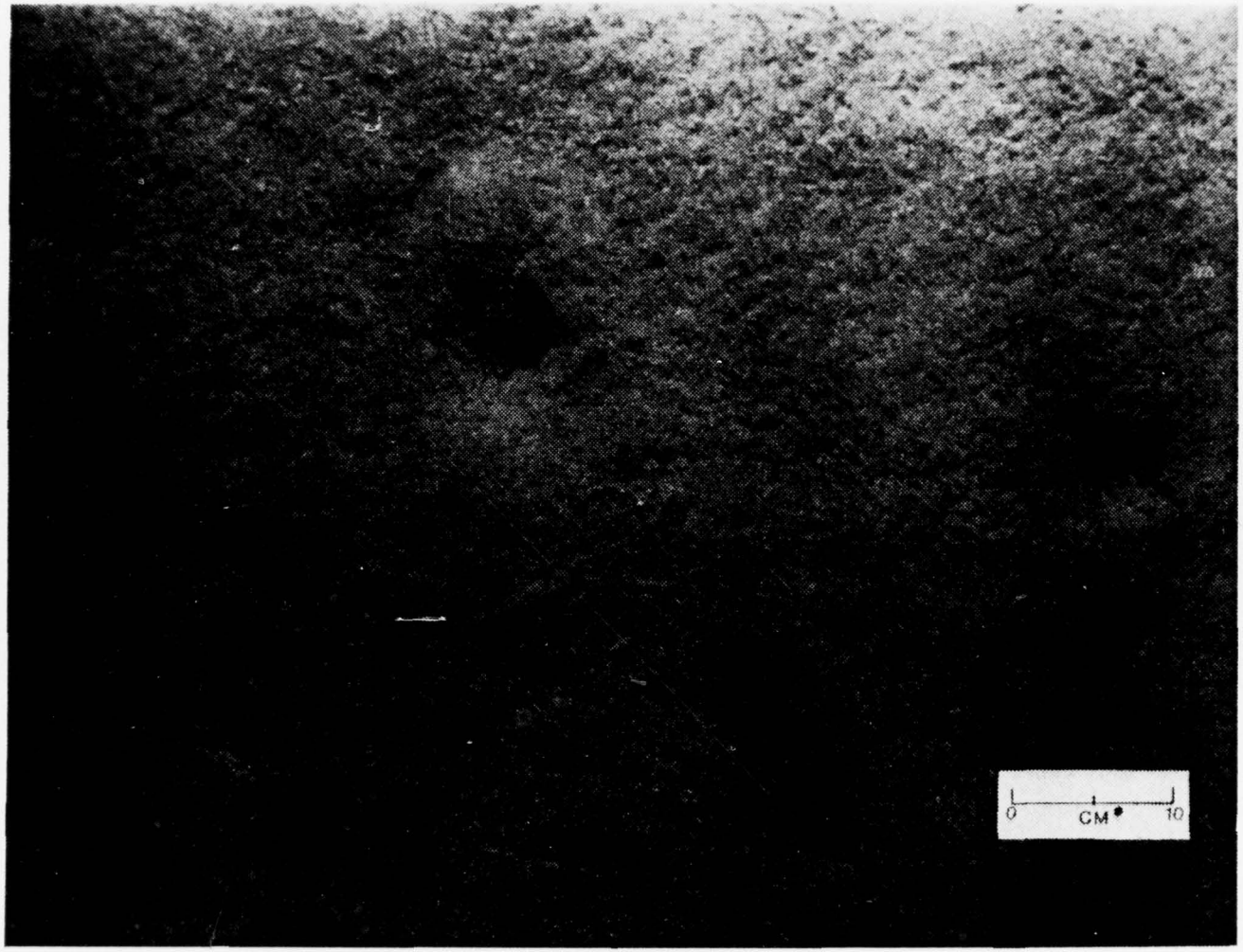


Fig. 17. Bottom Photograph Leg CD-2, 1103.3 hr, 200 m, Large rimless craters, small holes, Scaphopod shell



Fig. 18. Bottom Photograph Leg CD-2, 1120.6 hr, 220 m, Protruding sea pens, short tracks, poorly defined current lineations from UL to LR

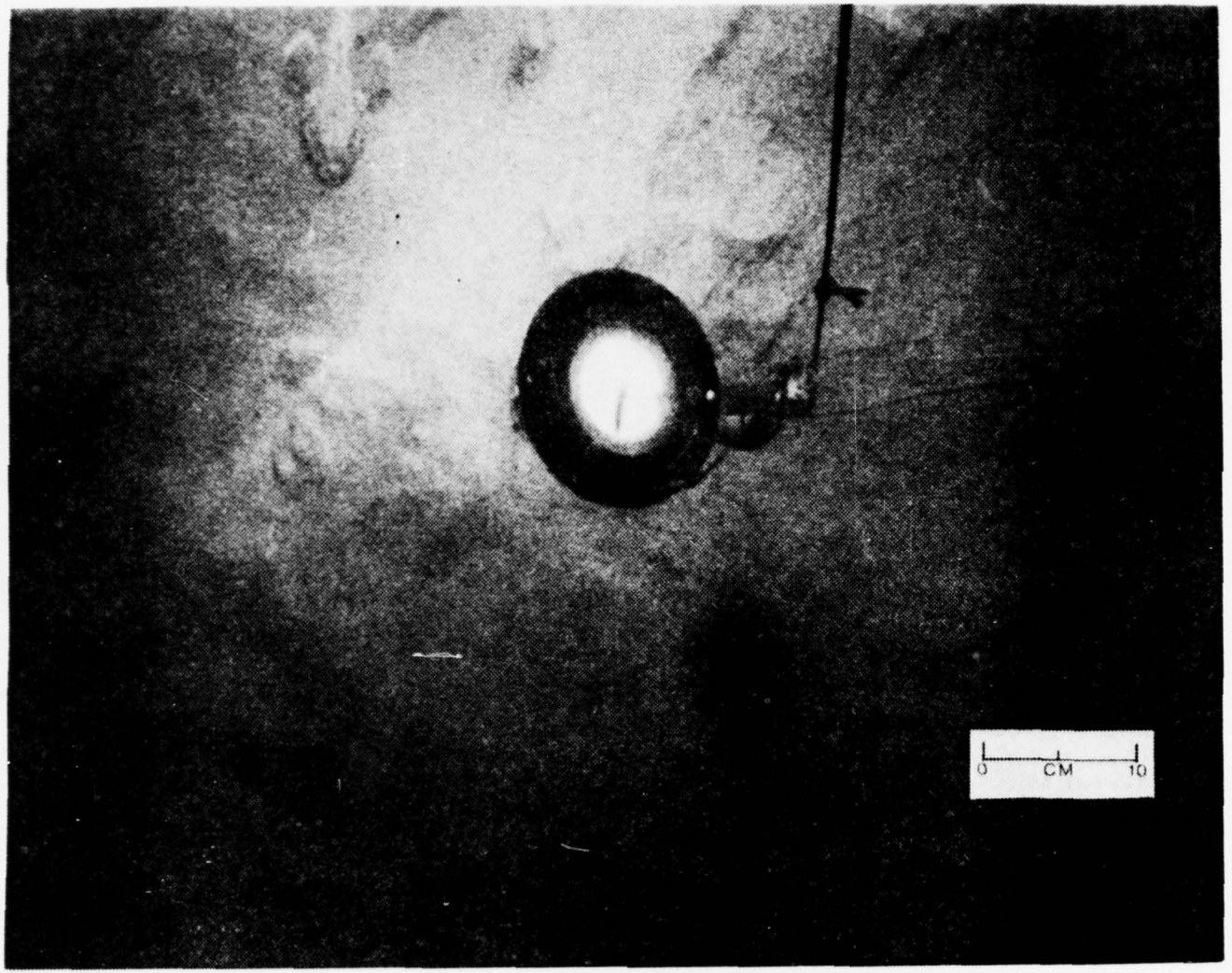


Fig. 19. Bottom Photograph Leg CD-2, 1116.7 hr, 210 m, Exposed layered rock with fish and sediment with ripple marks in a depression

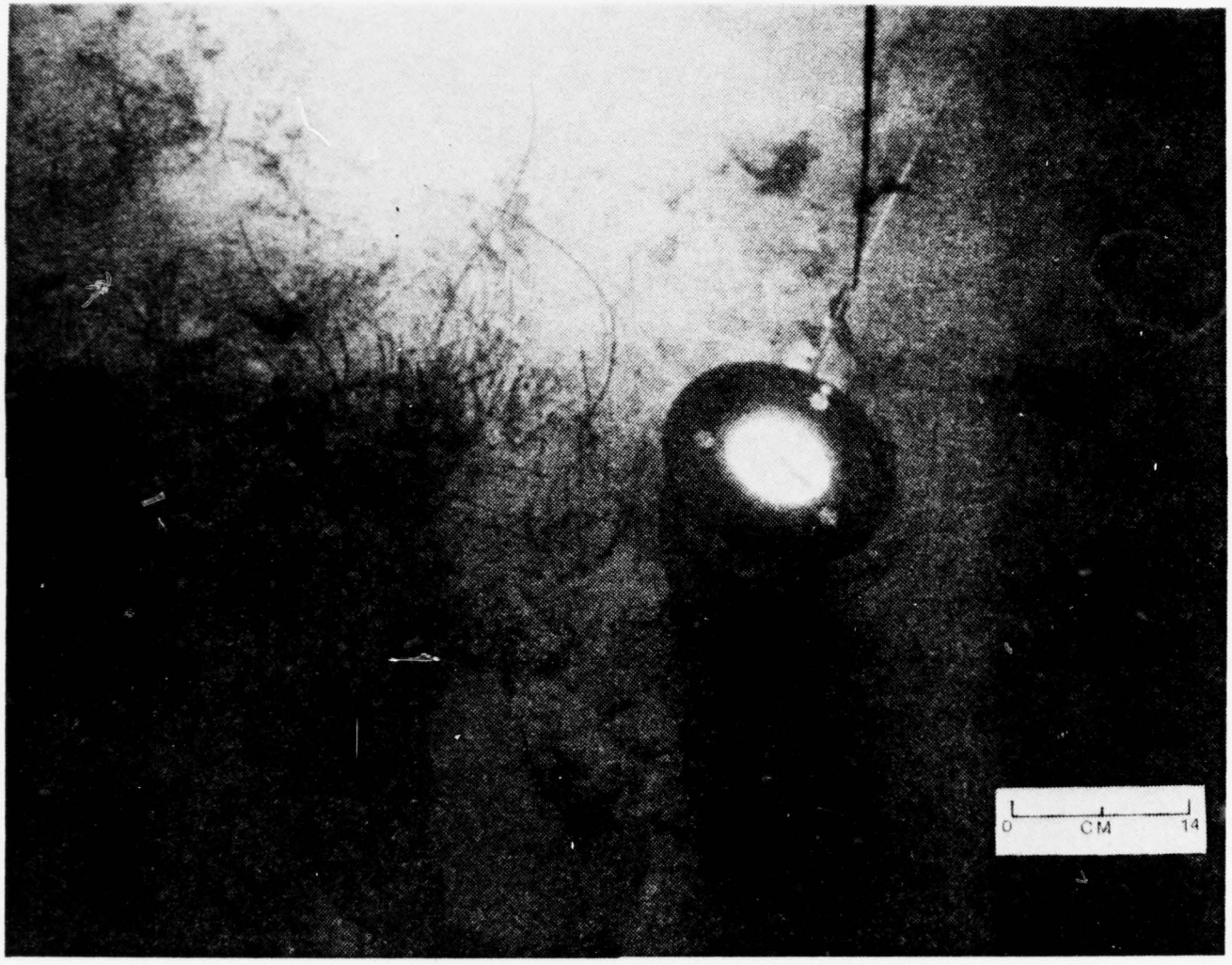


Fig. 20. Bottom Photograph Leg CD-2, 1118 hr, 214 m, Eel grass debris buried in sediment surrounded by angular rock fragments

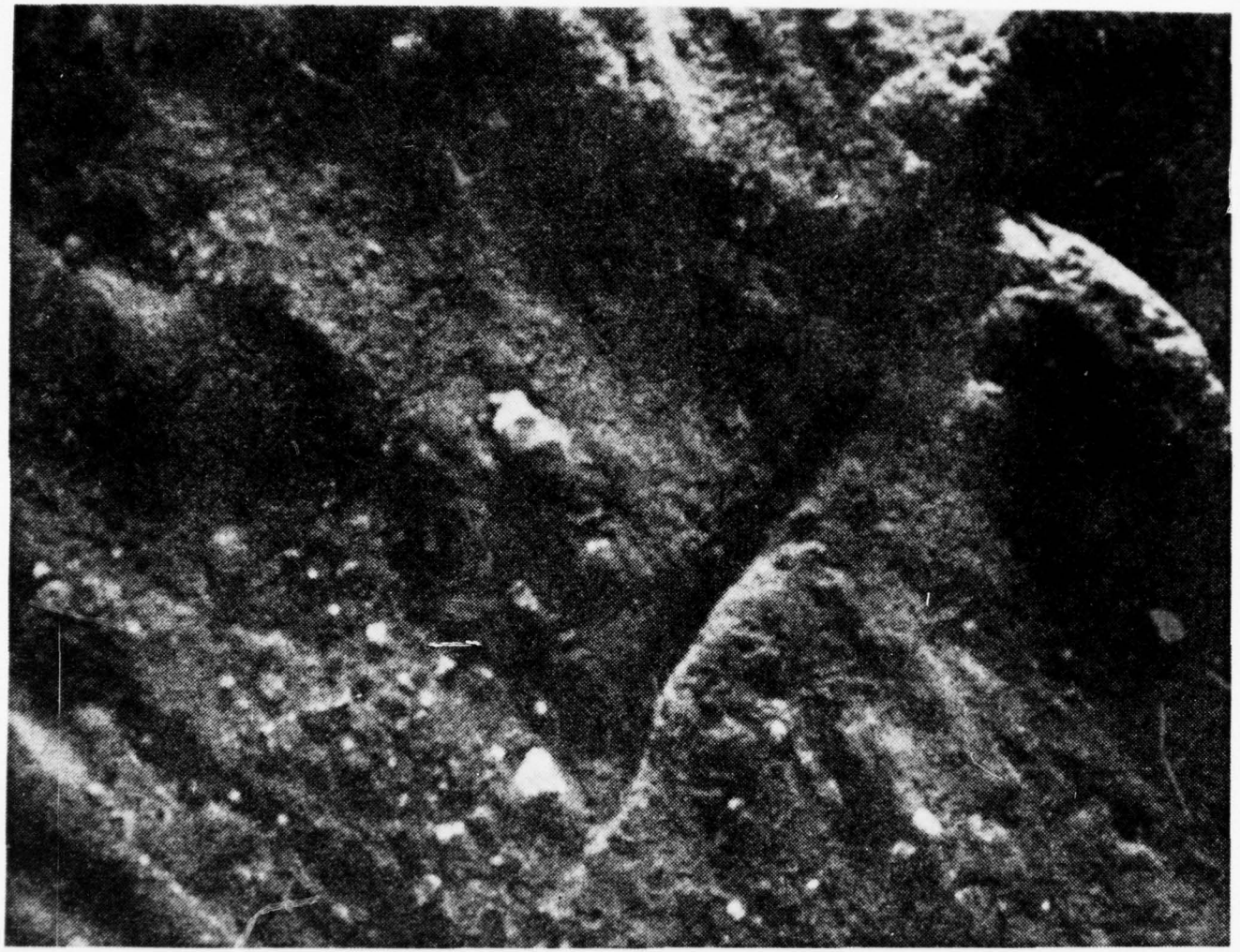


Fig. 21. Bottom Photograph Leg CD-2, 1118.6 hr, 215 m, Rock outcrop clean of sediment. Note the sediment free crack suggesting scouring

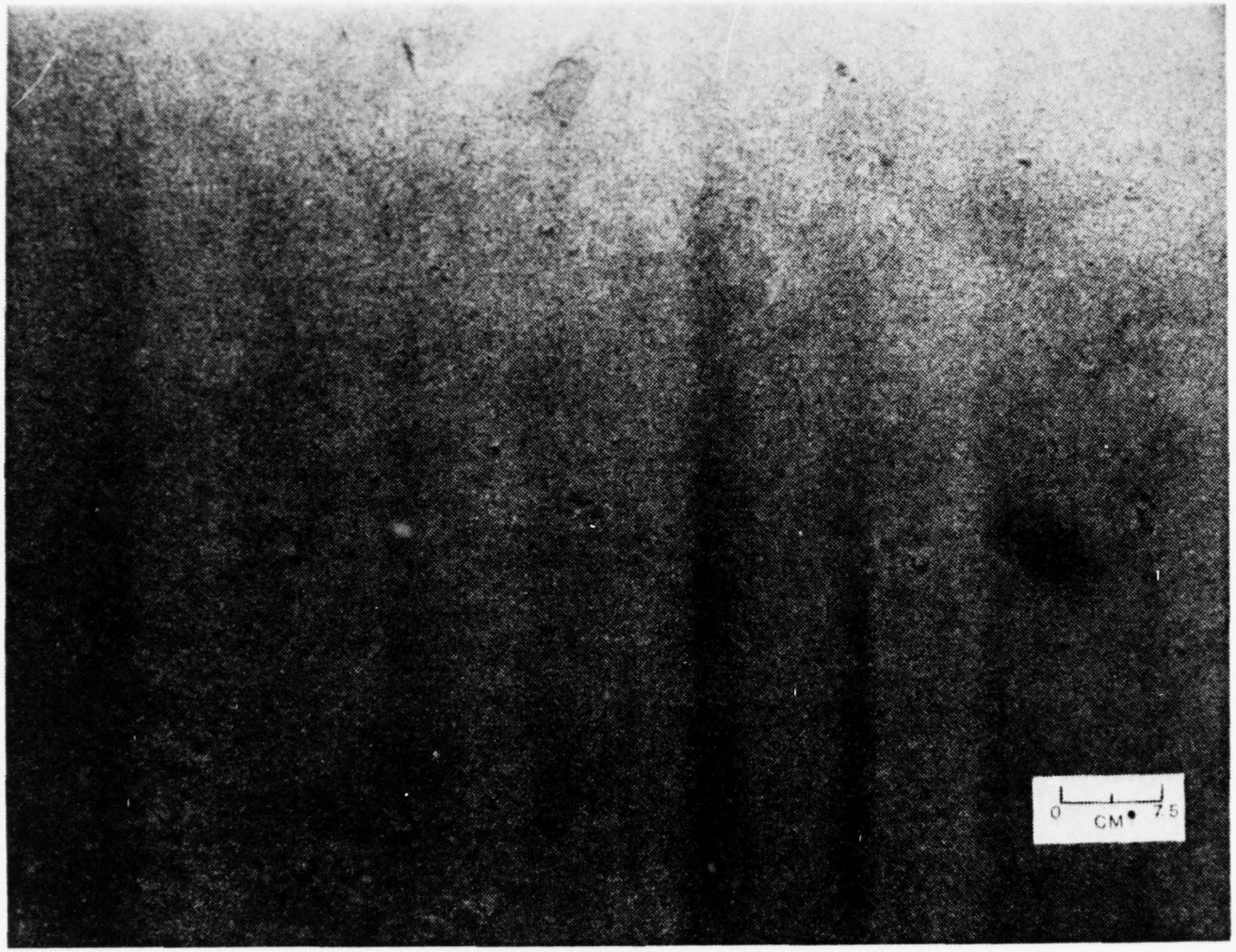


Fig. 22. Bottom Photograph Leg CD-2, 1118.9 hr, 215 m, Mud clumps bordering smoothed-over sediment containing some small holes and a few sea pens

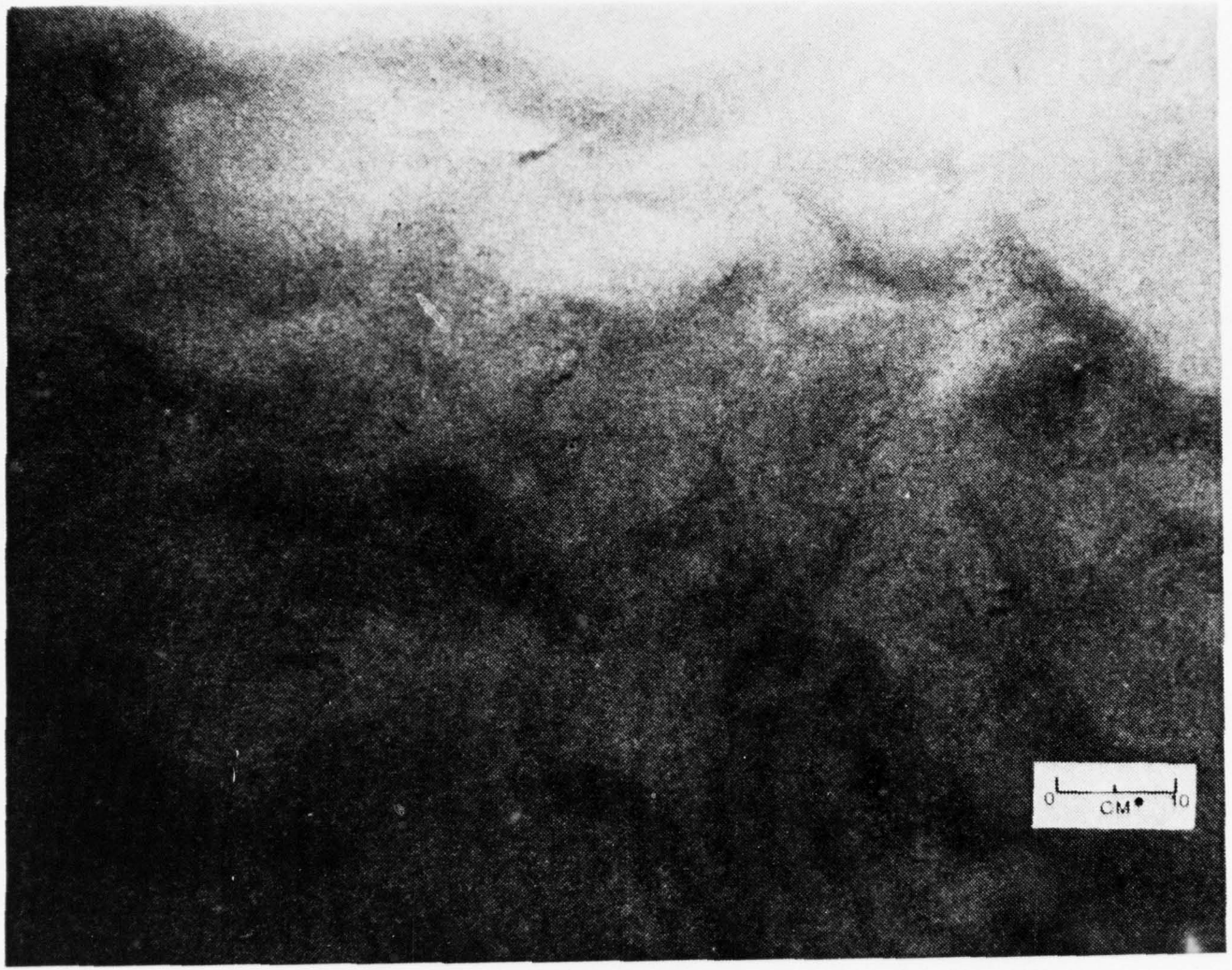


Fig. 23. Bottom Photograph Leg CD-2, 1122.5 hr, 220 m, Asymmetrical short crested ripple marks, rex sole, exposed broken worm tubes

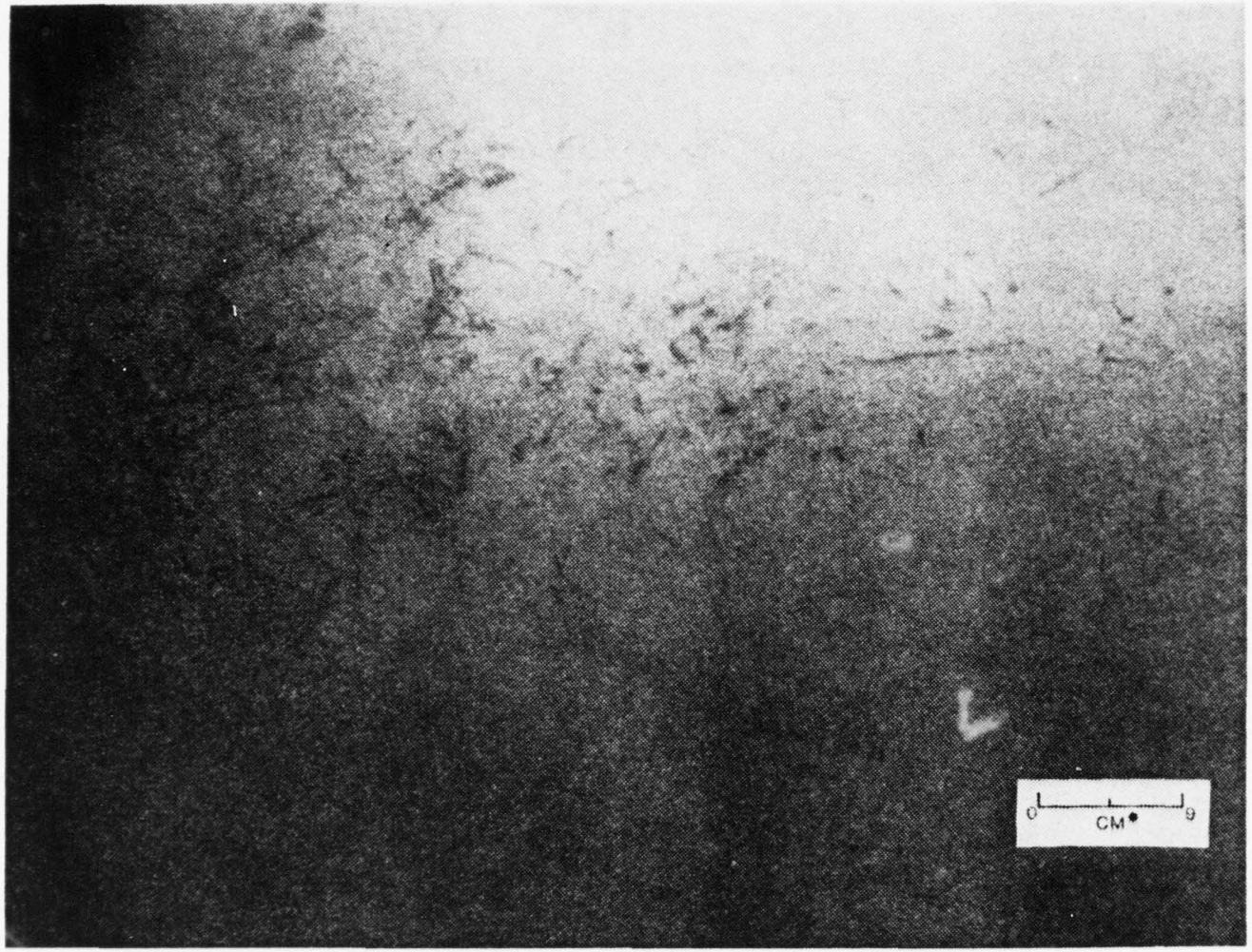


Fig. 24. Bottom Photograph Leg CD-2, 1122.3 hr, 220 m, Surface debris (eel grass and leaf) lying on smooth sediment

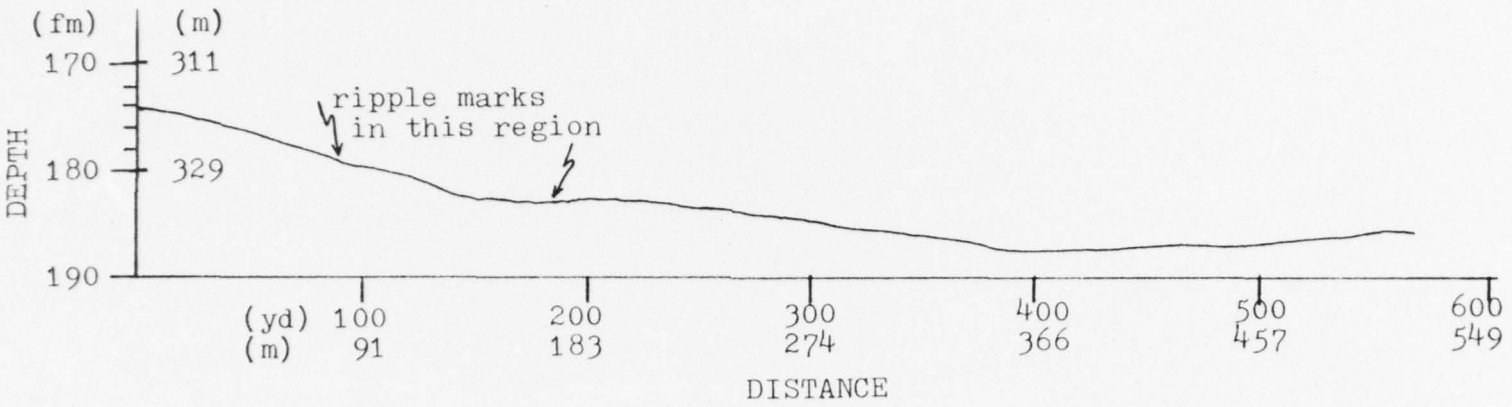


Fig. 25. Bathymetric Profile of Leg UV-1

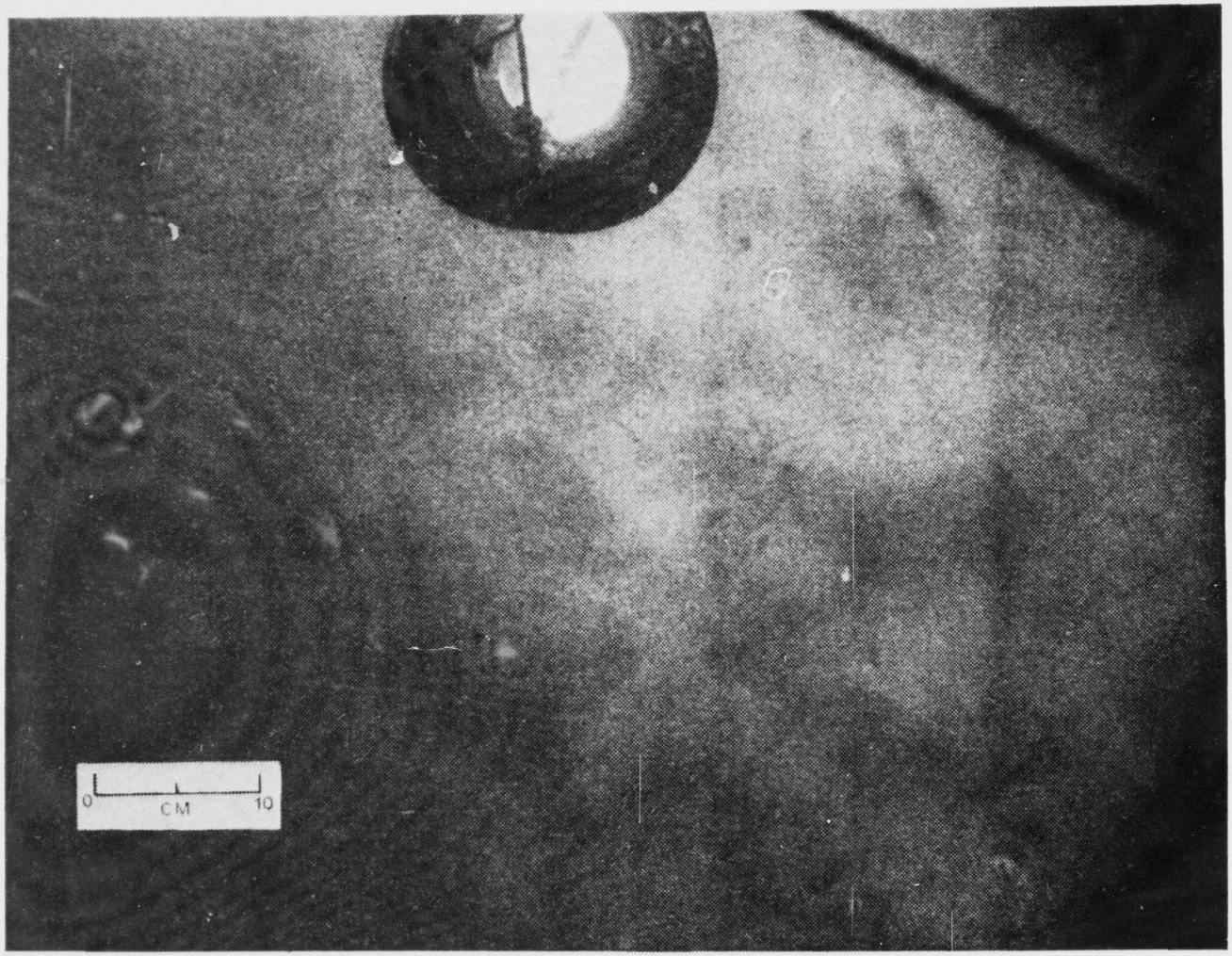


Fig. 26. Bottom Photograph Leg UV-1, 1039.25 hr, 330 m, Ripple marks, partially buried broken heart urchin

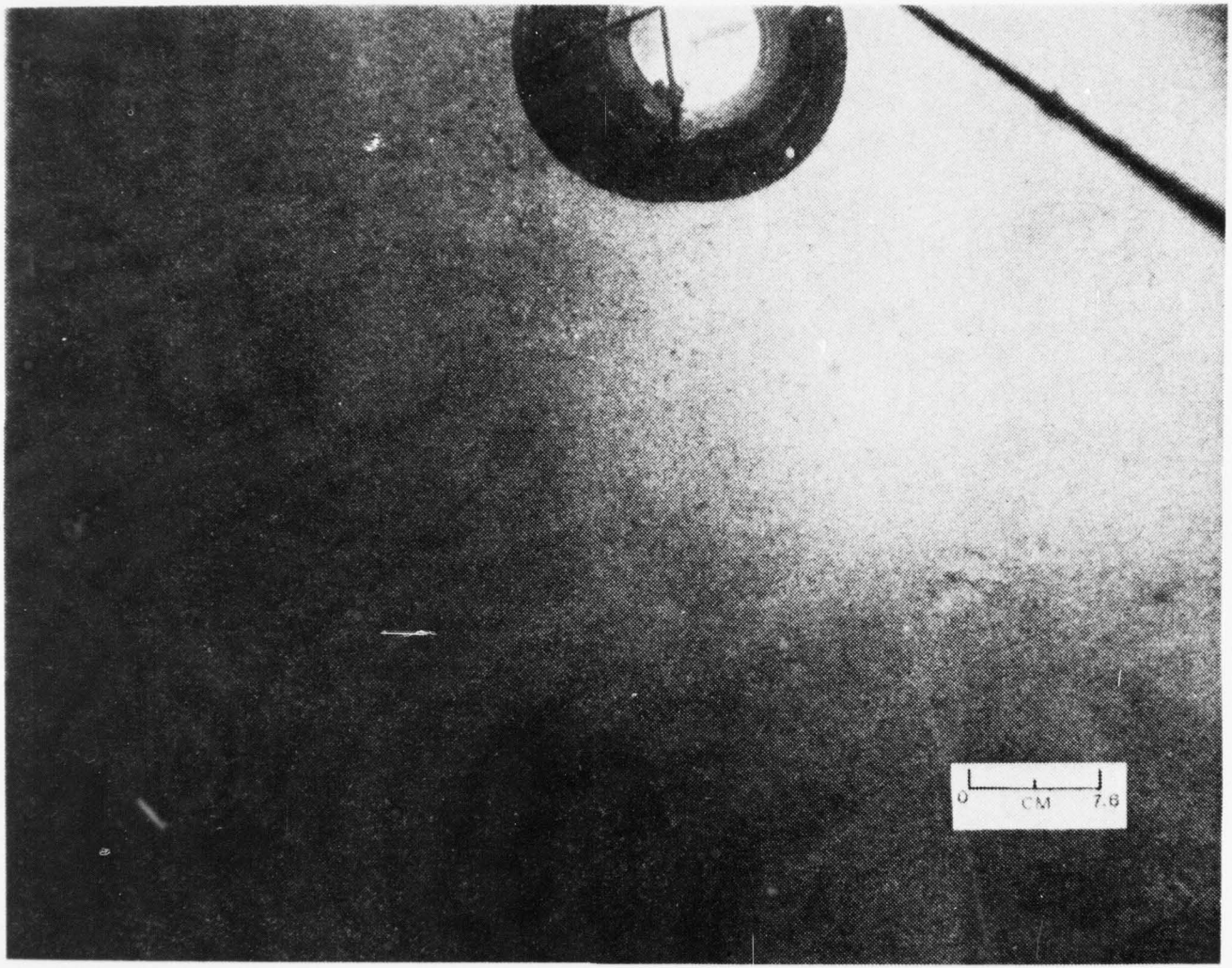


Fig. 27. Bottom Photograph Leg UV-1, 1049.1 hr, 340 m, Smooth sediment, rock in lower left may have an associated scour pit indicating transport

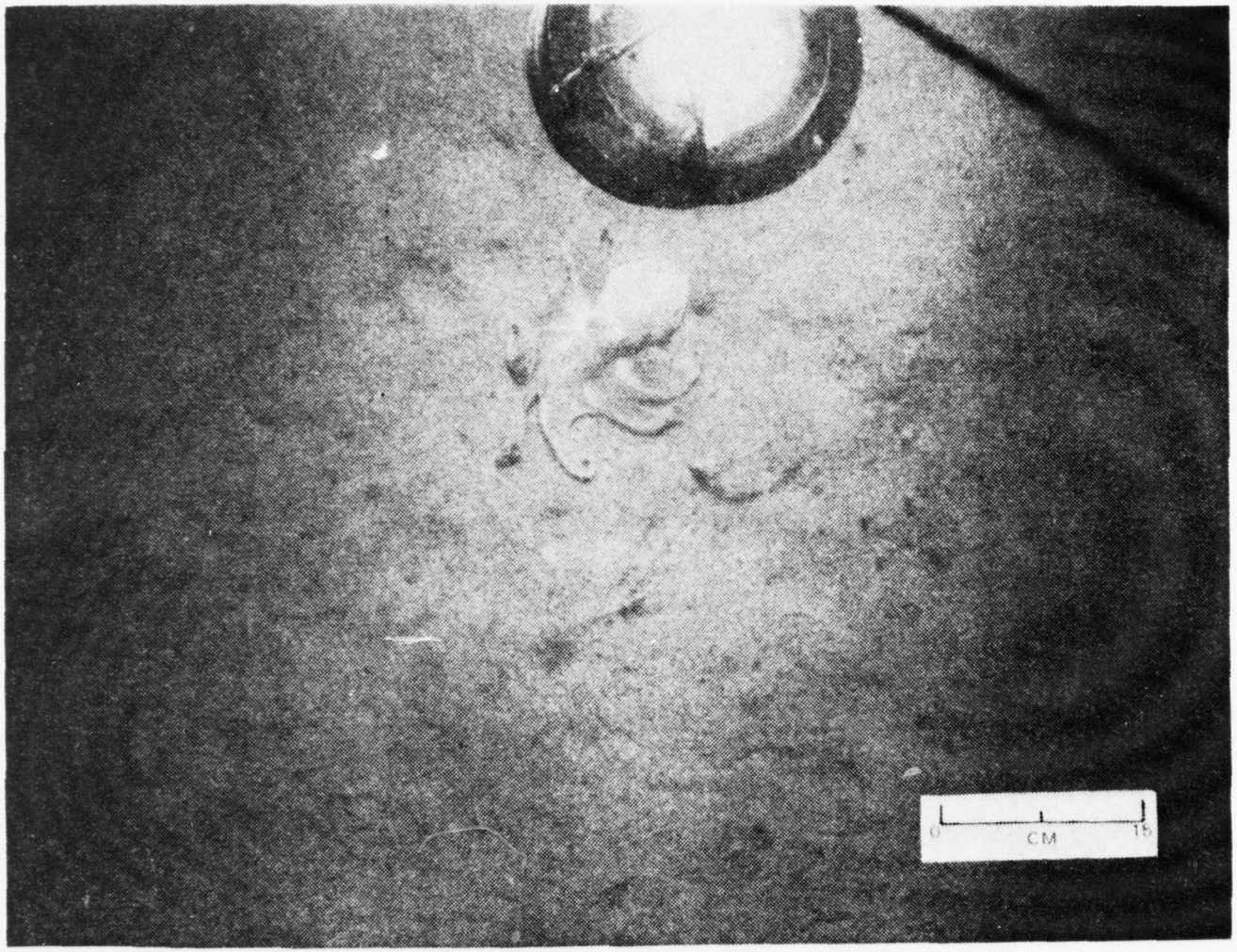


Fig. 28. Bottom Photograph Leg UV-1, 1107.8 hr, 400 m, Octopus and associated trail, sea pens, short tracks probably due to worms or holothurians

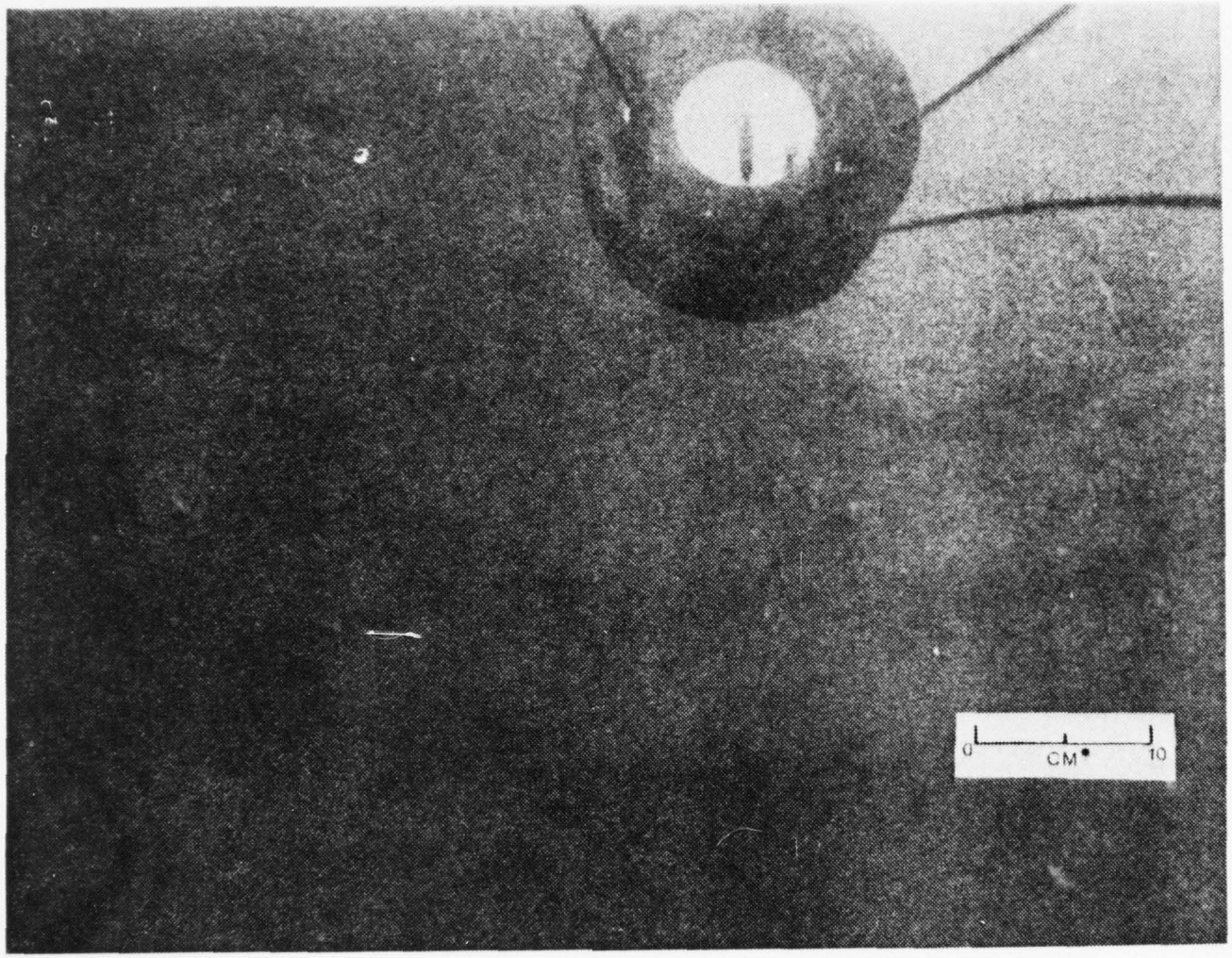


Fig. 29. Bottom Photograph Leg CD-3, 0946.4 hr, 360 m, Ripple marks, water looks slightly turbid

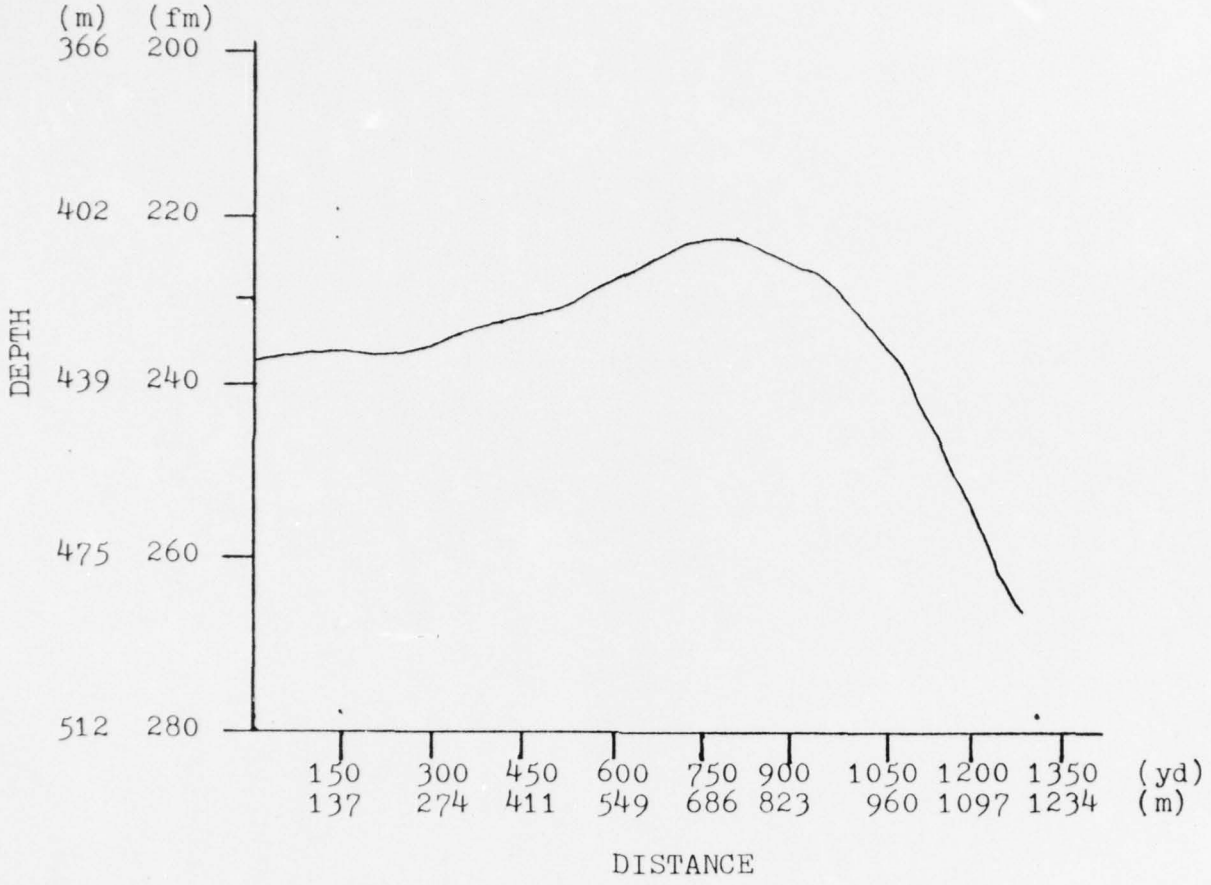


Fig. 30. Bathymetric Profile of Leg EF-2

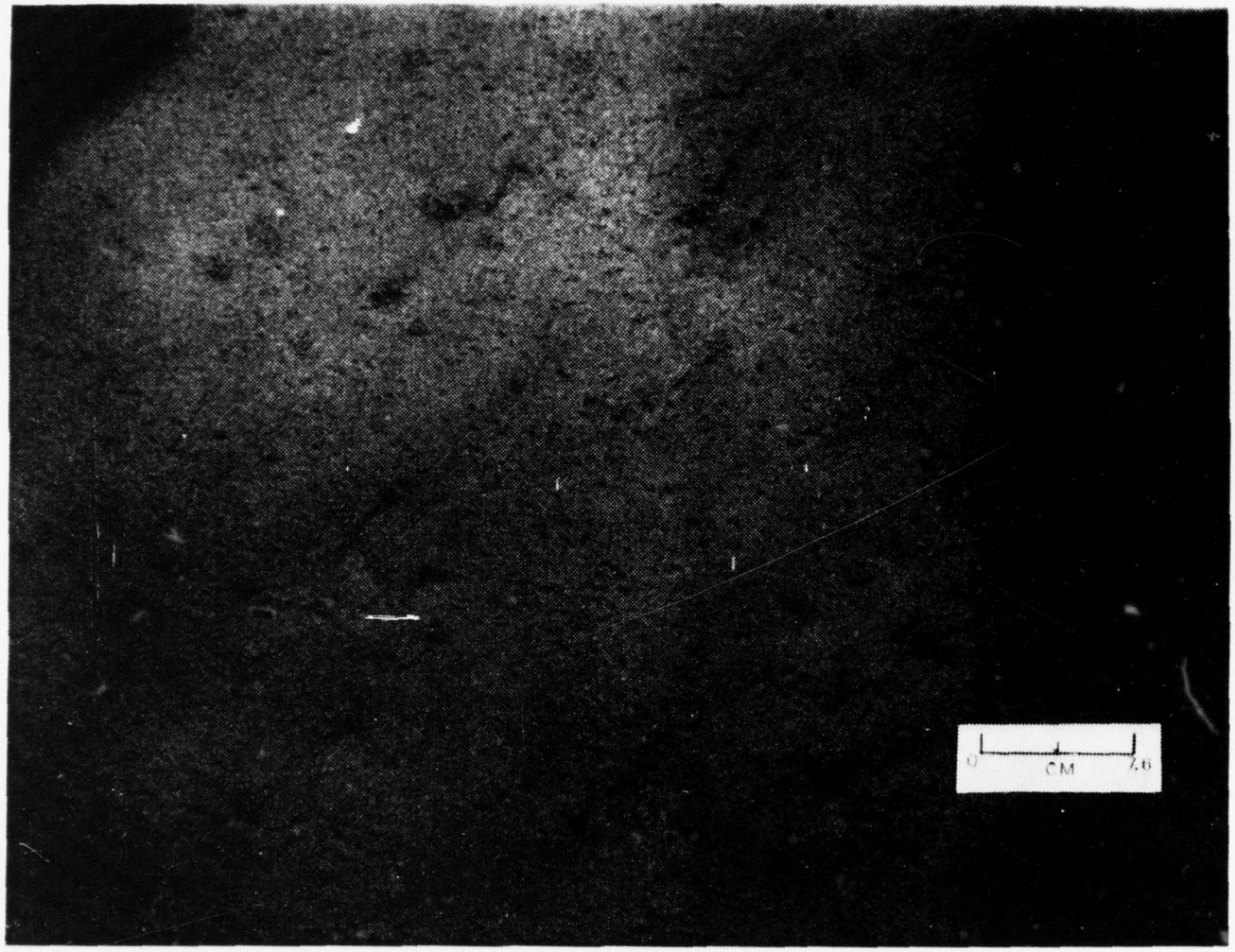


Fig. 31. Bottom Photograph Leg EF-2, 1430.4 hr, 420 m, coiled feces, tracks, small holes probably due to burrowing worms

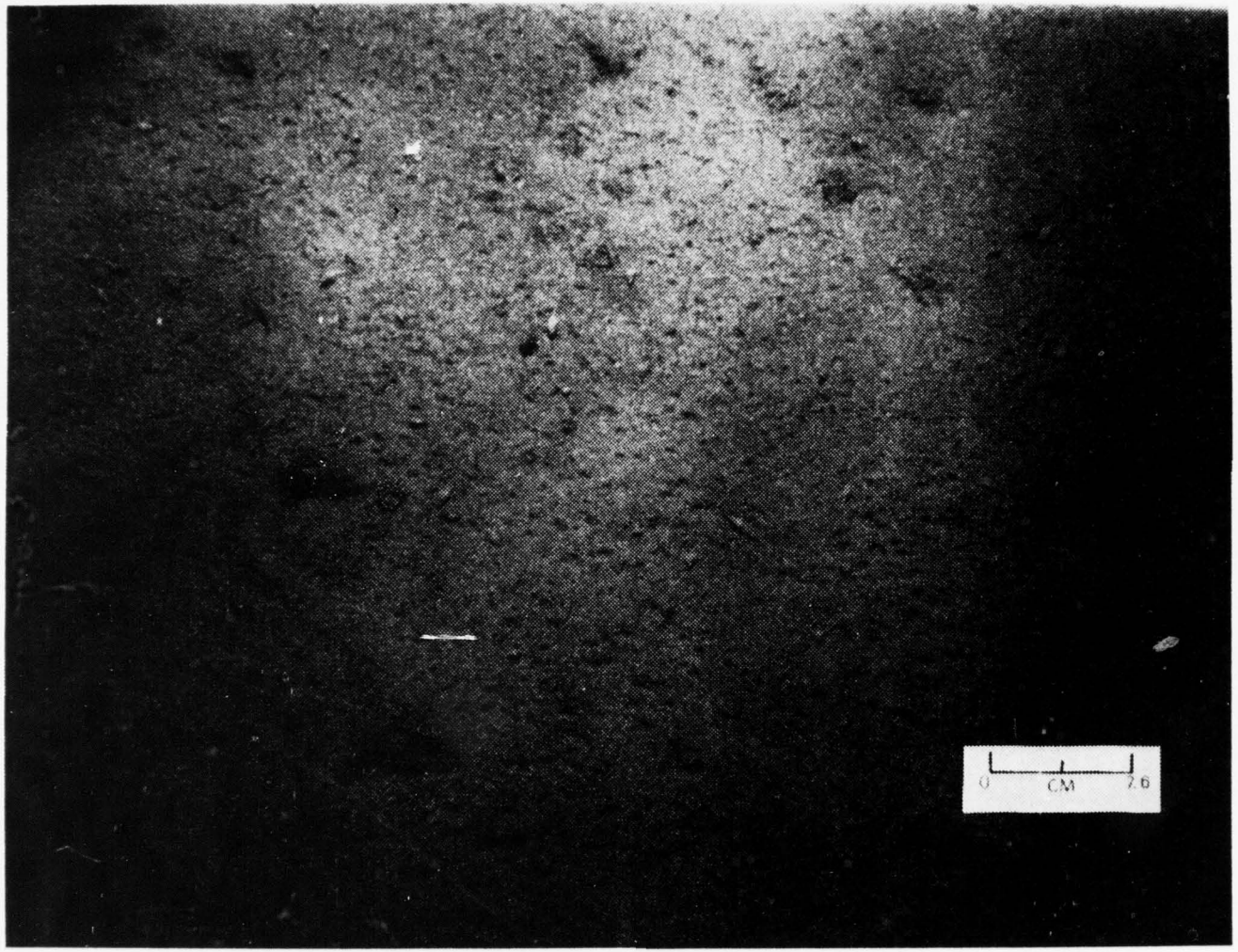


Fig. 32. Bottom Photograph Leg EF-2, 1429.8 hr, 420 m, Rimless craters, feces, gastropods and associated trails

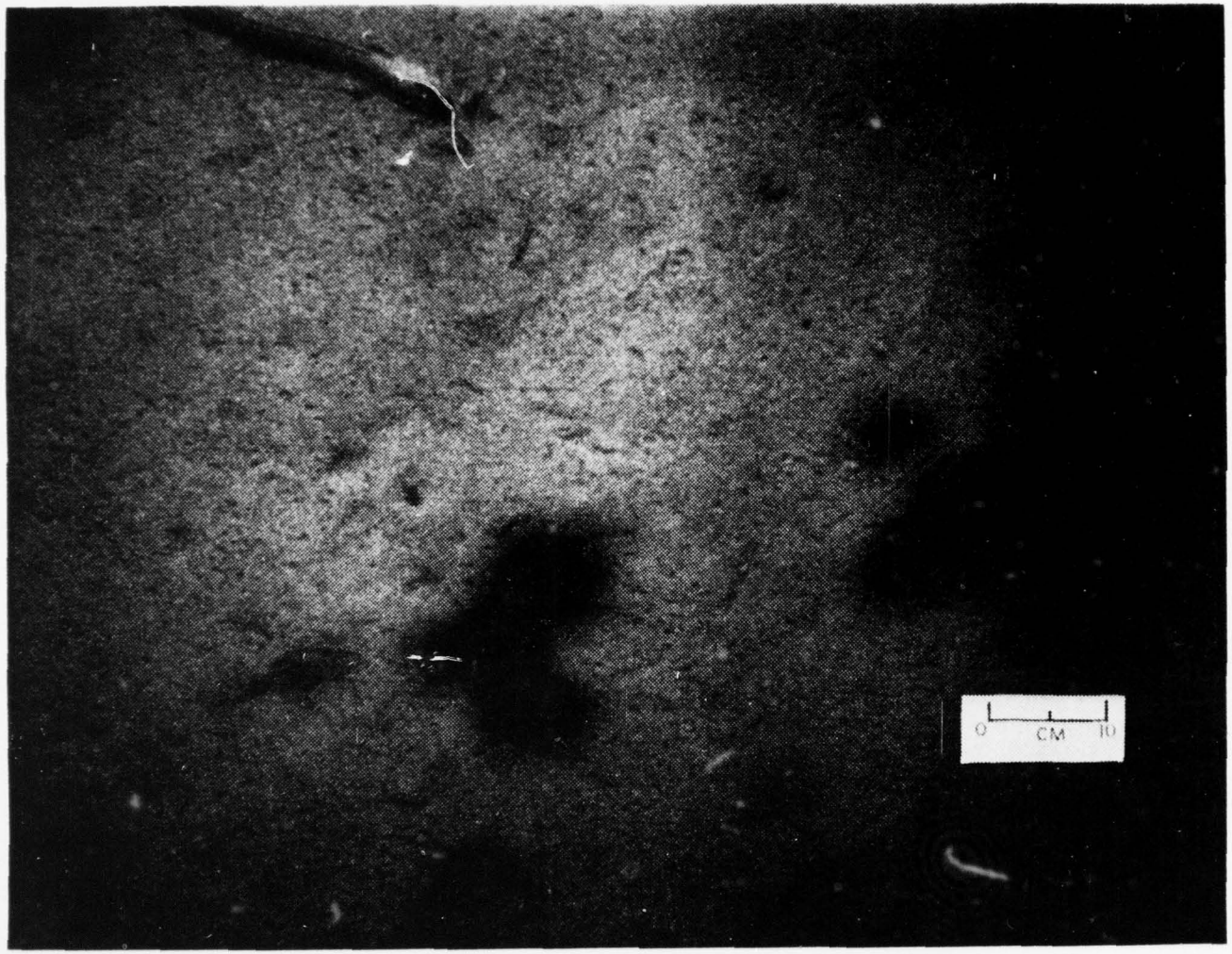


Fig. 33. Bottom Photograph Leg EF-2, 1433.9 hr, 420 m, Eel pout rooting in sediment, trails, brittle star impressions, gastropods

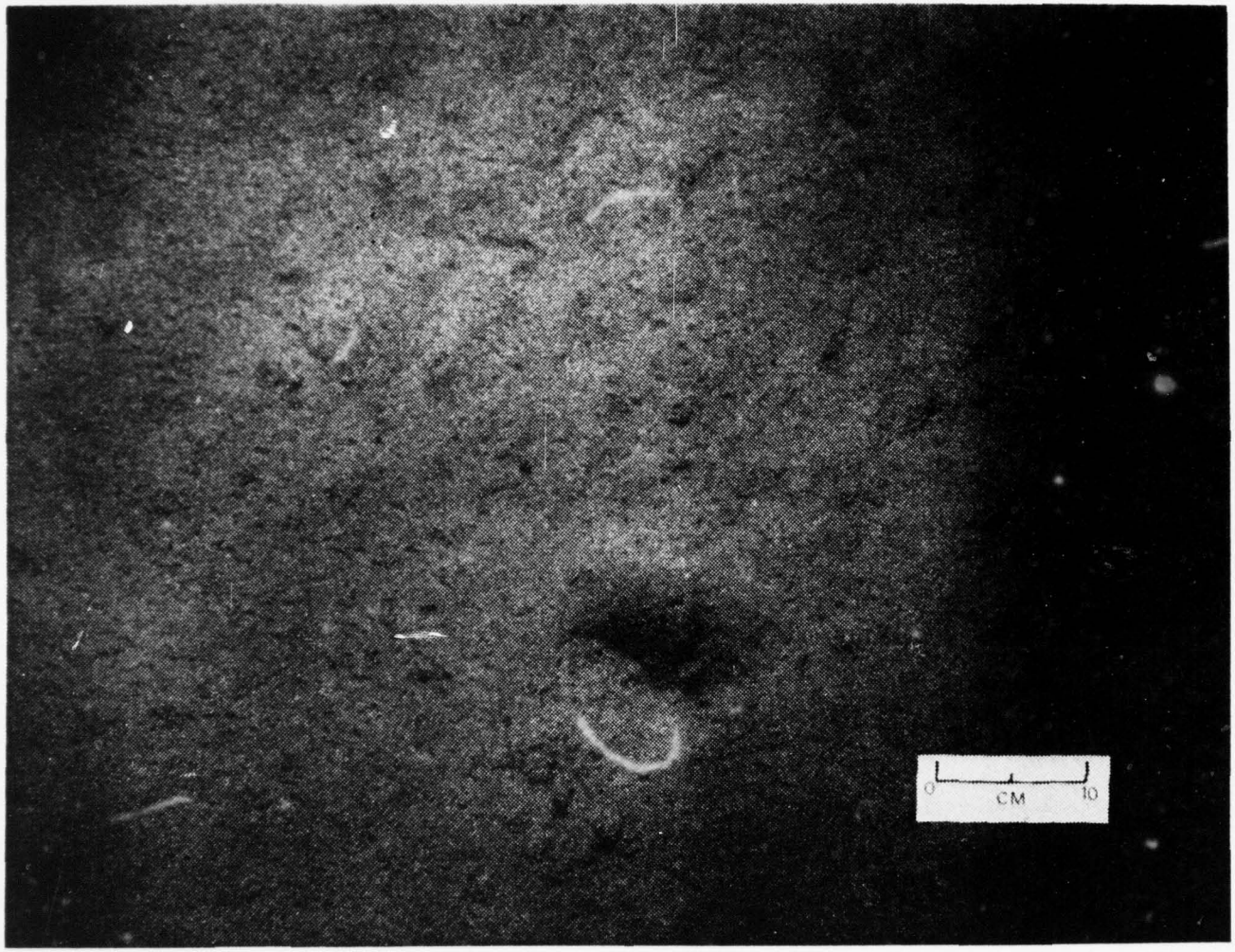


Fig. 34. Bottom Photograph Leg EF-2, 1434.5 hr, 415 m, Heart urchin may be burrowing at base of depression

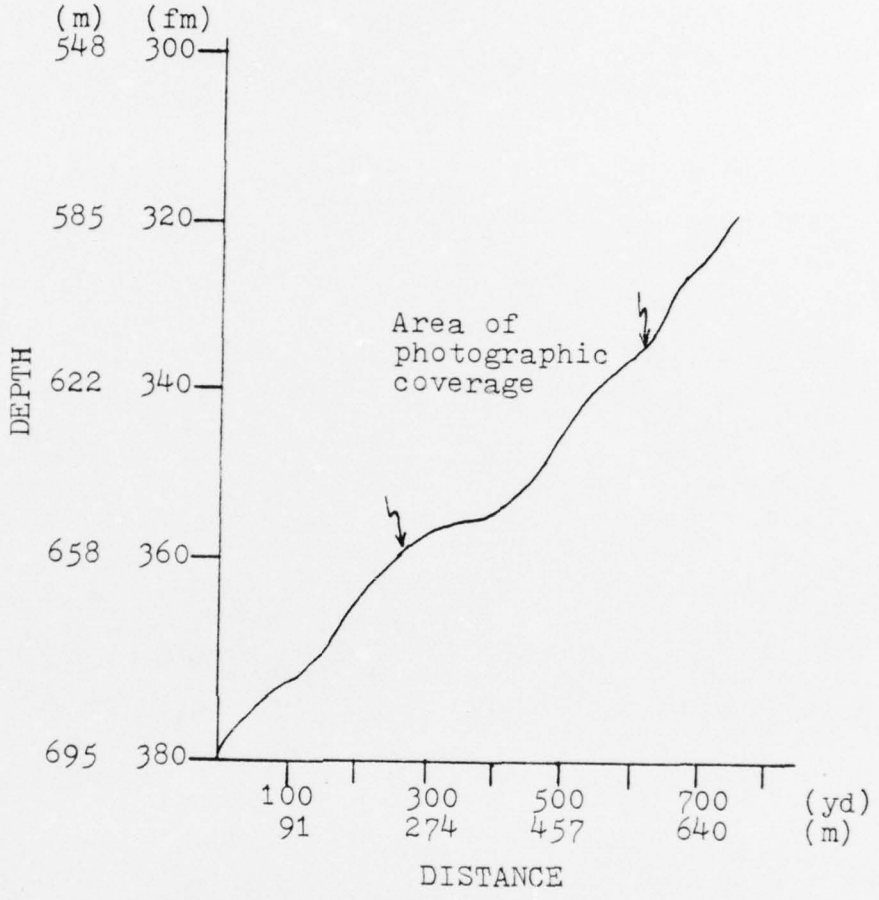


Fig. 35. Bathymetric Profile of Leg GH

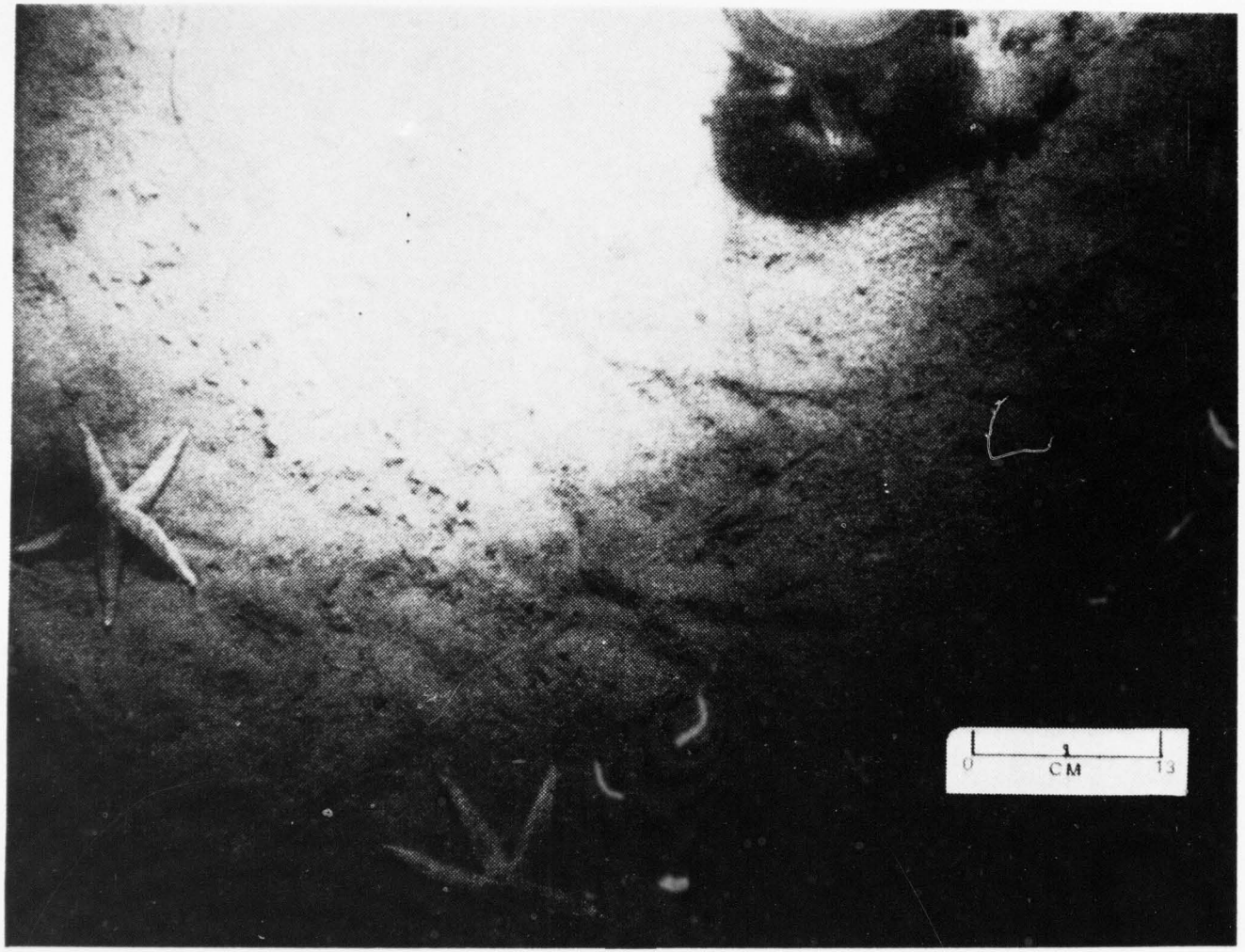


Fig. 36. Bottom Photograph Leg GH, 0922.2 hr, 624 m, Starfish, long straight furrows are due to the gastropod, two-hole tracks may be from a large holothurian

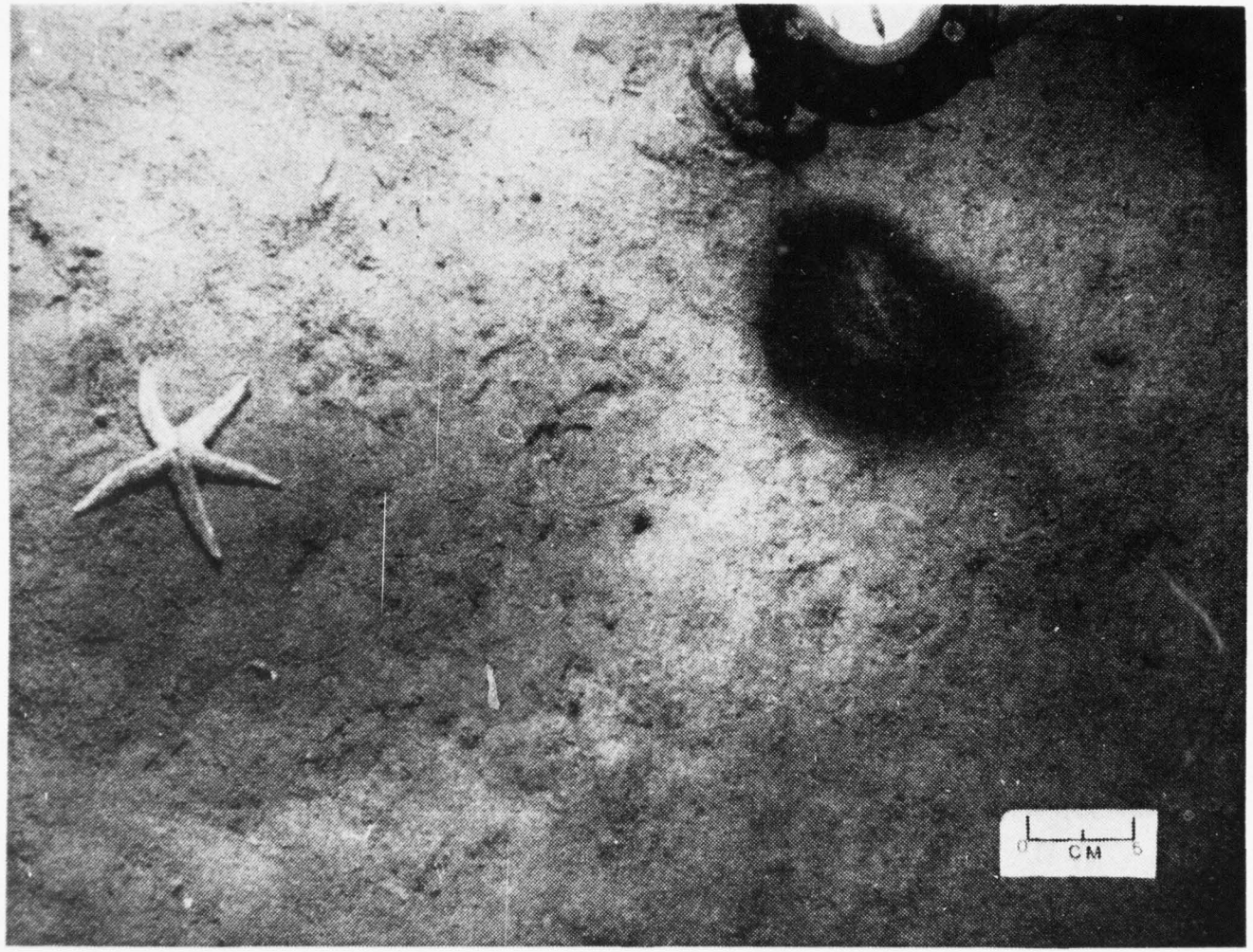


Fig. 37. Bottom Photograph Leg GH, 0931.1 hr, 650 m, Starfish and gastropods, small dense sediment cloud created by weight on compass

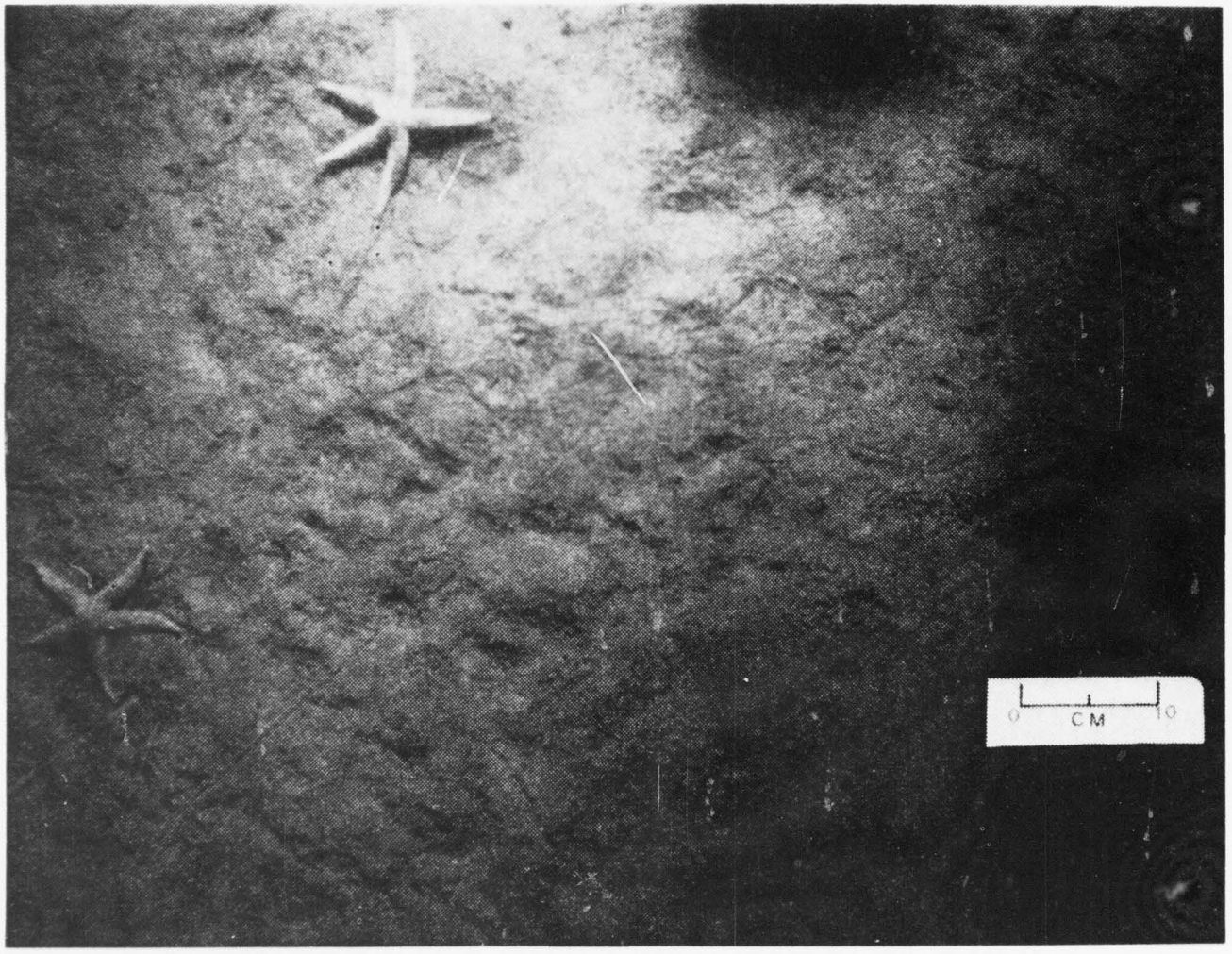


Fig. 38. Bottom Photograph Leg GH, 0921.25 hr, 622 m, Starfish, gastropods and their trails, feathery extension of a sea pen (LC)

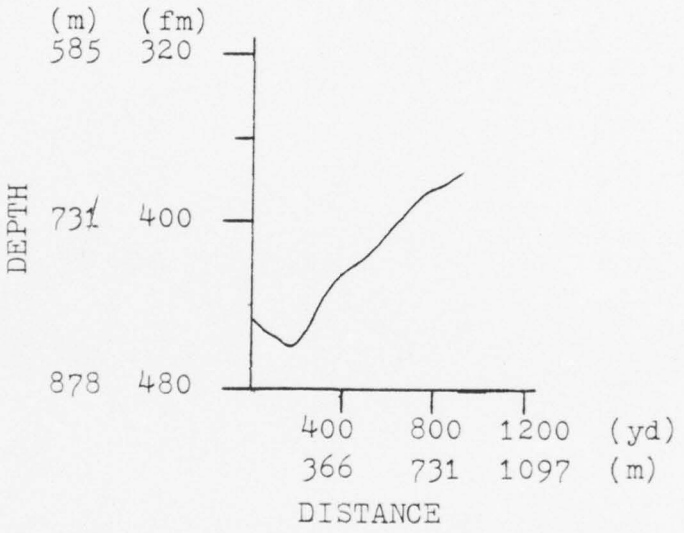


Fig. 39. Bathymetric Profile of Leg IJ

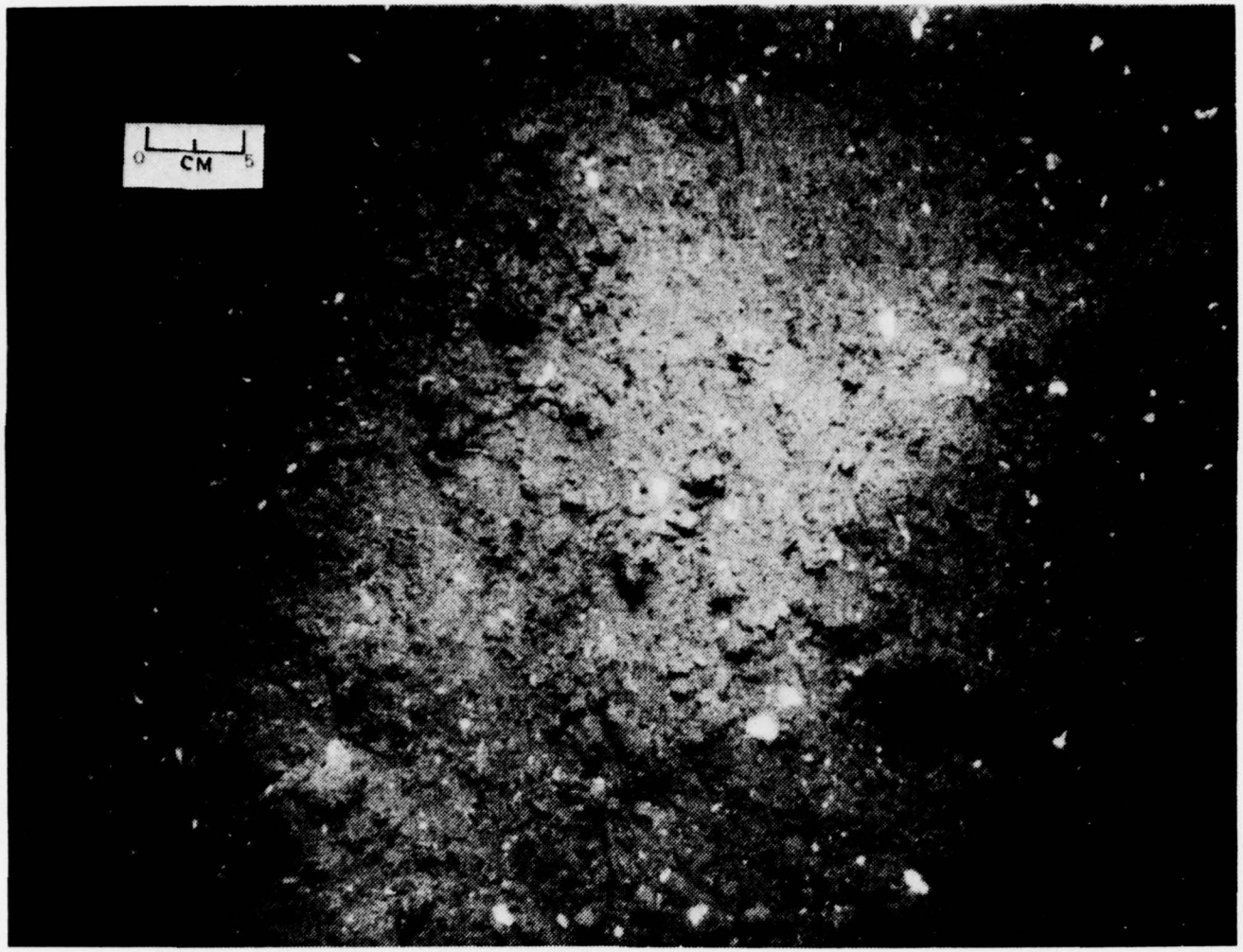


Fig. 40. Bottom Photograph Leg IJ, 1213.25 hr, 740 m, Mud clumps and many shell fragments

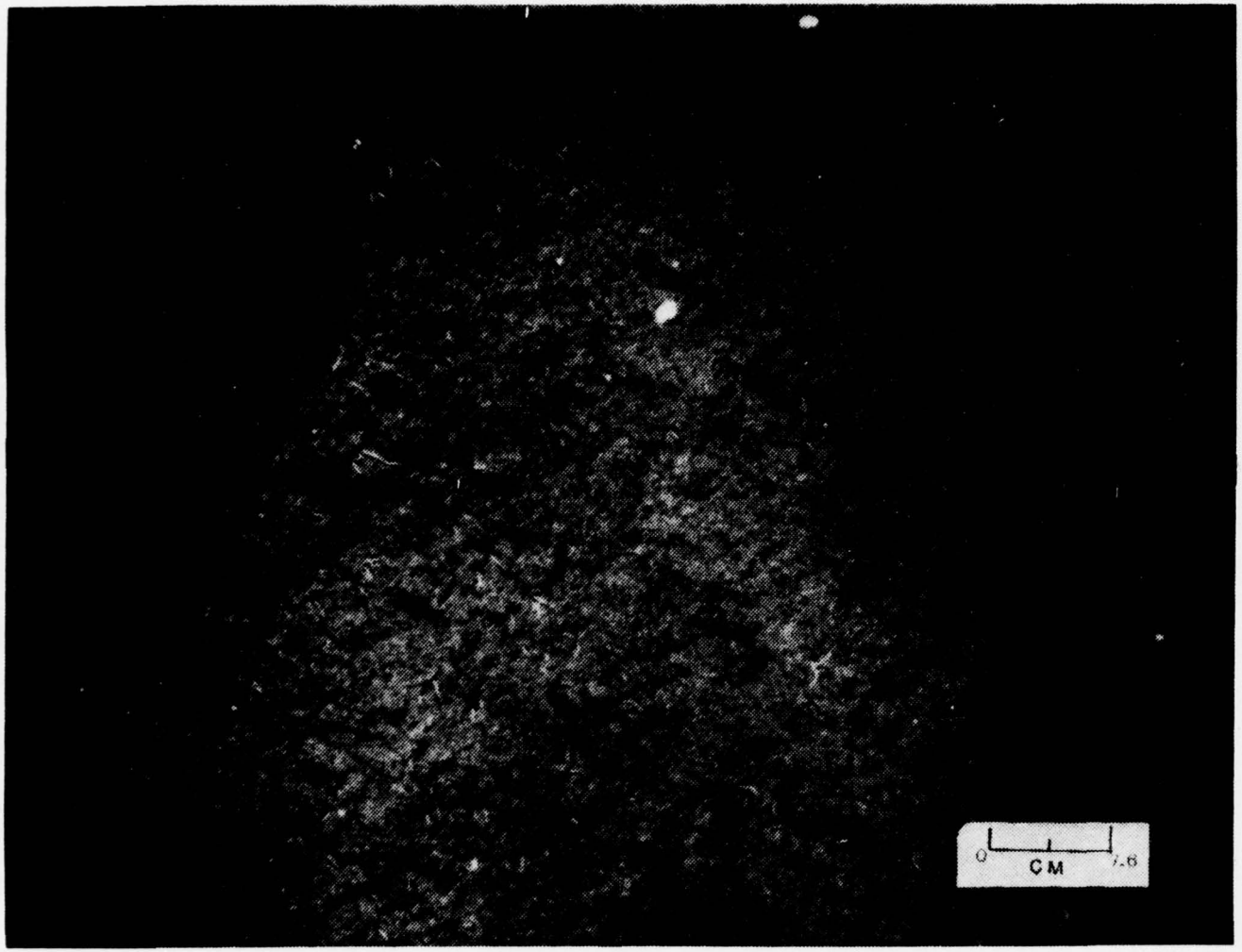


Fig. 41. Bottom Photograph Leg IJ, 1209.8 hr, 745 m, Numerous buried brittle stars and several shell fragments

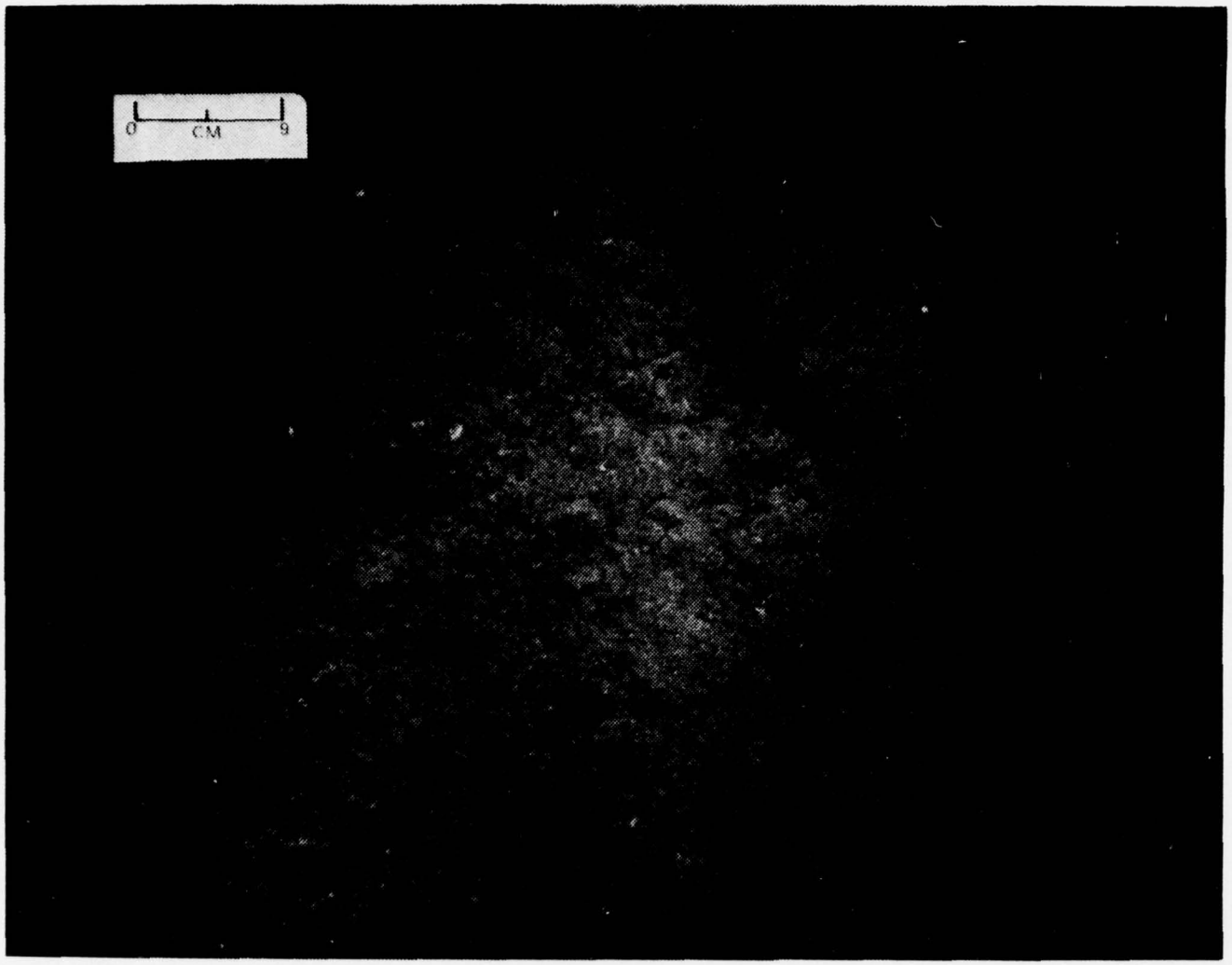


Fig. 42. Bottom Photograph Leg IJ, 1217.4 hr, 735 m, Sediment ridge probably due to an erosional process

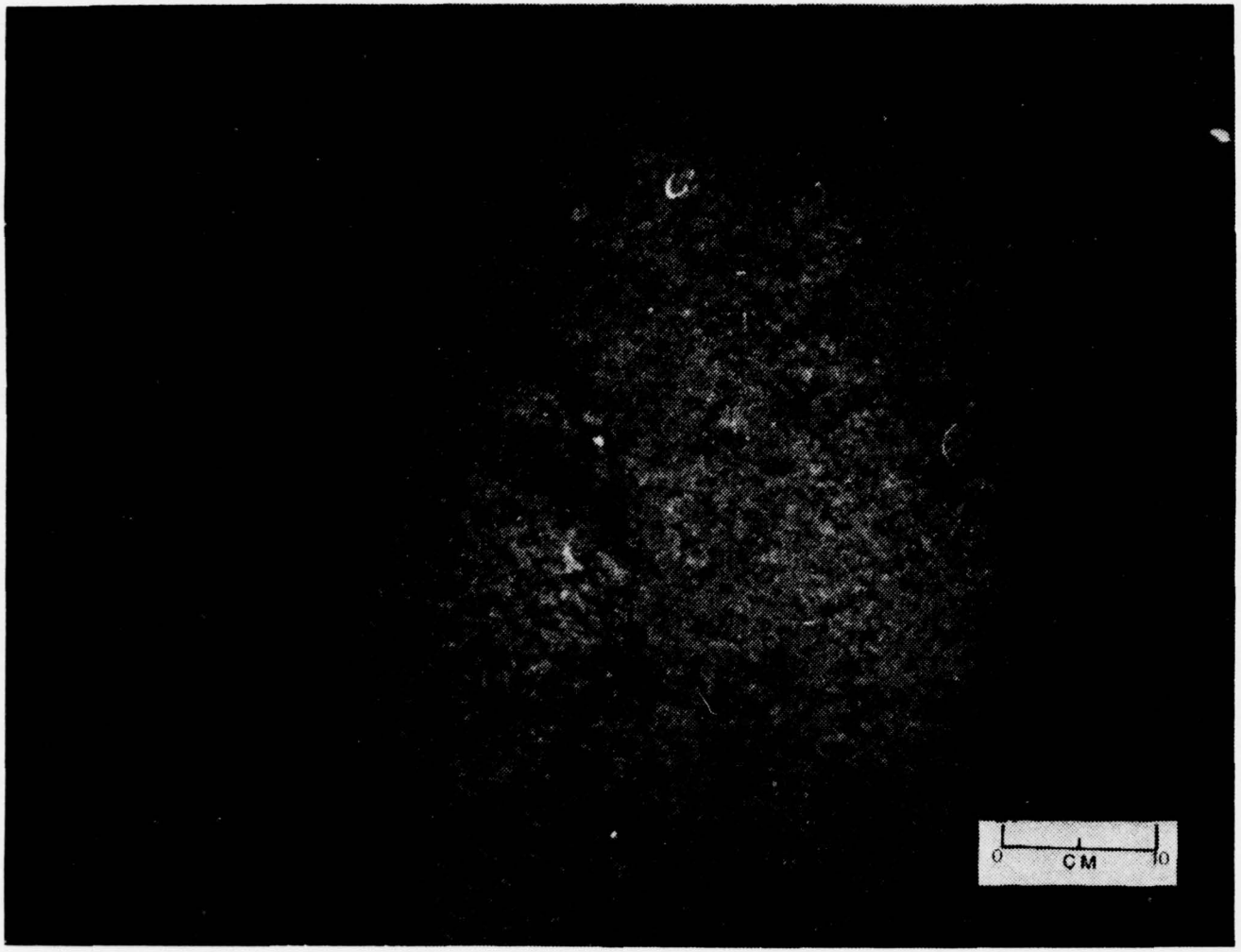


Fig. 43. Bottom Photograph Leg IJ, 1203.75 hr. 750 m, Sediment ridge and shell fragments

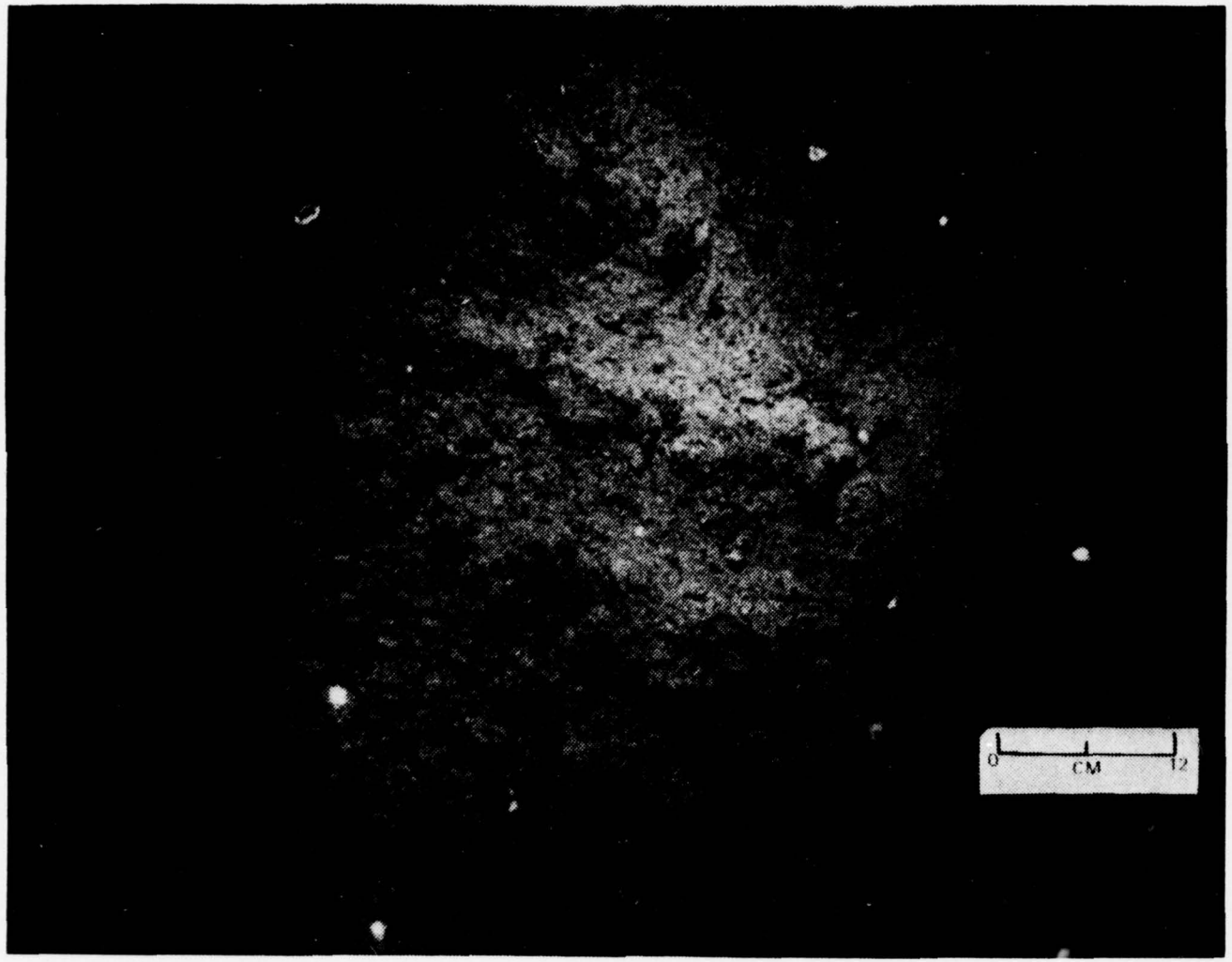


Fig. 44. Bottom Photograph Leg IJ, 1215.7 hr, 735 m, Several ridges resembling ripples, some shells

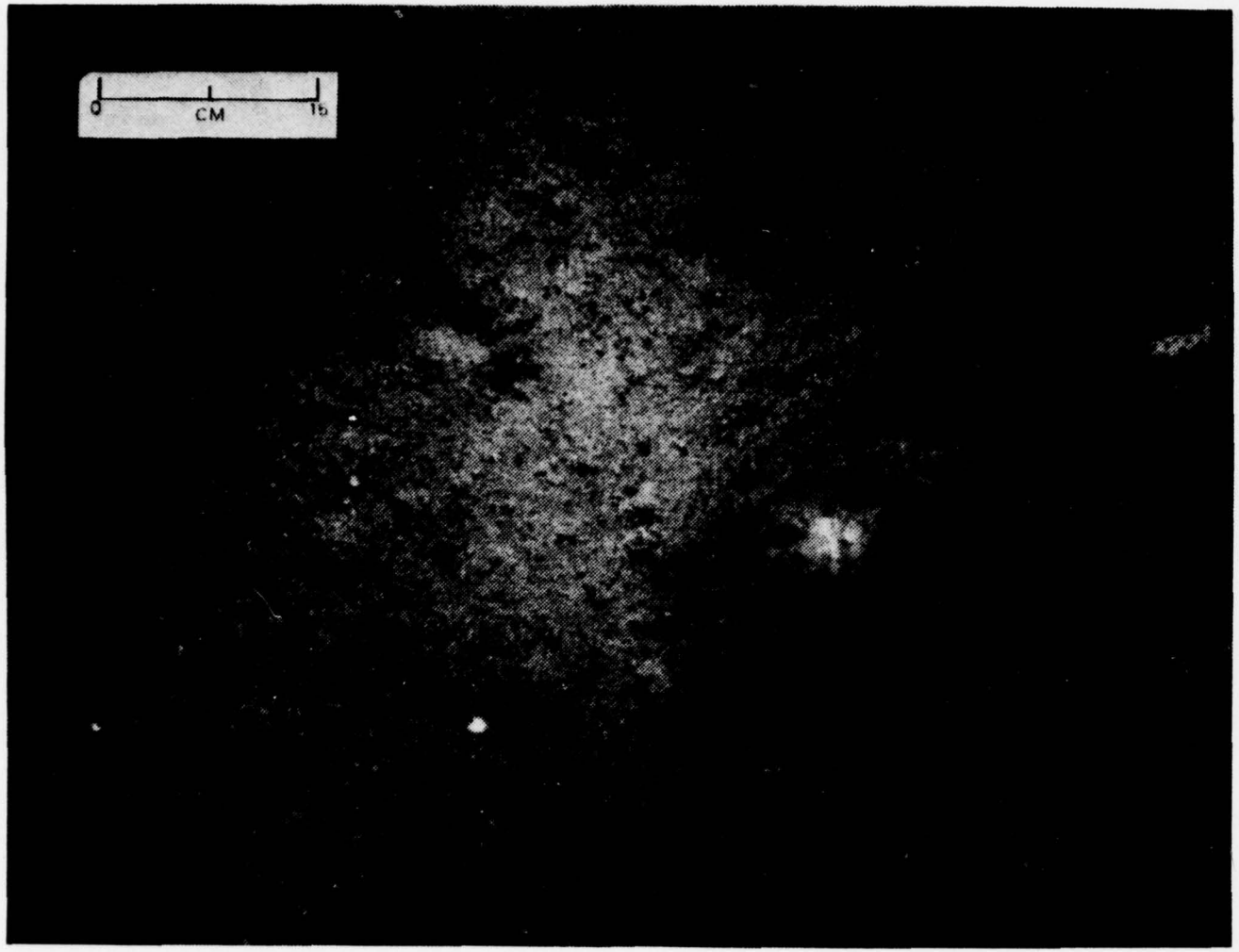


Fig. 45. Bottom Photograph Leg IJ, 1219.8 hr, 737 m, Soft coral and sea anemone attached to several rocks, lack of sediment on one side of rock may indicate sediment transport

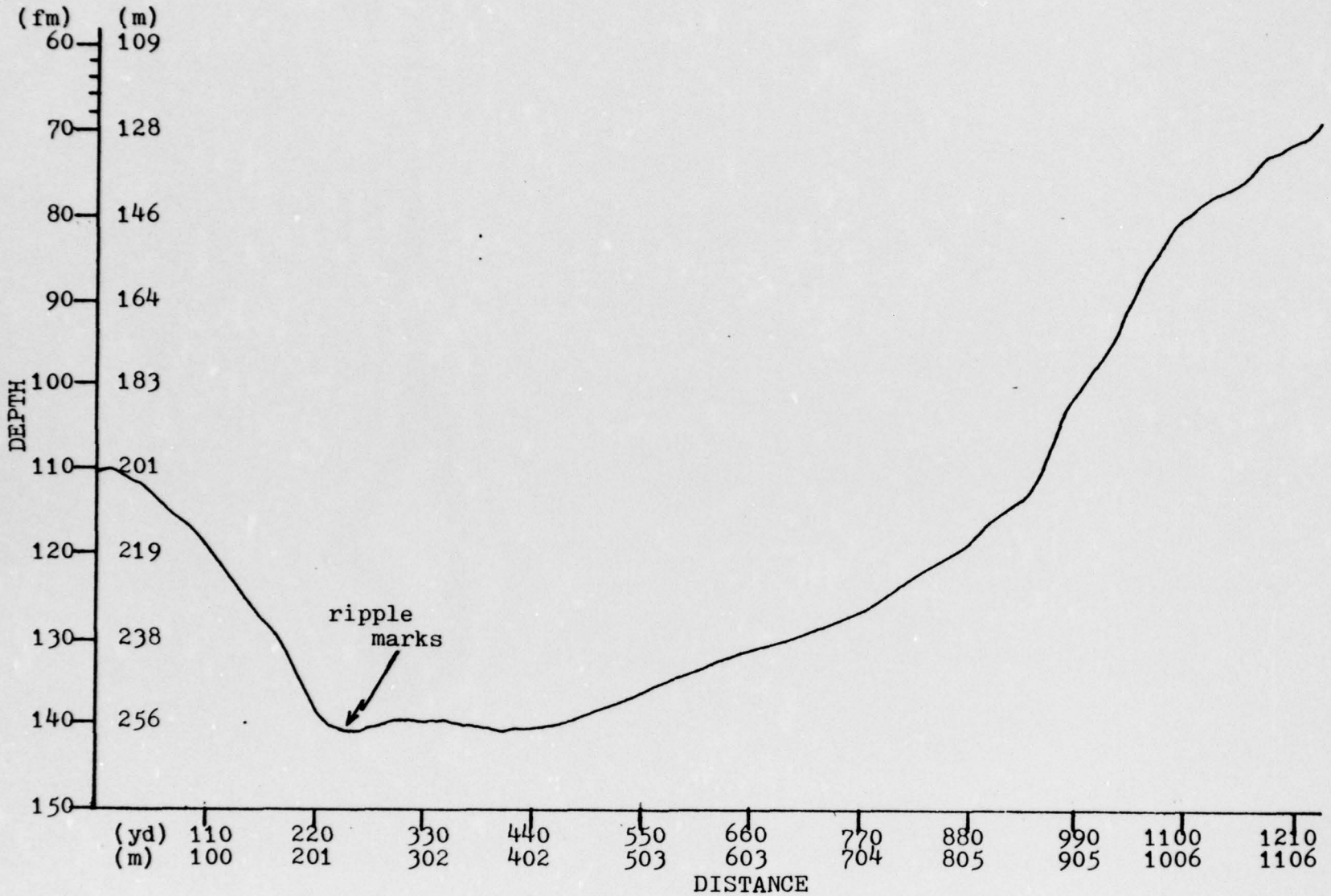


Fig. 46. Bathymetric Profile of Leg TU

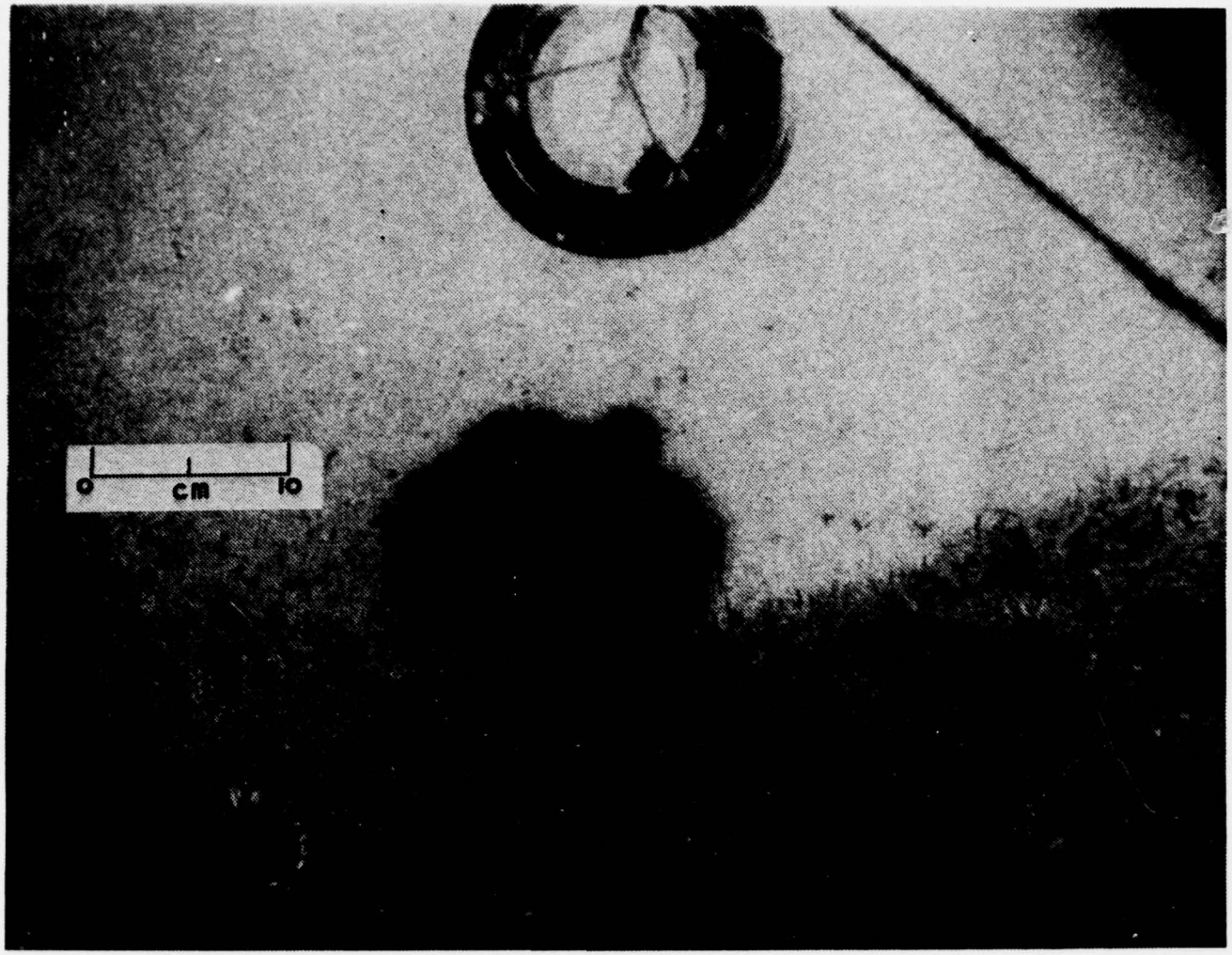


Fig. 47. Bottom Photograph Leg TU, 1403 hr, 200 m, Sediment covered and biologically encrusted rocks bordering sediment, crabs (Galatheid)

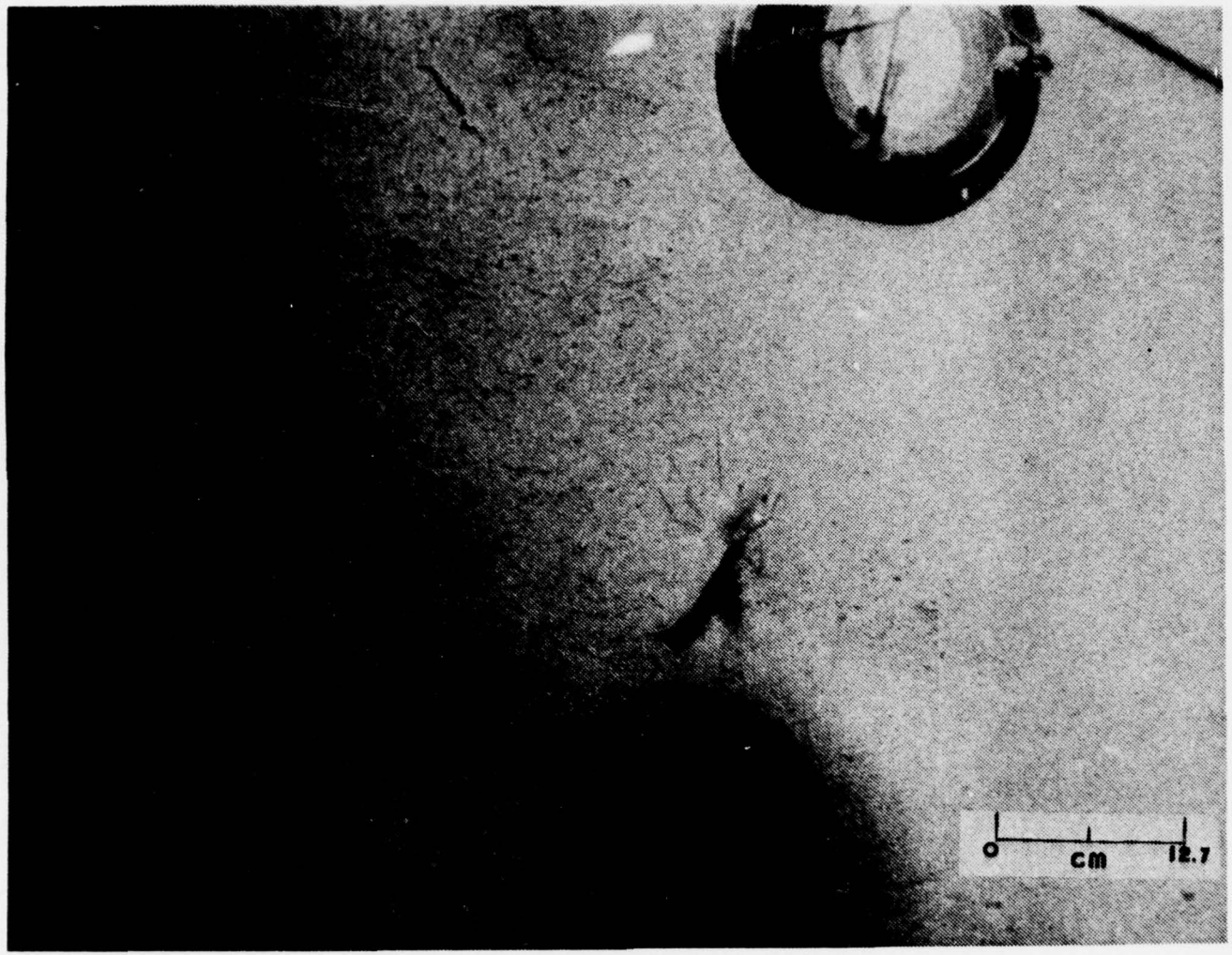


Fig. 48. Bottom Photograph Leg TU, 1341.9 hr, 70 m, Shrimp, sea pens, trails

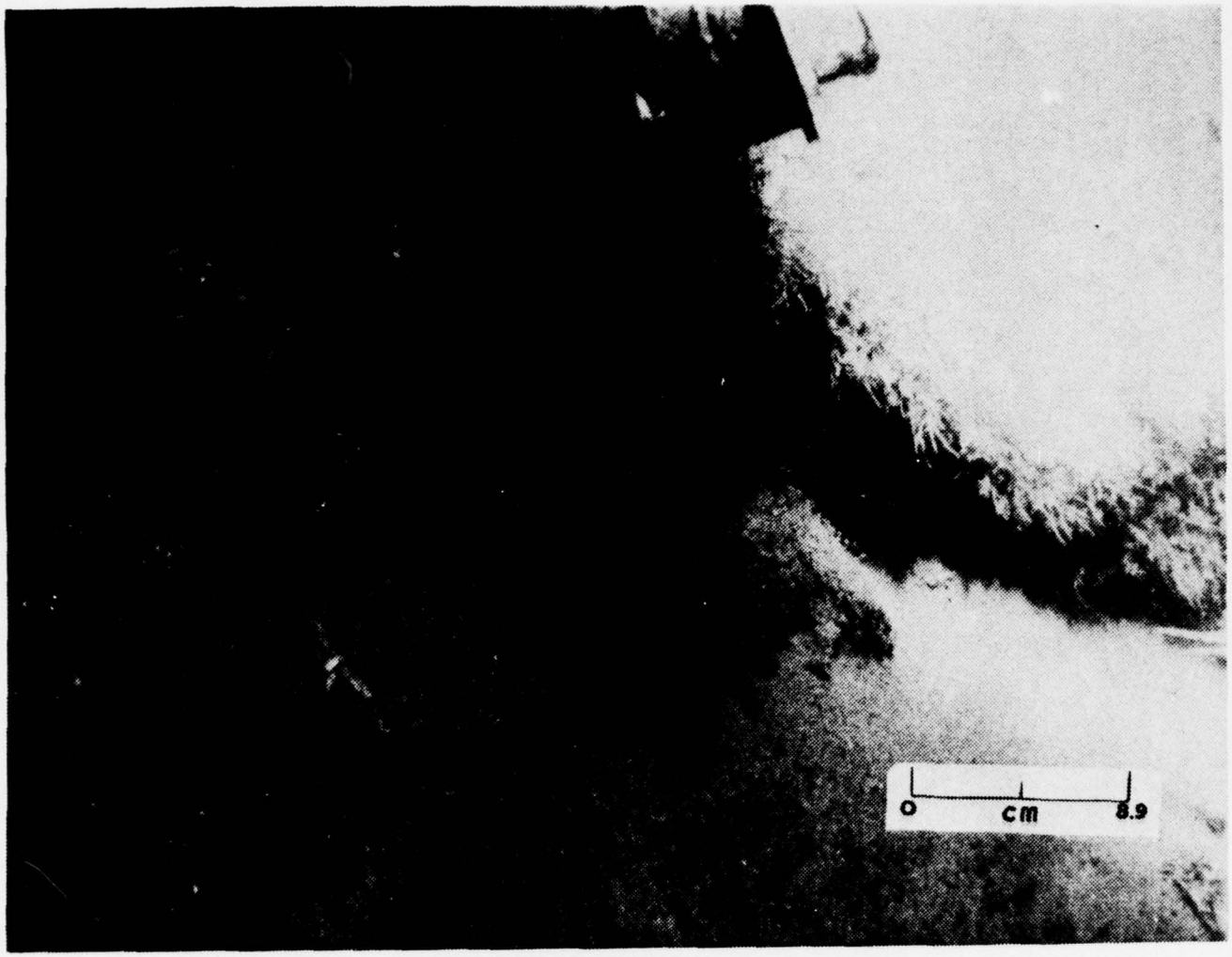


Fig. 49. Bottom Photograph Leg TU, 1350.8 hr, 240 m, Crab hiding under biologically covered rocks, starfish partially buried, sandy bottom (LR)



Fig. 50. Bottom Photograph Leg TU, 1401.7 hr, 219 m, Biologically encrusted rocks with some sediment cover, crab hiding under rock ledge

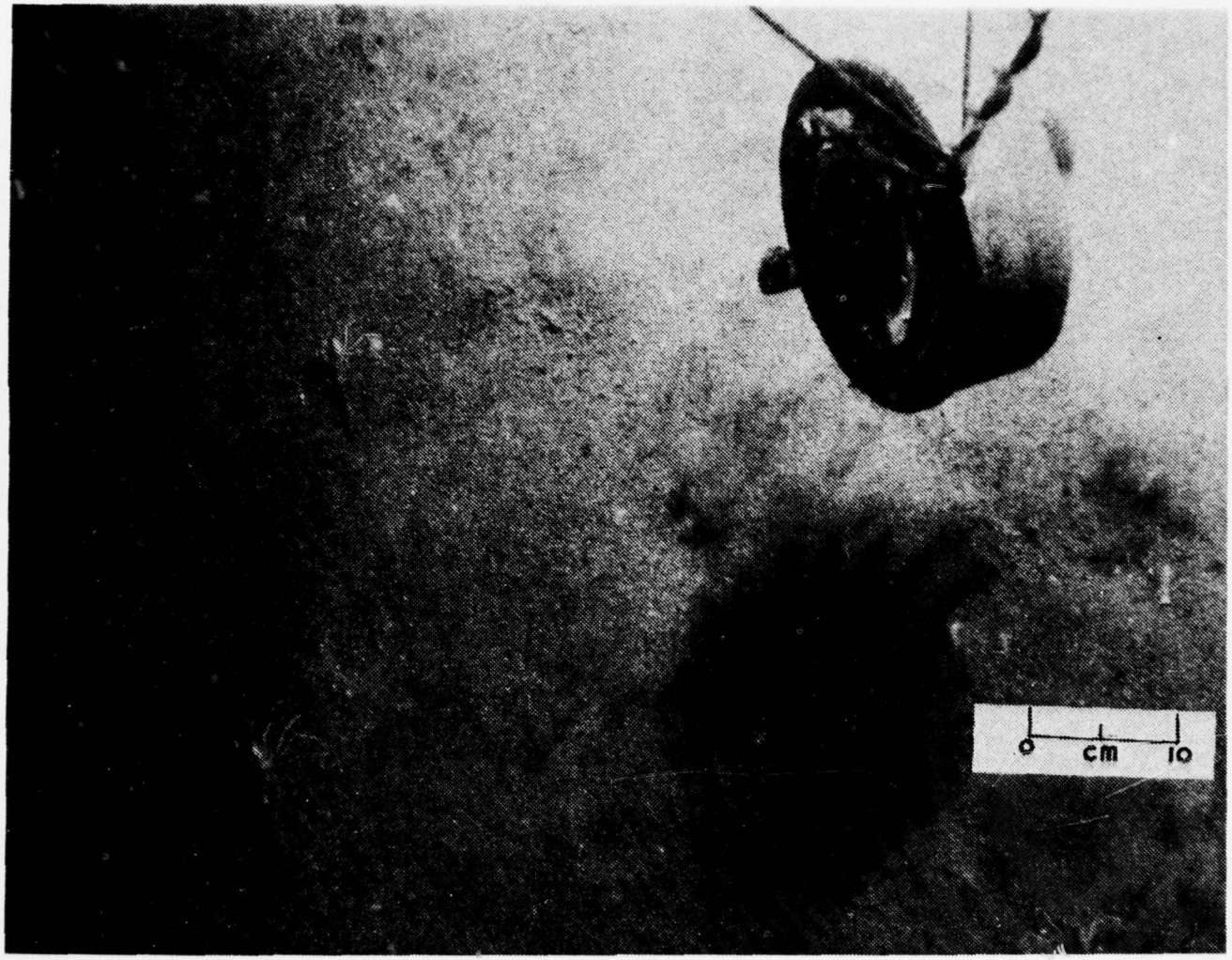


Fig. 51. Bottom Photograph Leg TU, 1400.9 hr, 221 m, Group of shrimp walking across sandy bottom

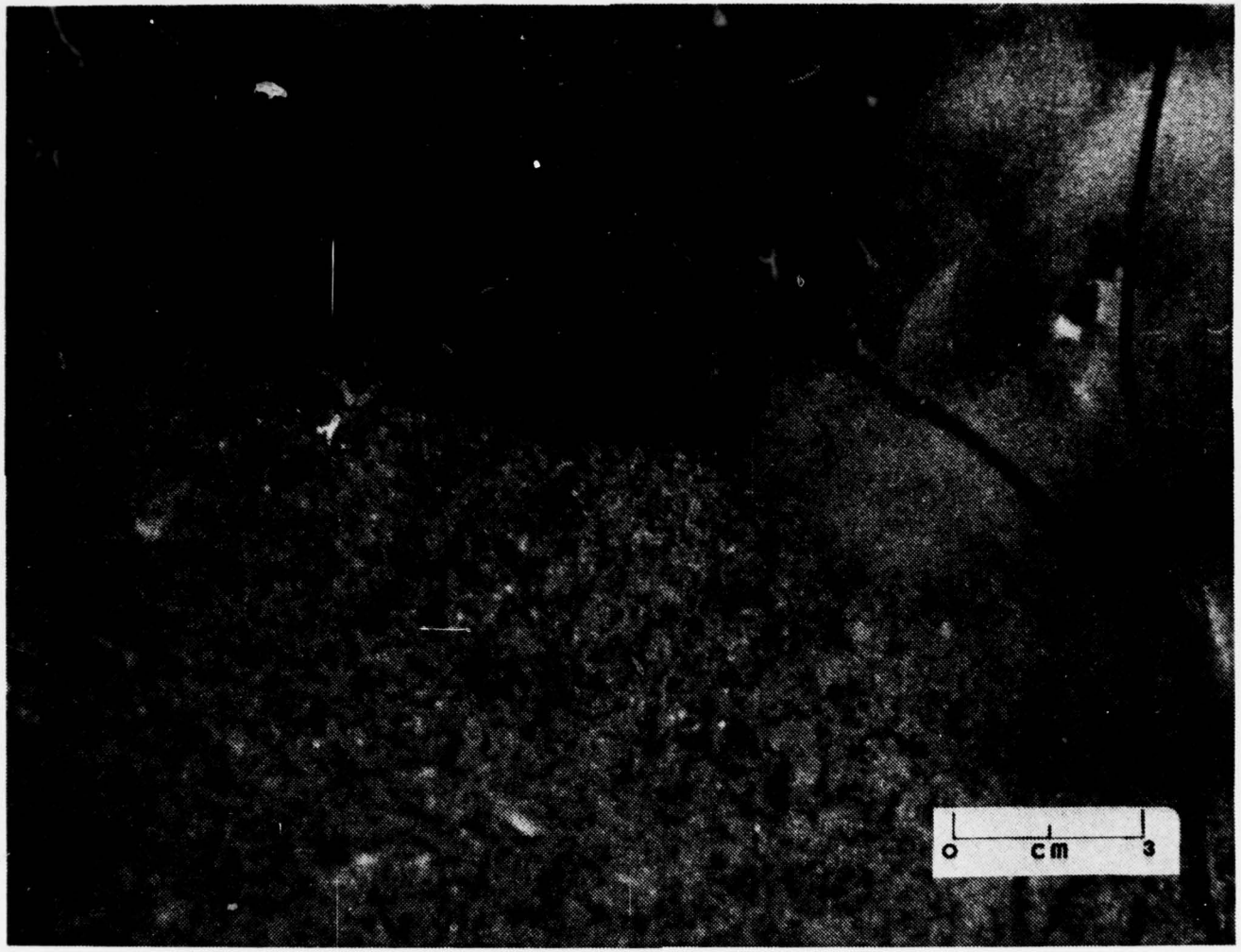


Fig. 52. Bottom Photograph Leg TU, 1326.3 hr, 217 m, Compass hitting biologically and sediment covered rock with unidentified organism (UL)

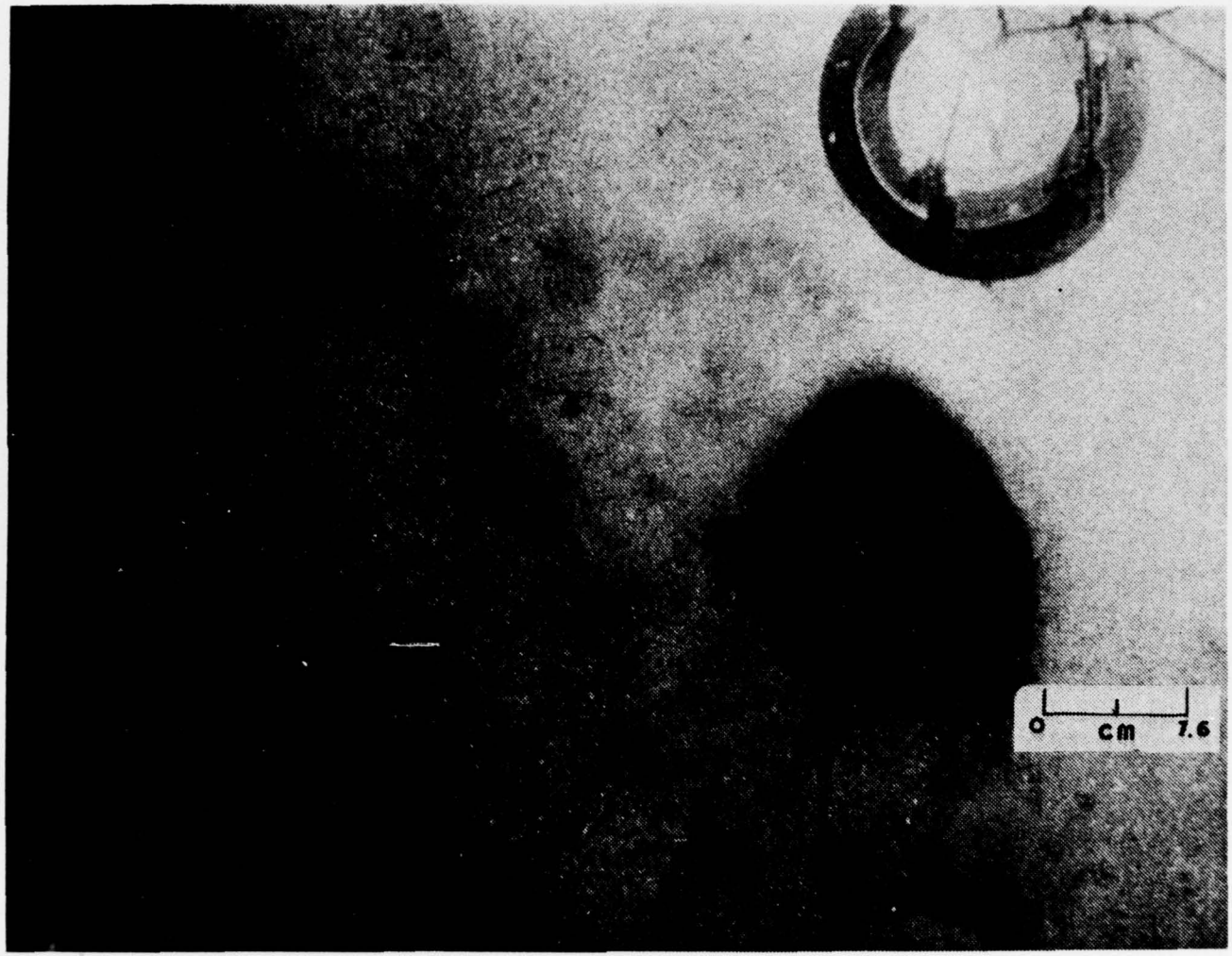


Fig. 53. Bottom Photograph Leg TU, 1329.8 hr, 256 m, Ripple marks in sandy sediment

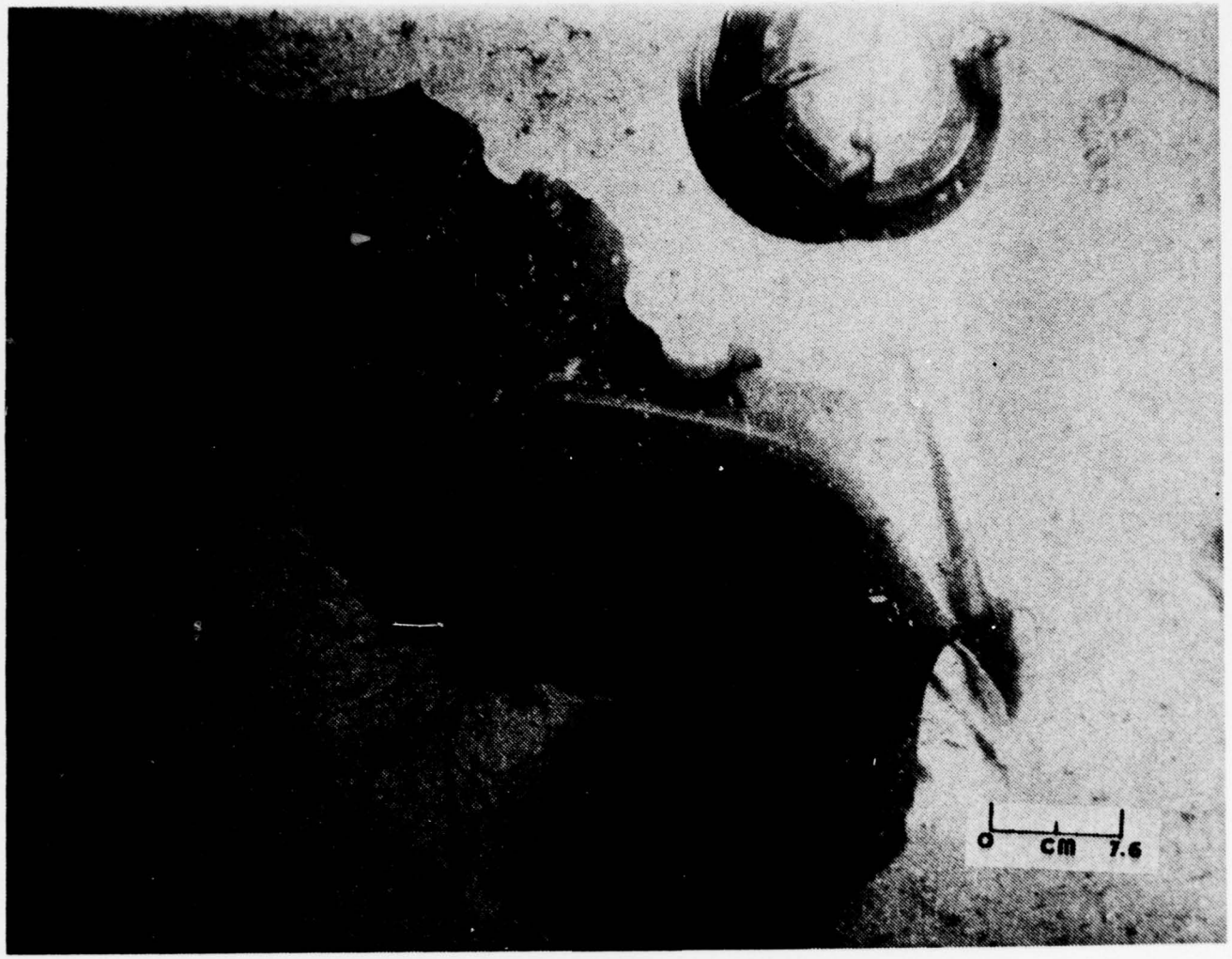


Fig. 54. Bottom Photograph Leg TU, 1338 hr, 254 m, Large kelp leaf (Alaria) and other surface debris, trail marks

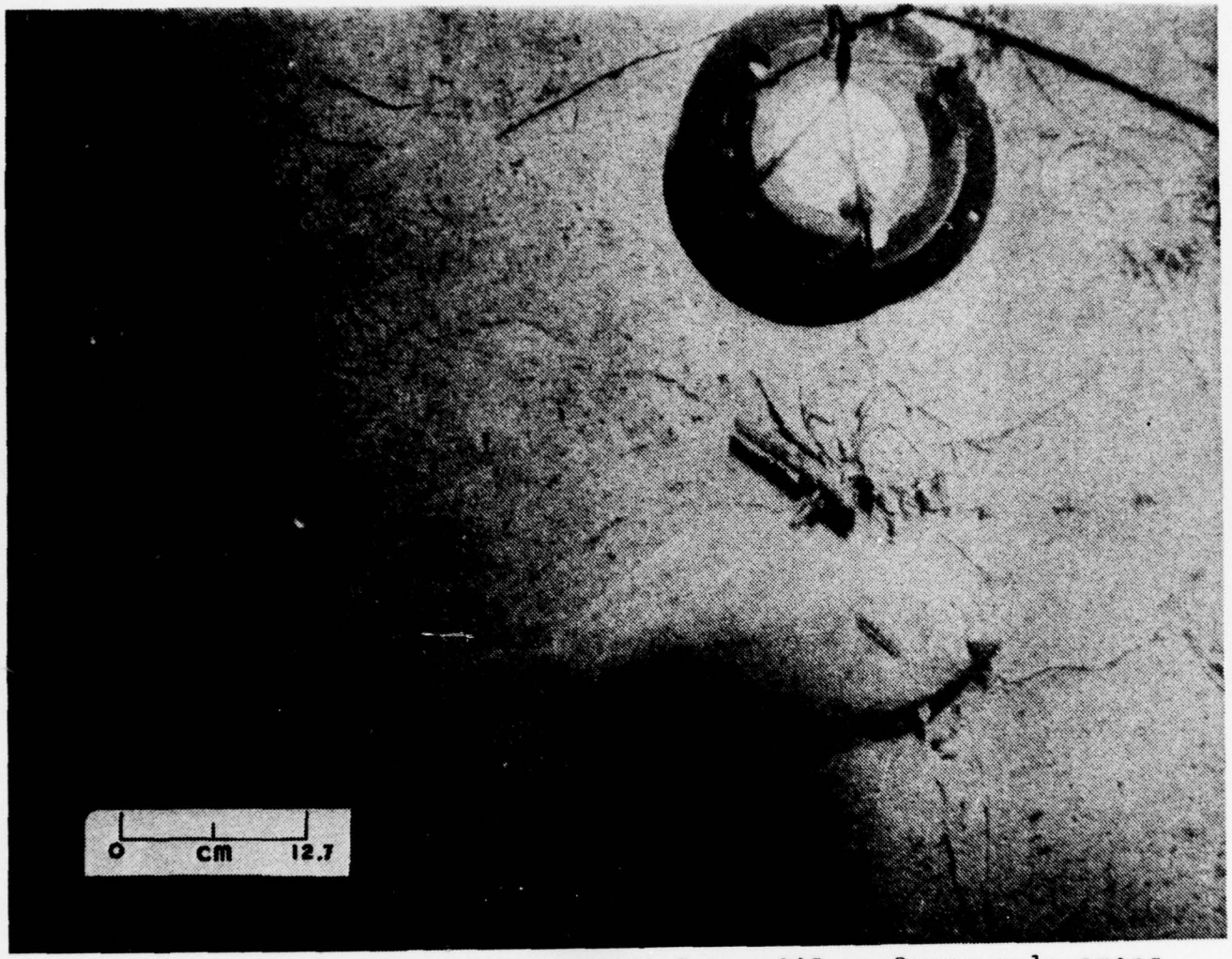


Fig. 55. Bottom Photograph Leg TU, 1344.7 hr, 245 m, Dover sole among surface debris and some shell fragments, short furrowed trails

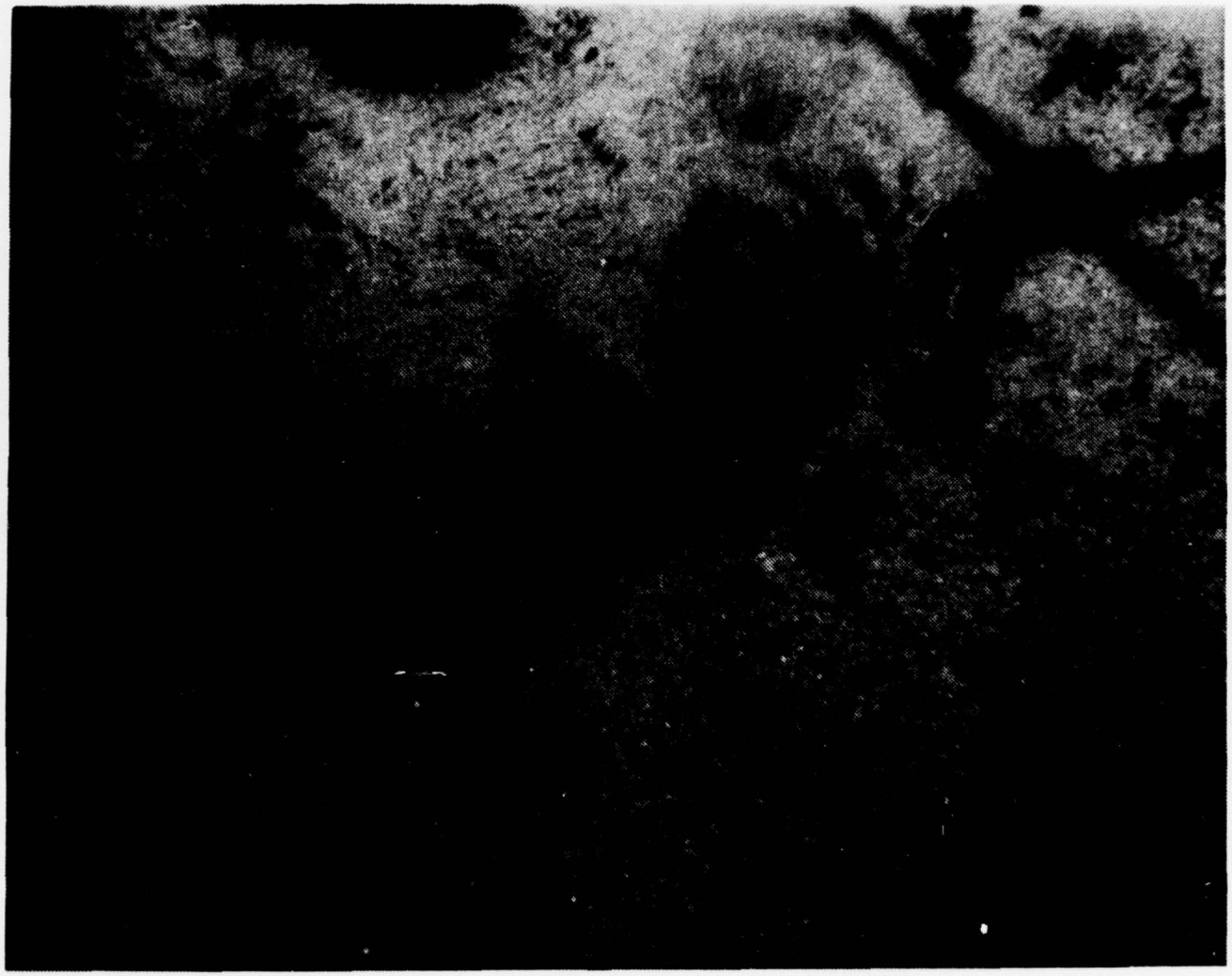


Fig. 56. Bottom Photograph Leg TU, 1358.5 hr, 230 m, Compass striking bottom creating thin large sediment cloud

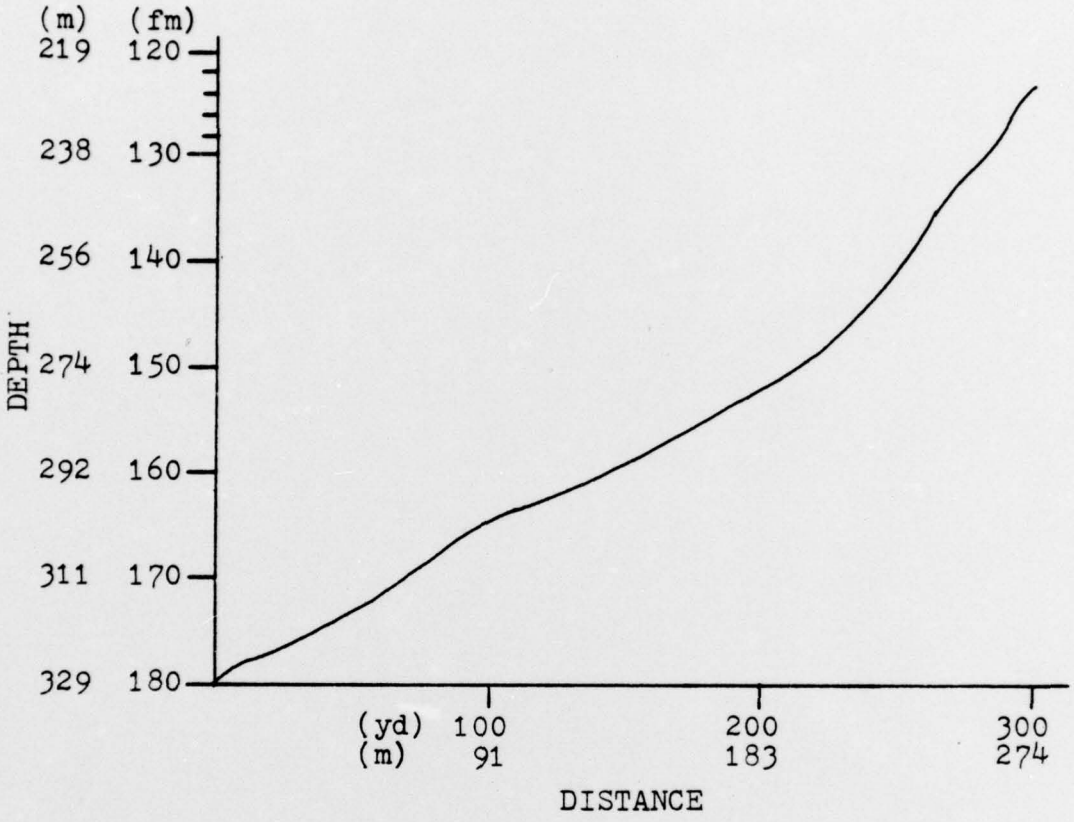


Fig. 57. Bathymetric Profile of Leg ST-1

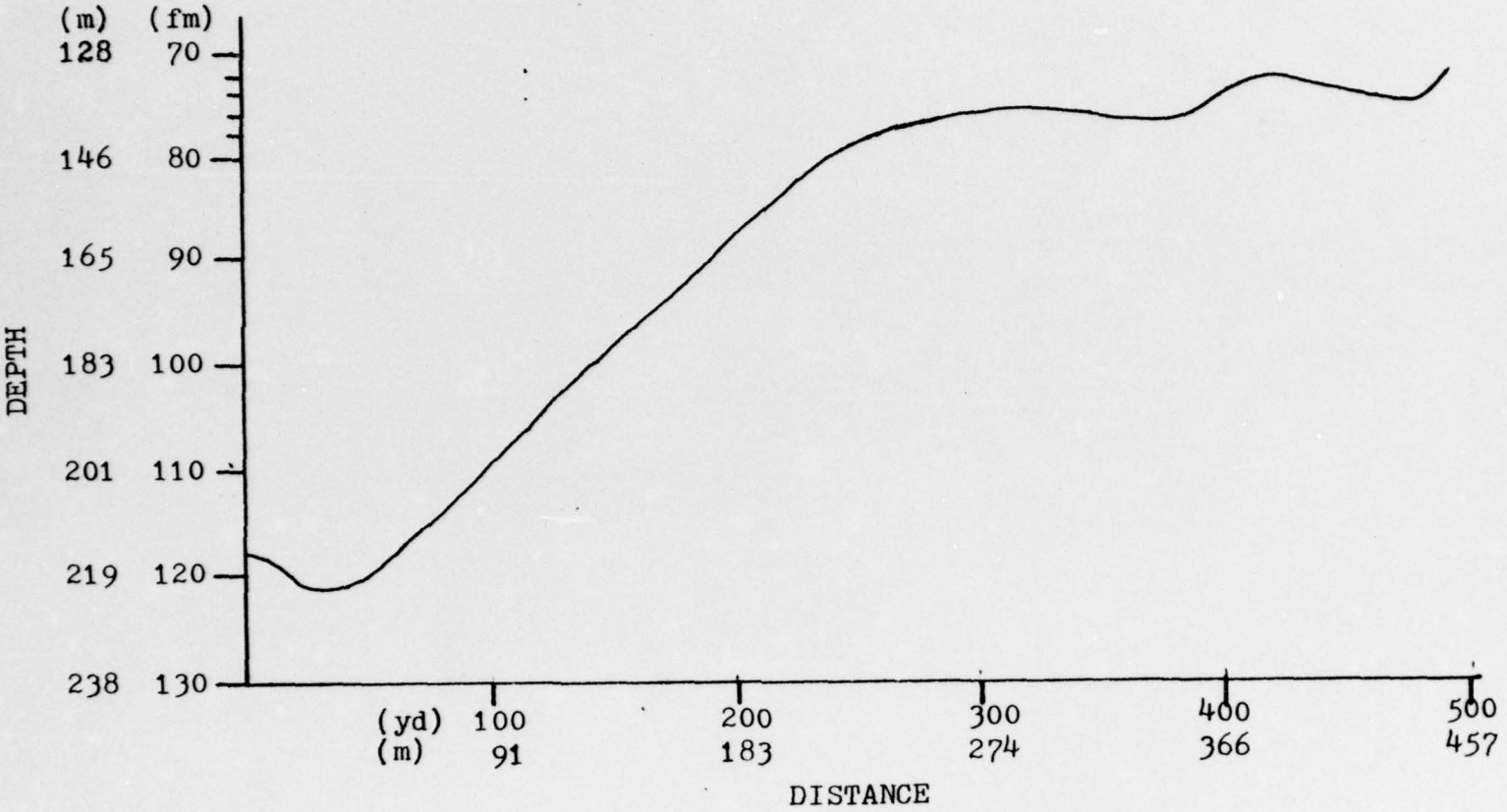


Fig. 58. Bathymetric Profile of Leg ST-2

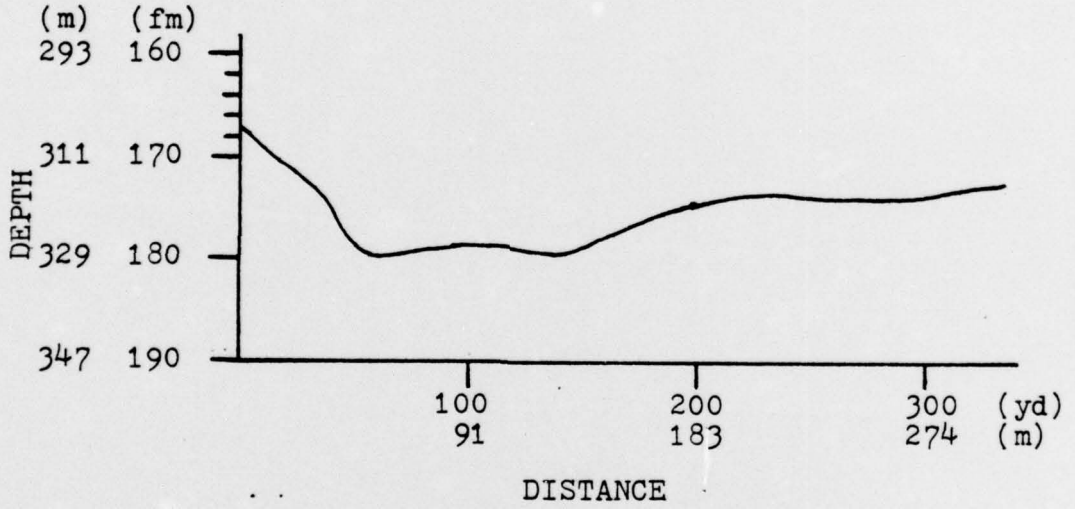


Fig. 59. Bathymetric Profile of Leg ST-3

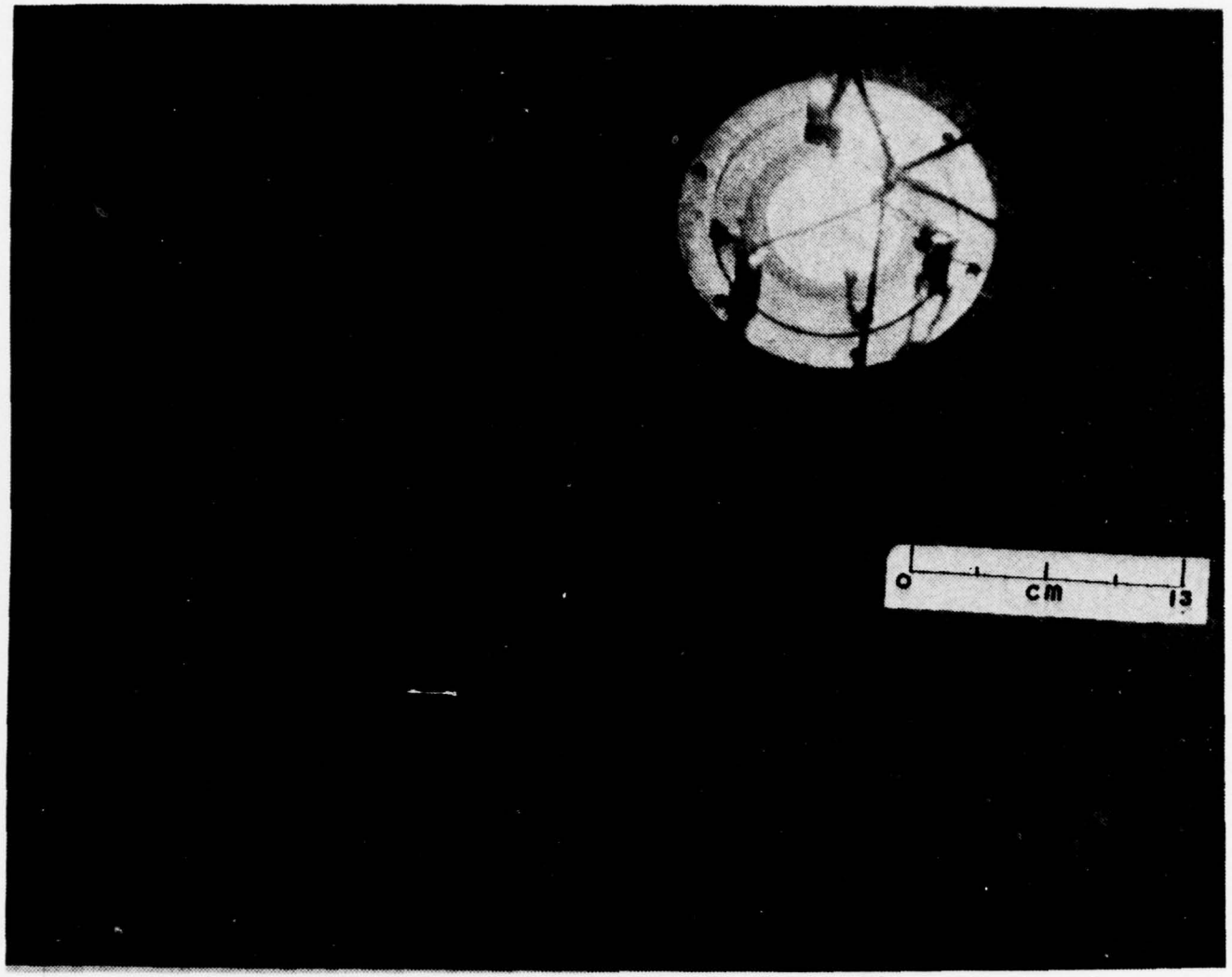


Fig. 60. Bottom Photograph Leg ST-1, 0958.5 hr, 230 m, Rock outcrops covered with sediment and biologics

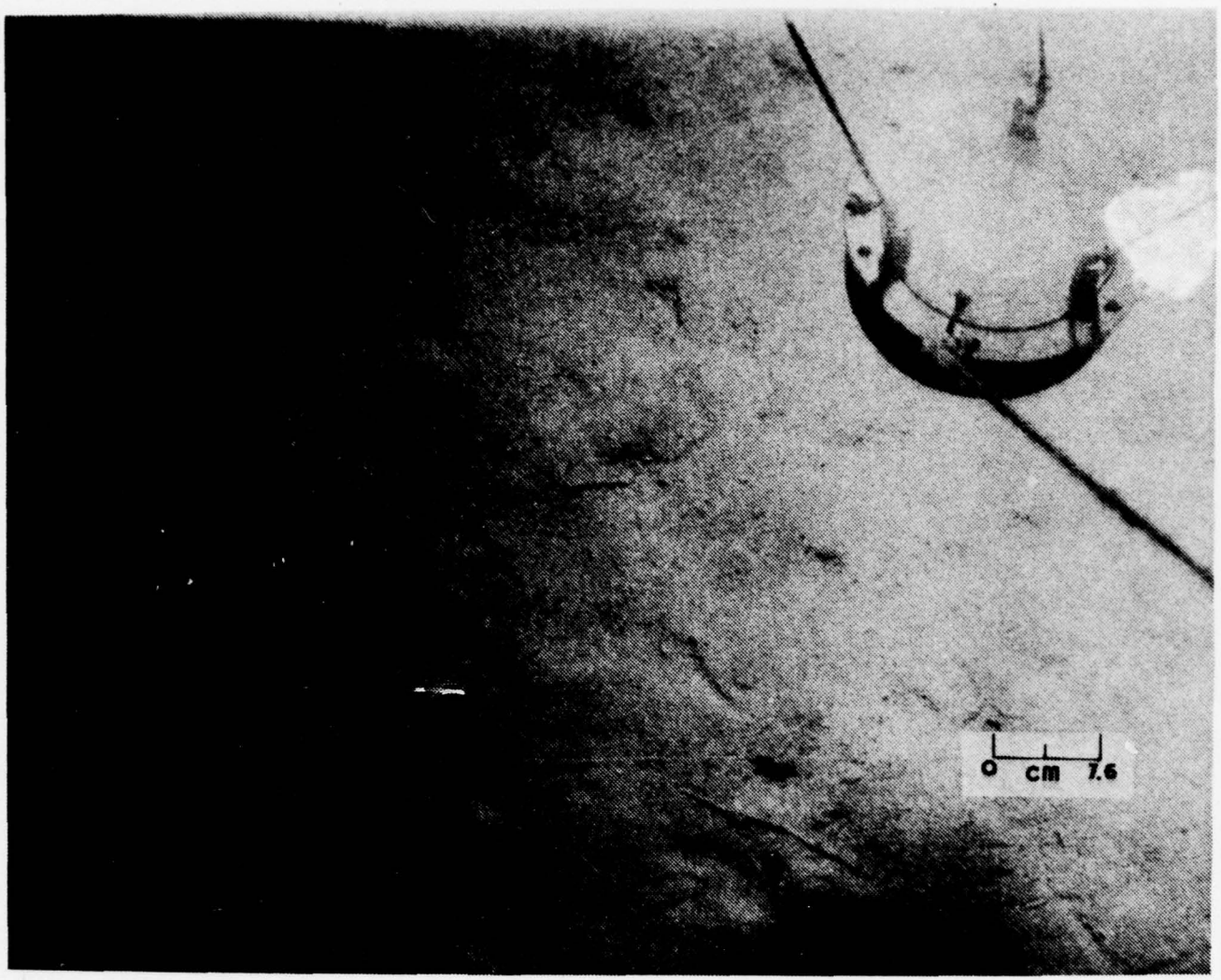


Fig. 61. Bottom Photograph Leg ST-3, 1140.75 hr, 256 m, Rimless depressions, poorly defined current lineations

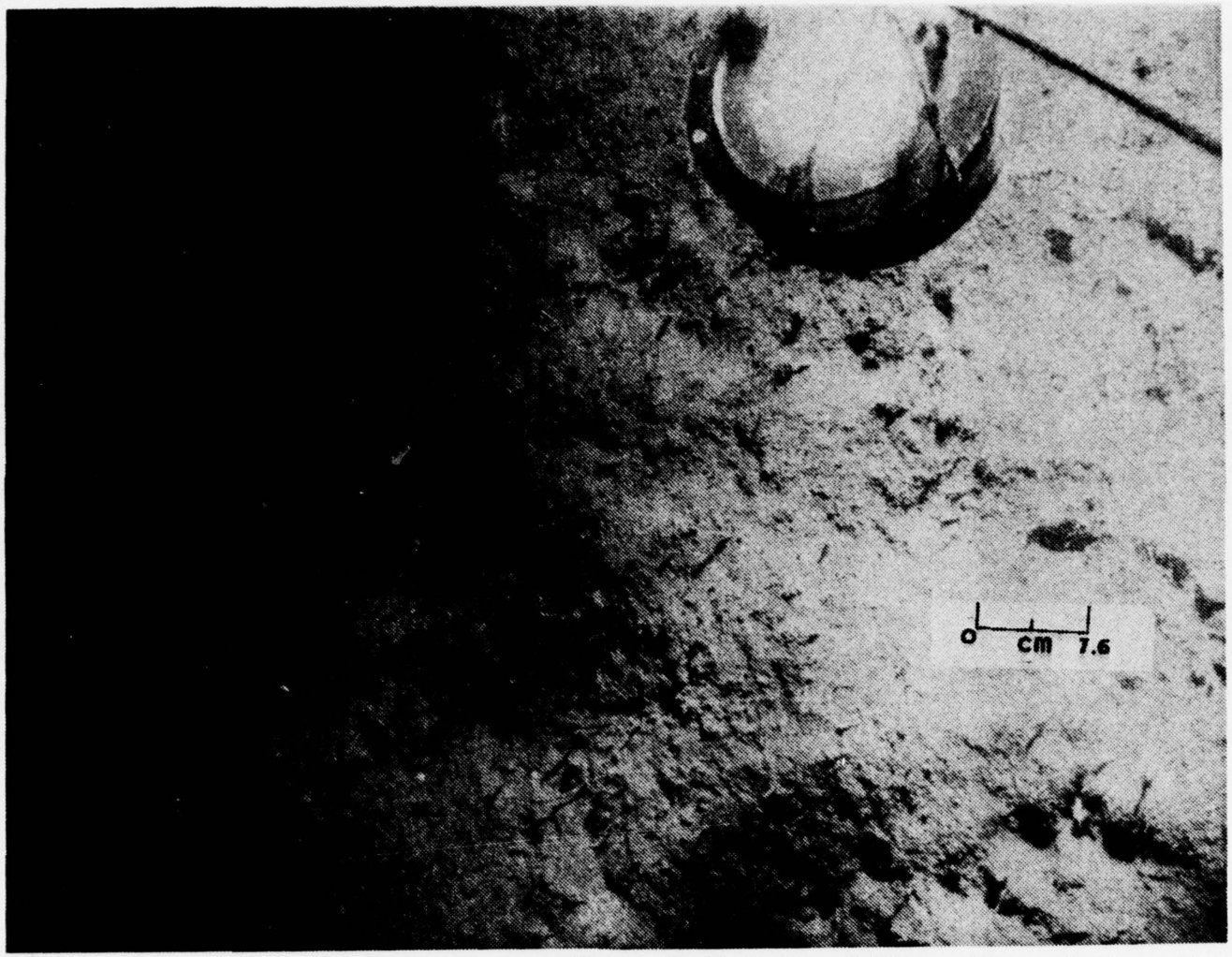


Fig. 62. Bottom Photograph Leg ST-2, 1041.4 hr, 146 m, Disturbed sediment with exposed worm tubes and several shell fragments

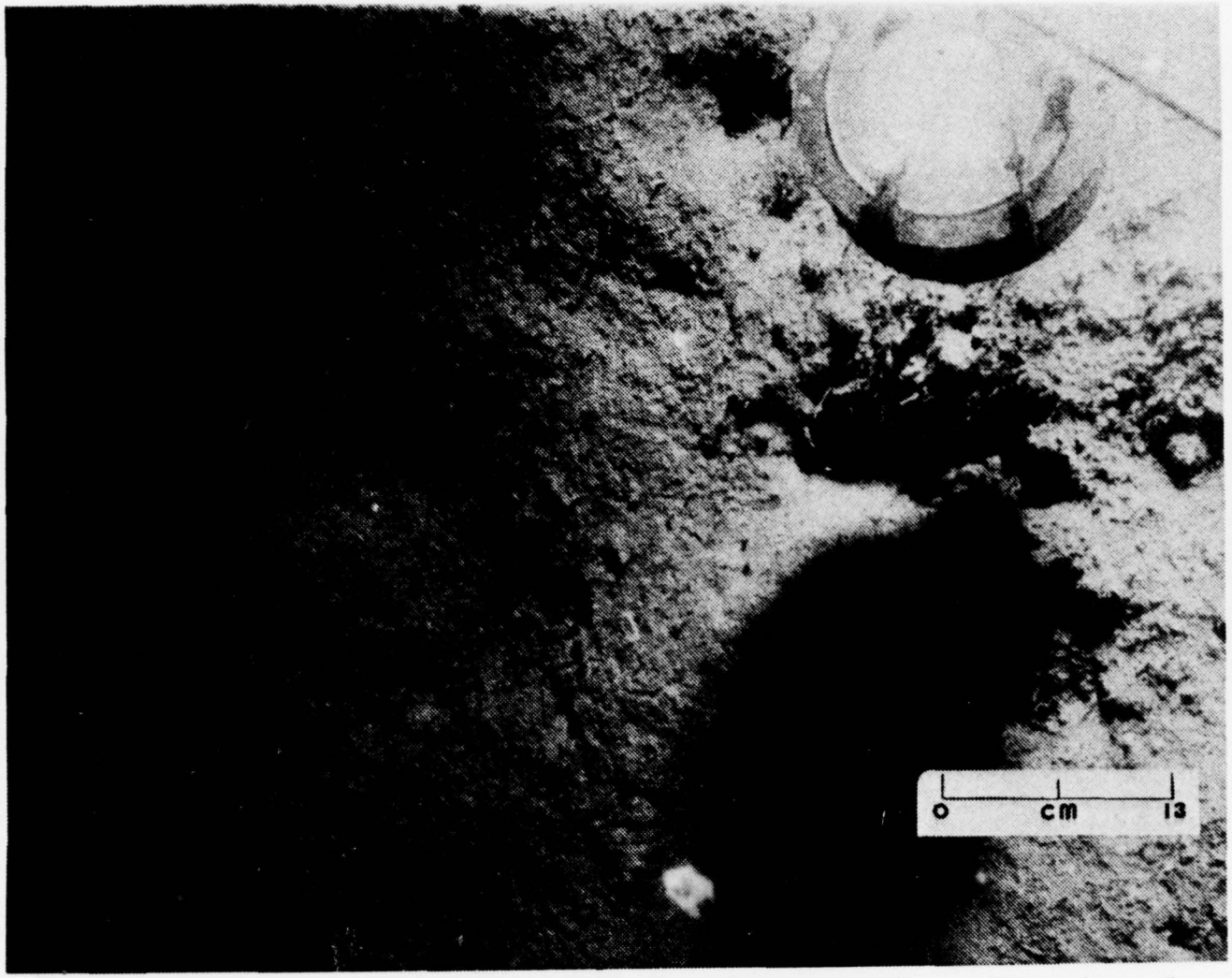


Fig. 63. Bottom Photograph Leg ST-2, 1043.2 hr, 142 m, Sloped surface appears to have experienced minor sediment slumping, many exposed worm tubes.

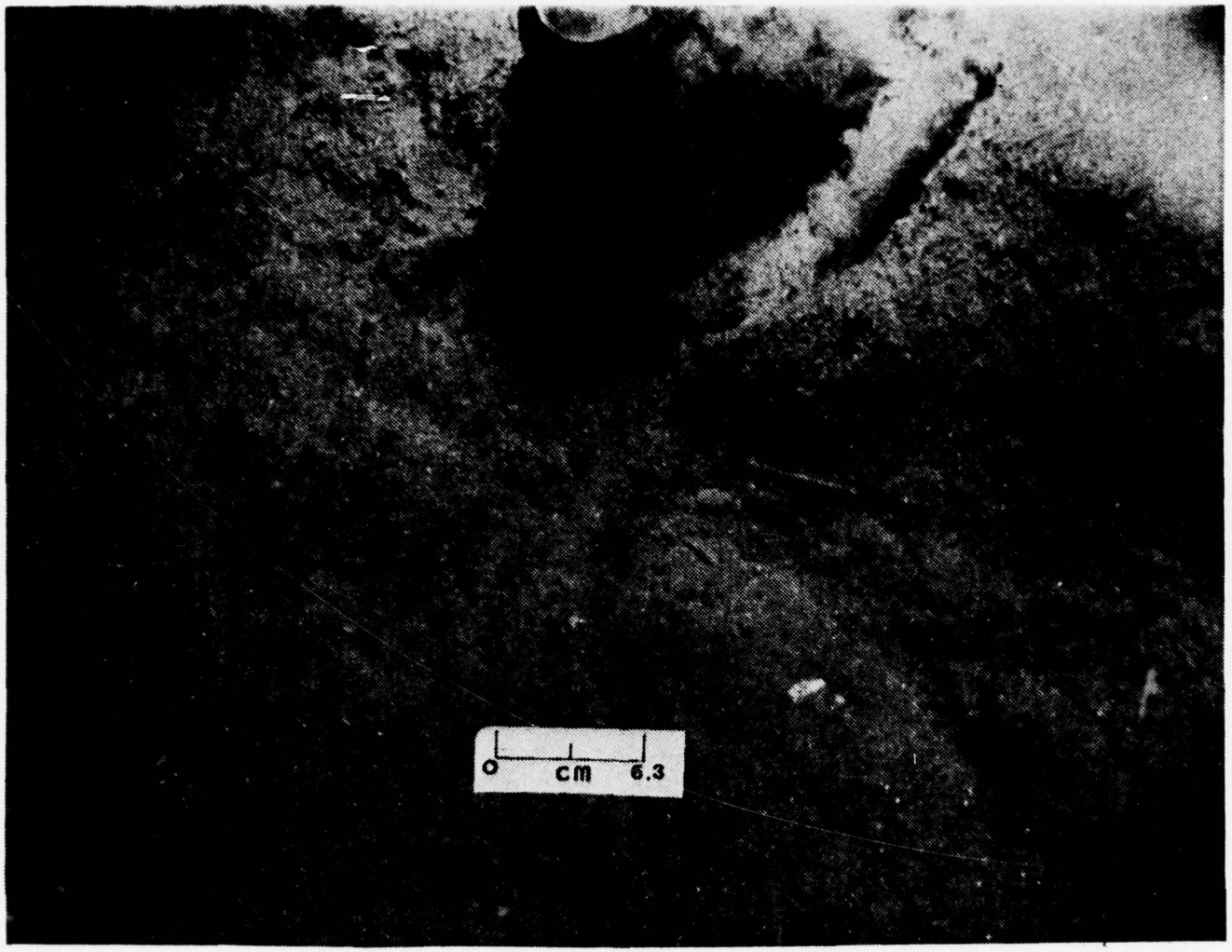


Fig. 64. Bottom Photograph Leg ST-2, 1050.25 hr, 120 m, Shell fragments and exposed worm tubes indicate disturbed sediment, hydroid colony (ML)

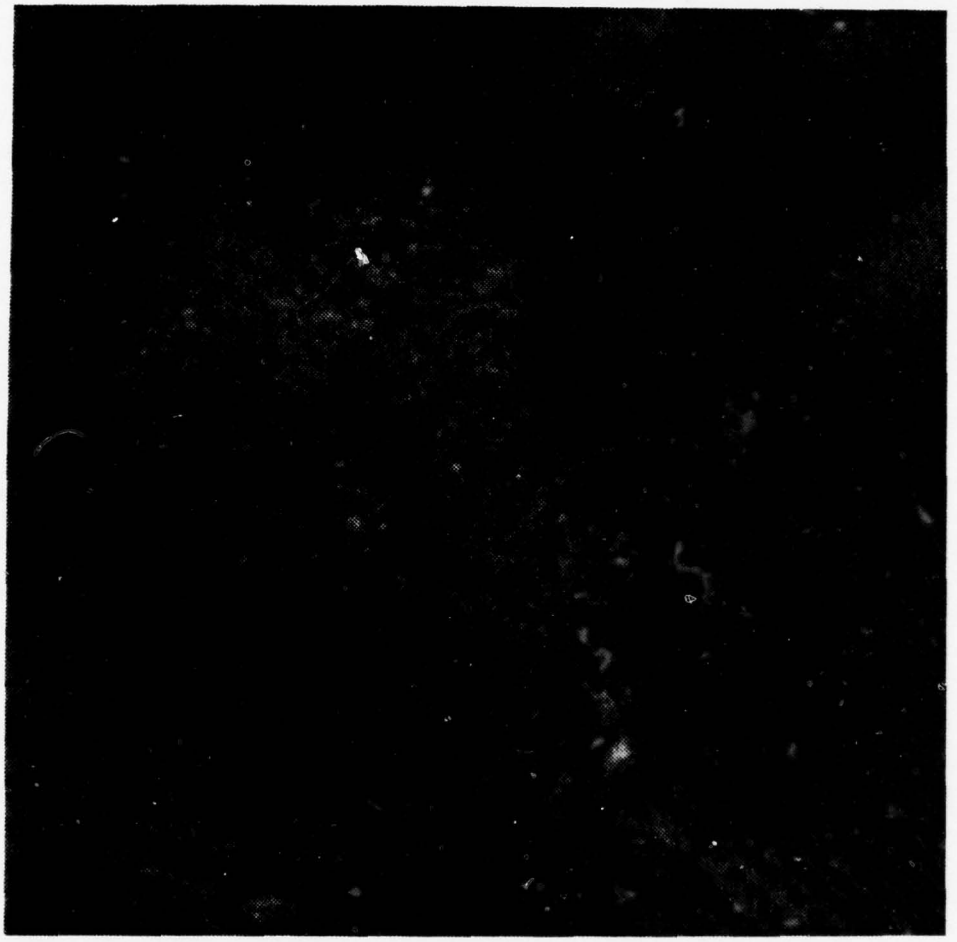


Fig. 65. Bottom Photograph Leg QR-1, 0958.6 hr, 270 m, Biologically encrusted rock with unidentified protruding organism



Fig. 66. Bottom Photograph Leg QR-1, 1006.6 hr, 260 m, Sea lilies attached to rocks, distortion due to water in camera case

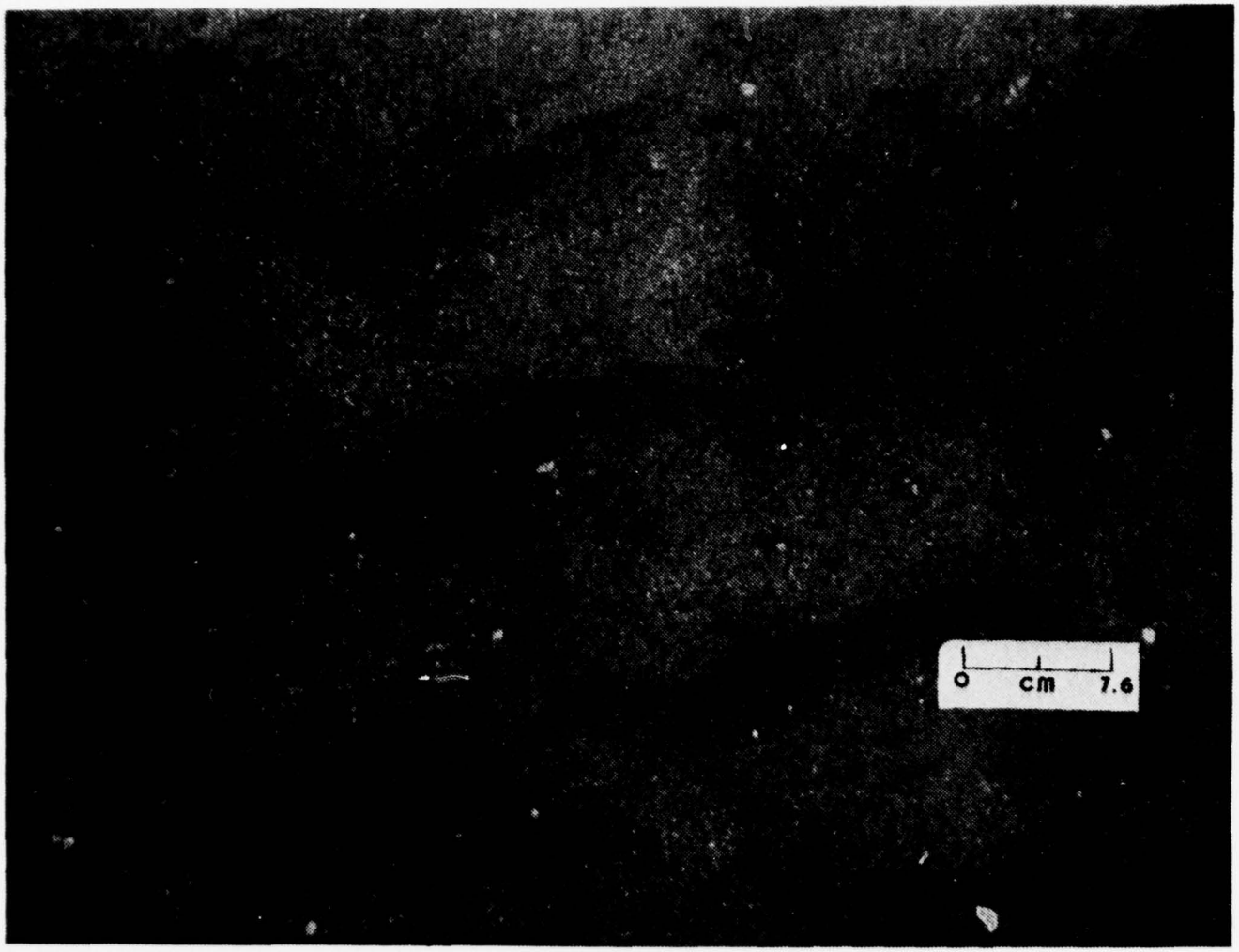


Fig. 67. Bottom Photograph Leg KL-1, 0930.7 hr, 528 m, Irregular asymmetrical ripple marks, some shell fragments

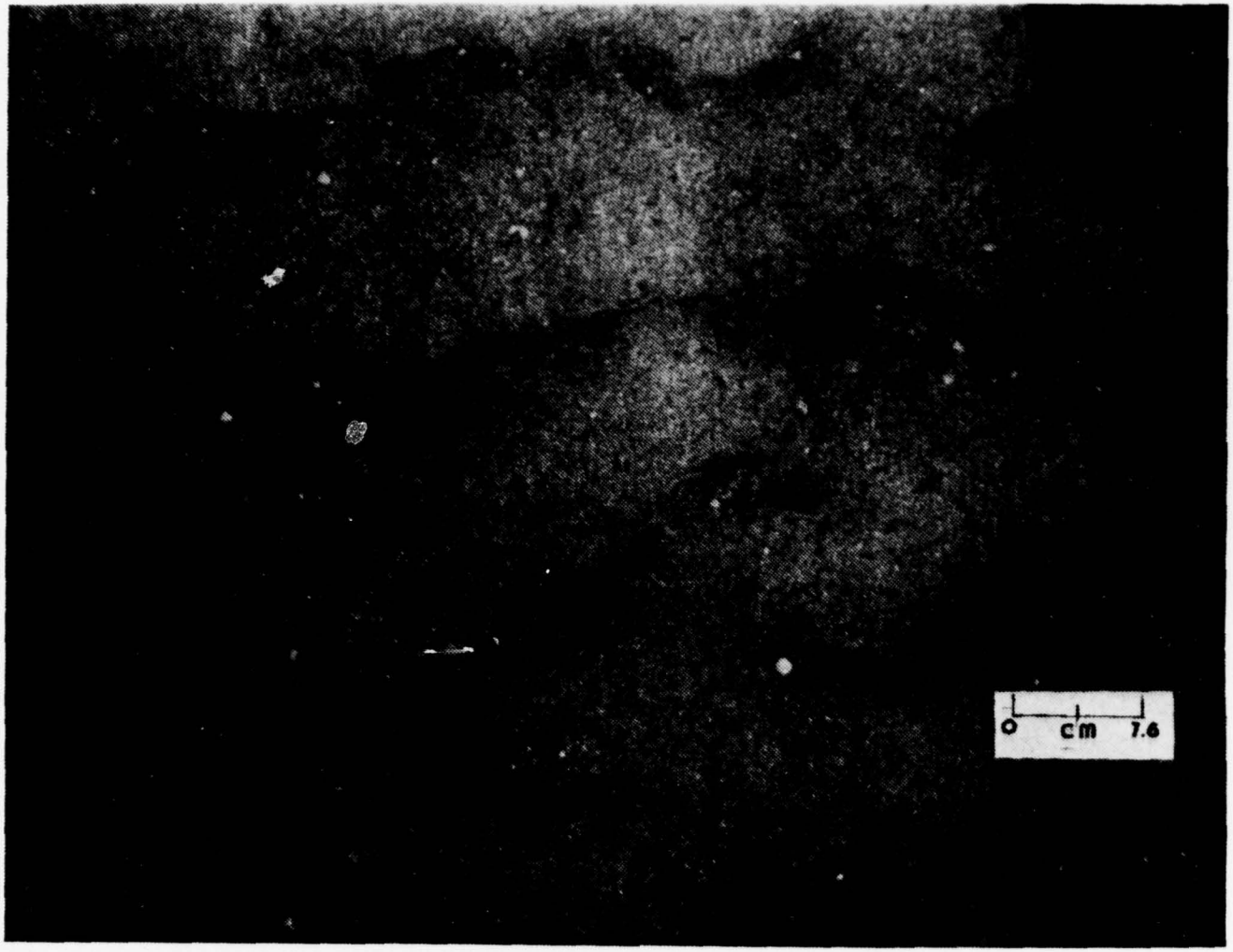


Fig. 68. Bottom Photograph Leg KL-1, 0933.6 hr, 528 m, Short crested irregular asymmetrical ripple marks, exposed worm tubes and shell

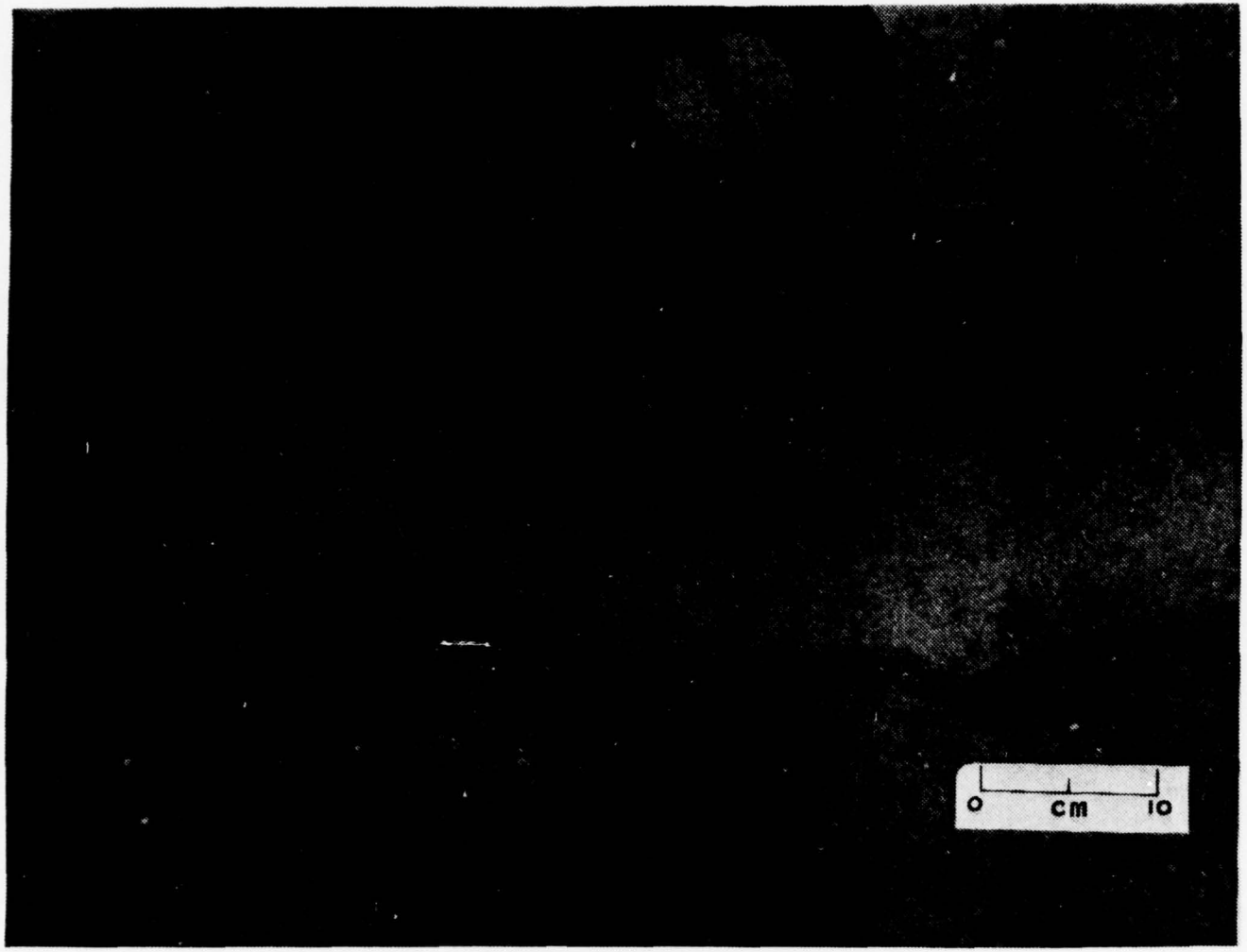


Fig. 69. Bottom Photograph Leg KL-1, 0934.3 hr, 528 m, Long crested asymmetrical ripple marks with coarse material and shell fragments in troughs

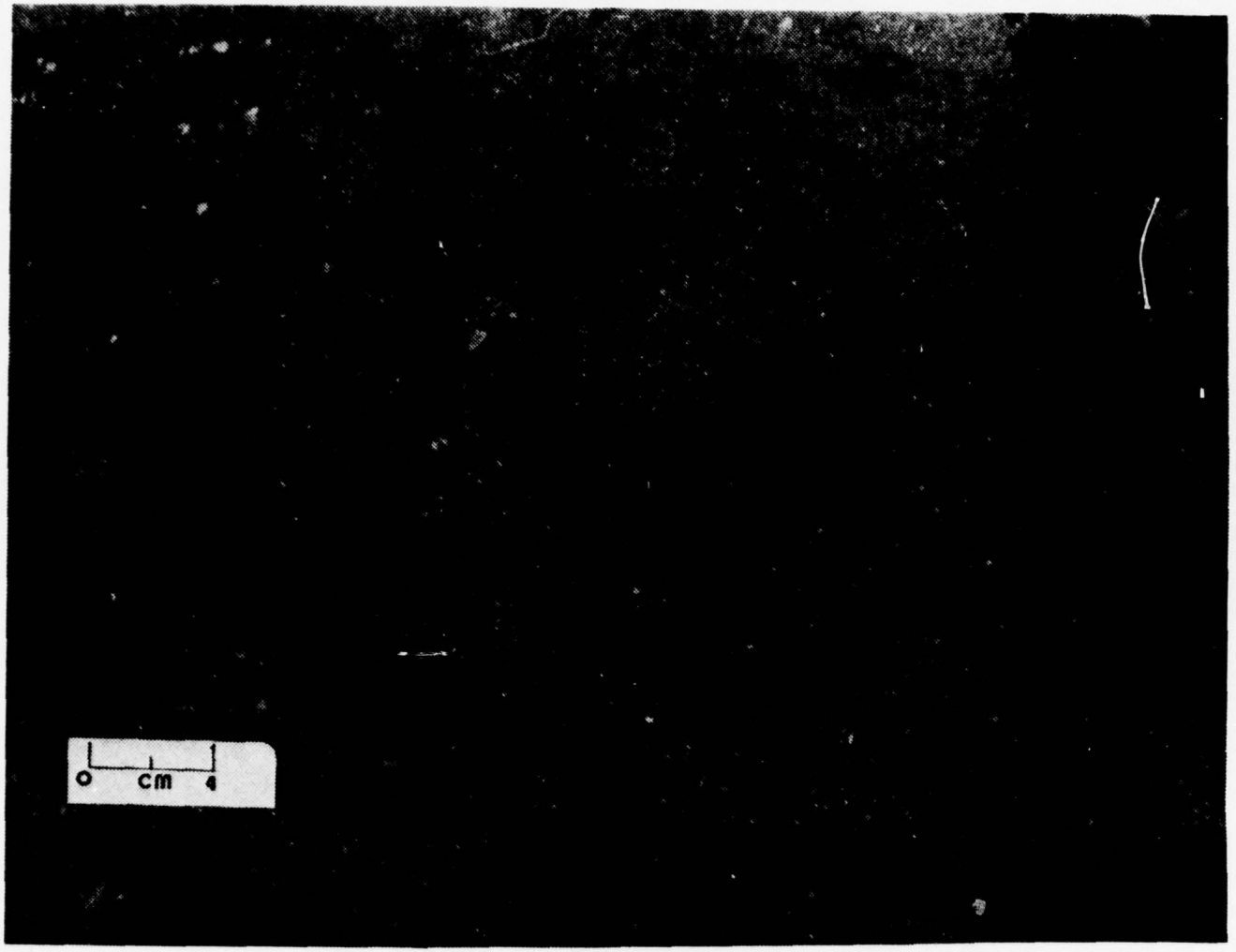


Fig. 70. Bottom Photograph Leg KL-1, 0936.2 hr, 528 m, Nearly destroyed ripple marks, coarse sand and a pebble (about 1.9 cm), shell fragments and a brittle star

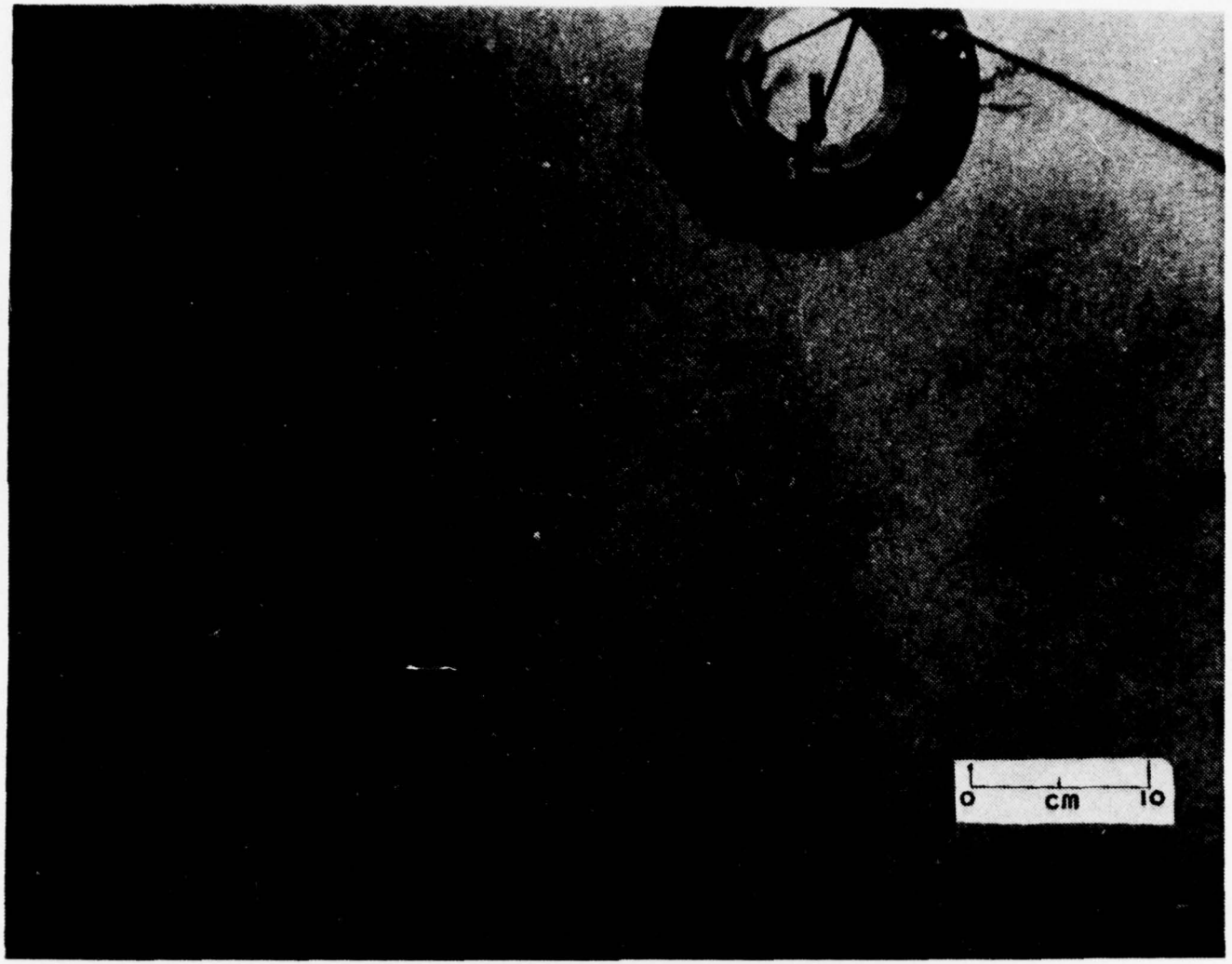


Fig. 71. Bottom Photograph Leg KL-1, 0941.2 hr, 520 m, Remnant ripples in sandy bottom with pockets of coarser material

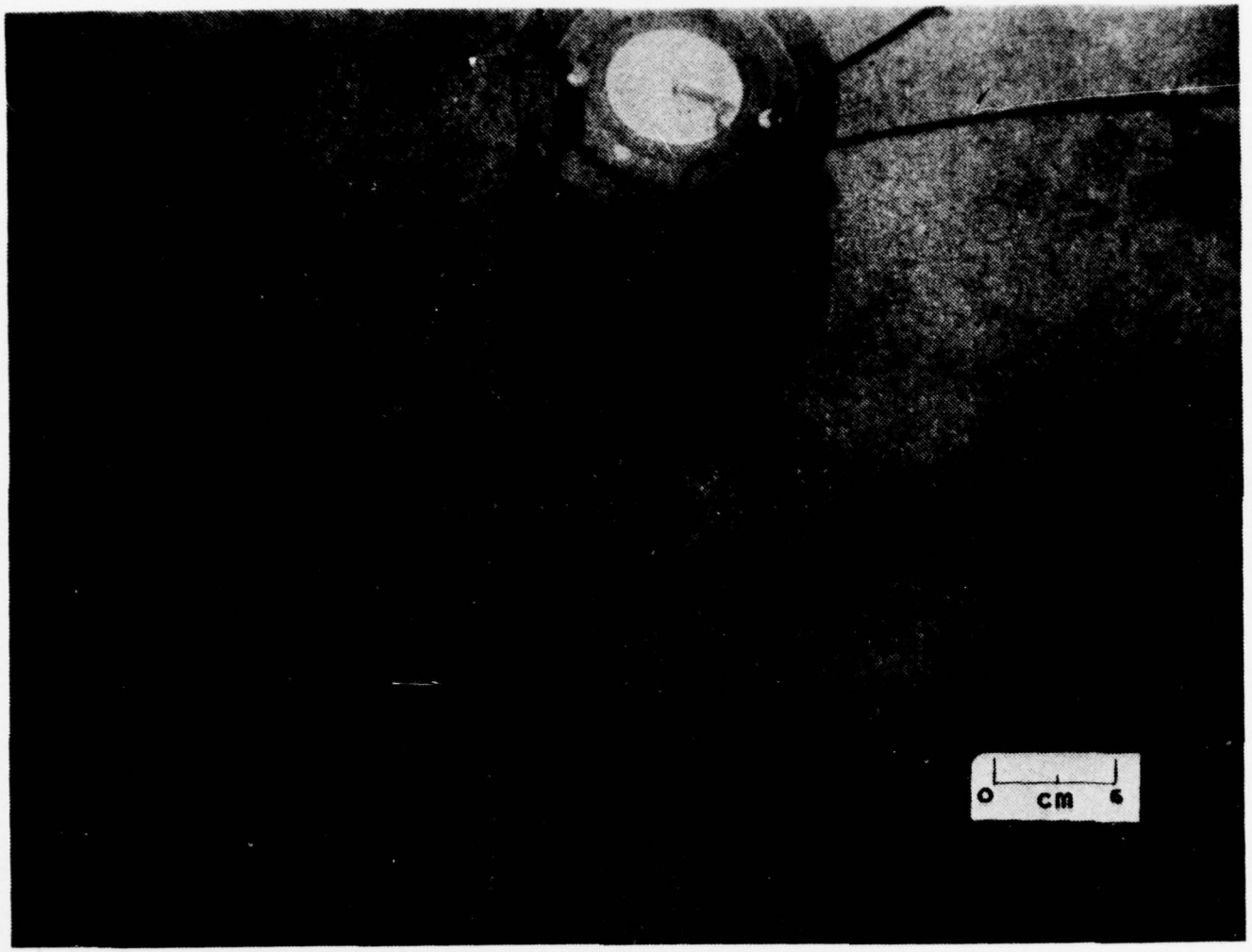


Fig. 72. Bottom Photograph Leg KL-3, 1228 hr, 480 m, Poorly defined current lineations, short grooves and sea pens, sea cucumber (UR)

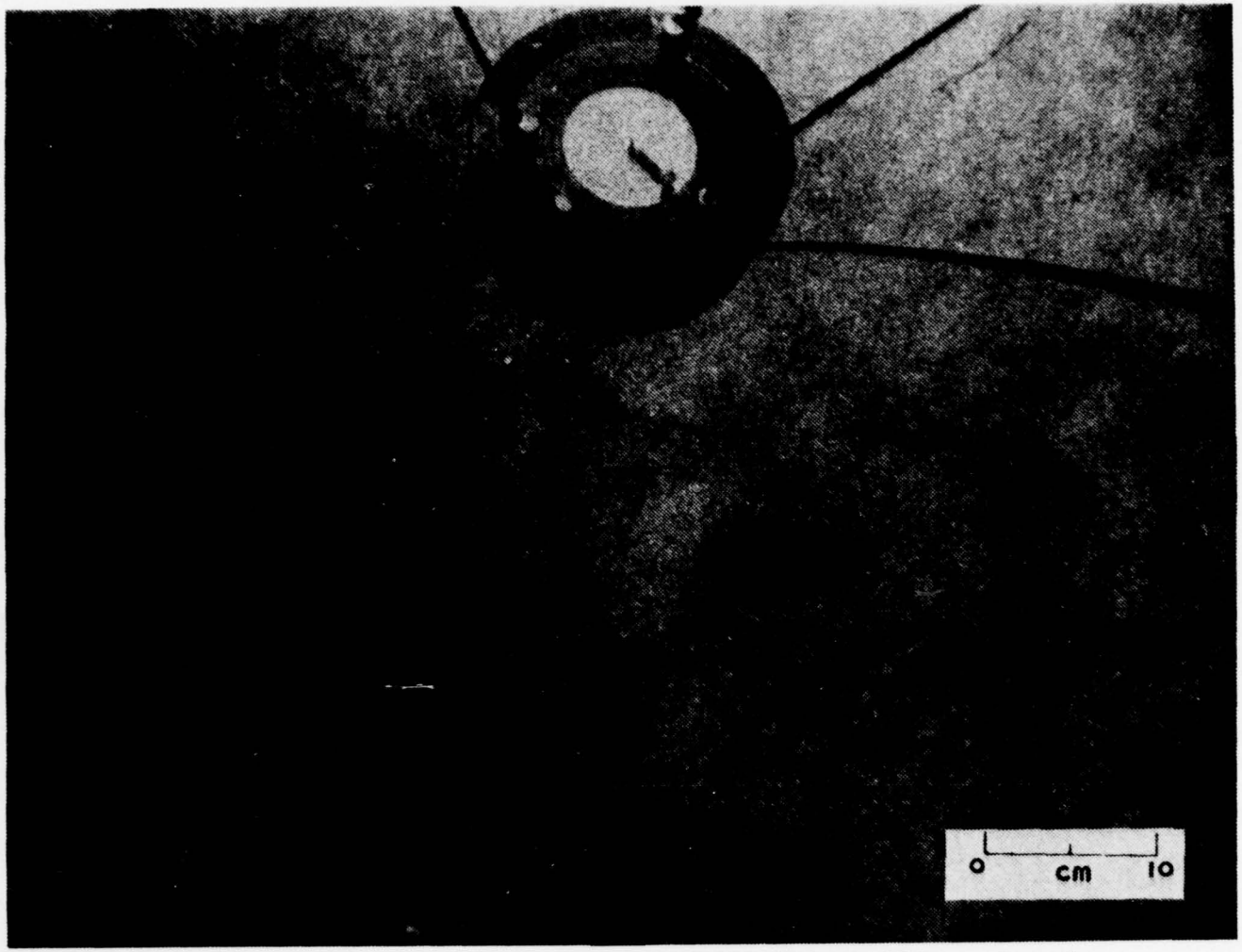


Fig. 73. Bottom Photograph Leg KL-3, 1235.5 hr, 478 m, Subtle current lineations, piece of sea grass, some small holes indicating burrowing

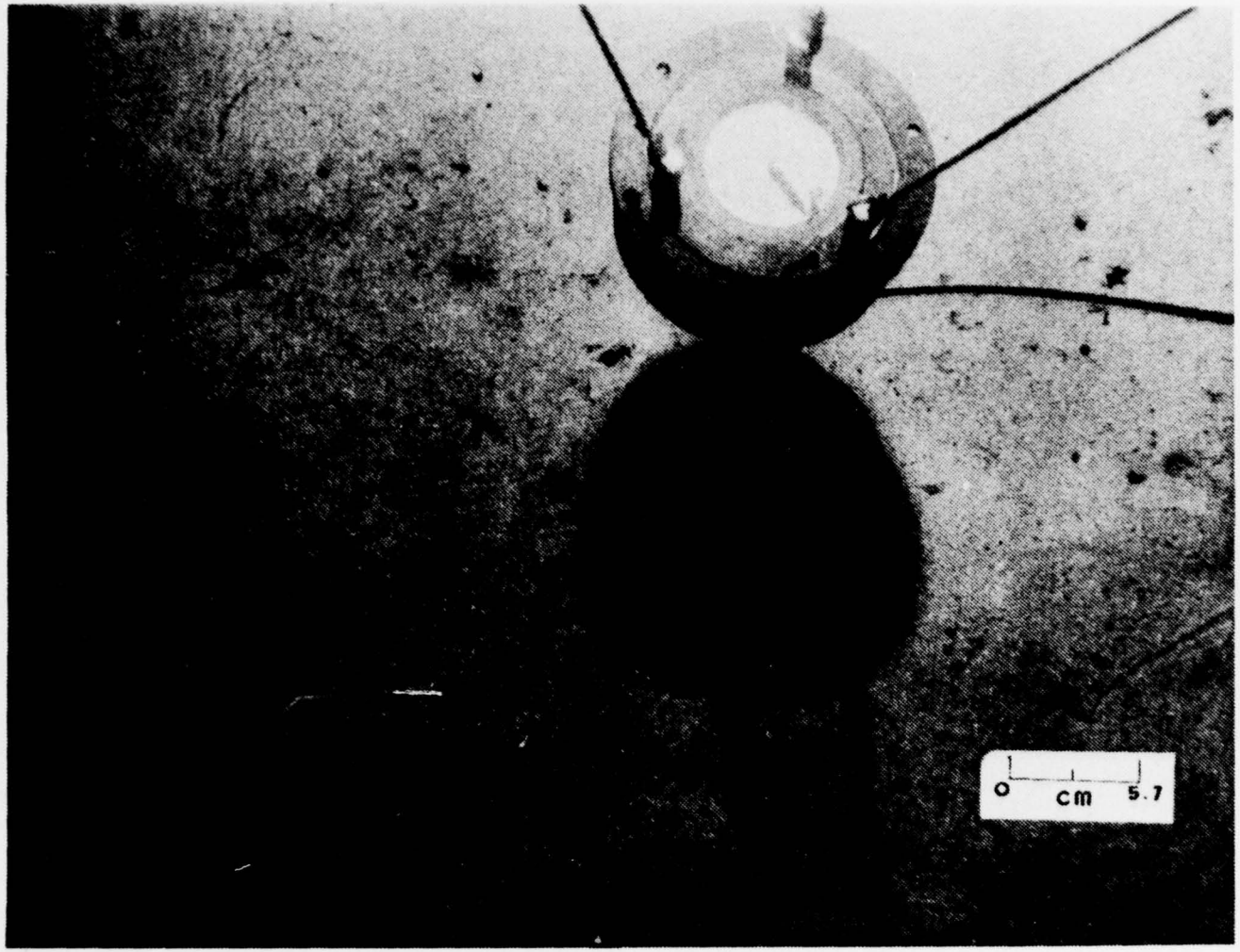


Fig. 74. Bottom Photograph Leg KL-2, 1043.2 hr, 400 m, Small holes and larger rimless craters, short groove marks, sea pen

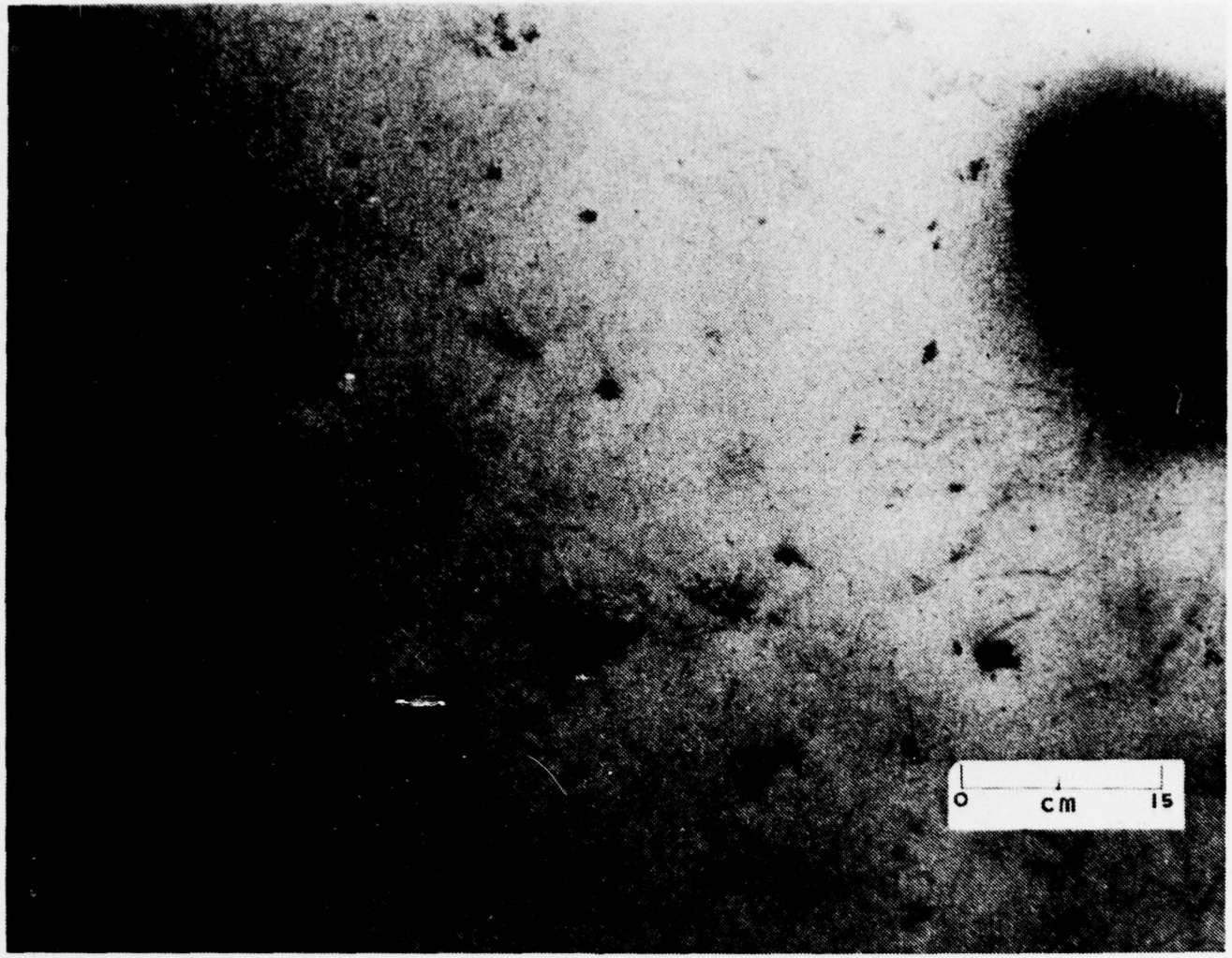


Fig. 75. Bottom Photograph Leg KL-2, 1044.5 hr, 400 m, Piles of feces, plow marks, many larger depressions

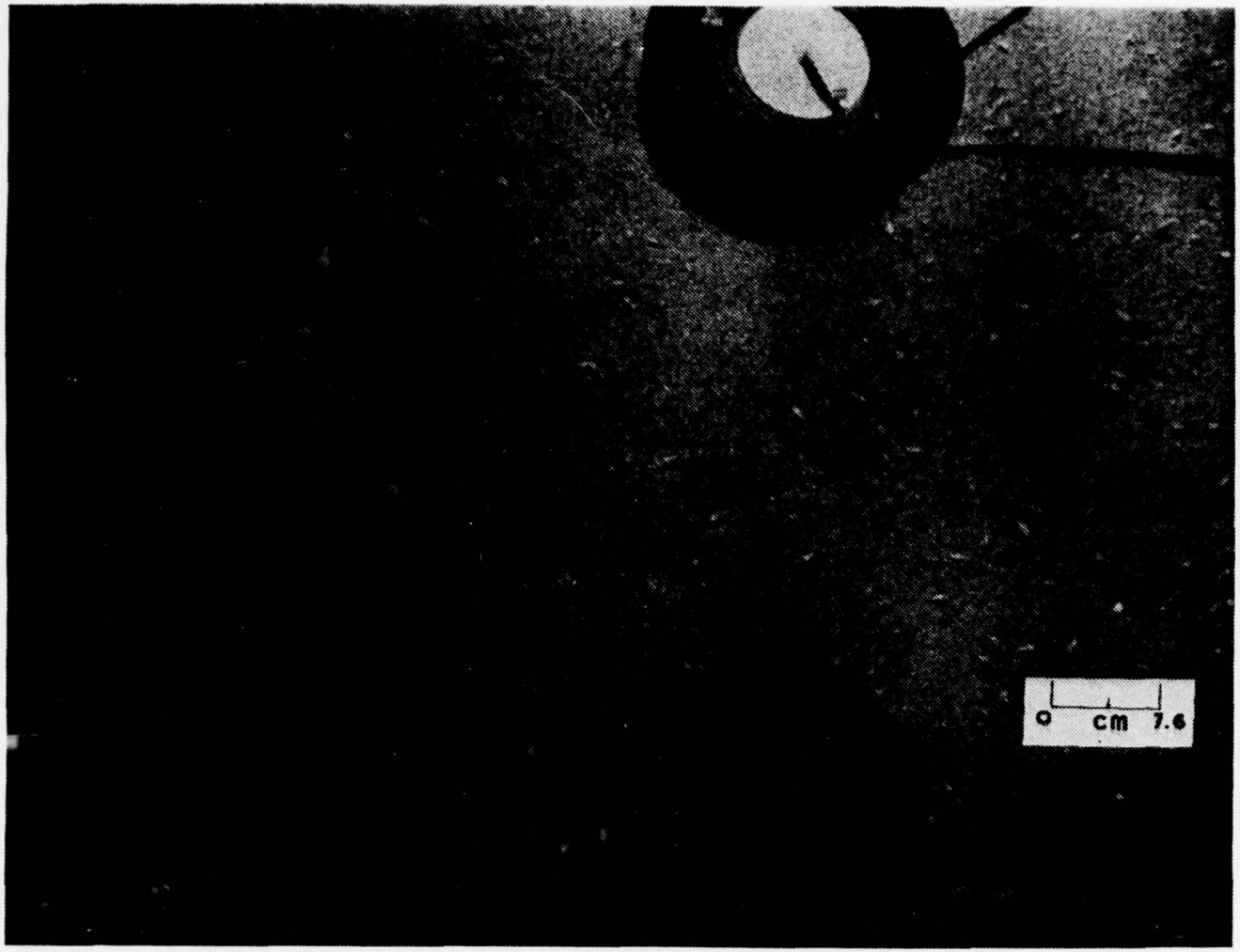


Fig. 76. Bottom Photograph Leg MN, 1340.9 hr, 660 m, Gastropods feeding on organically rich sediments, sea cucumber (LR)

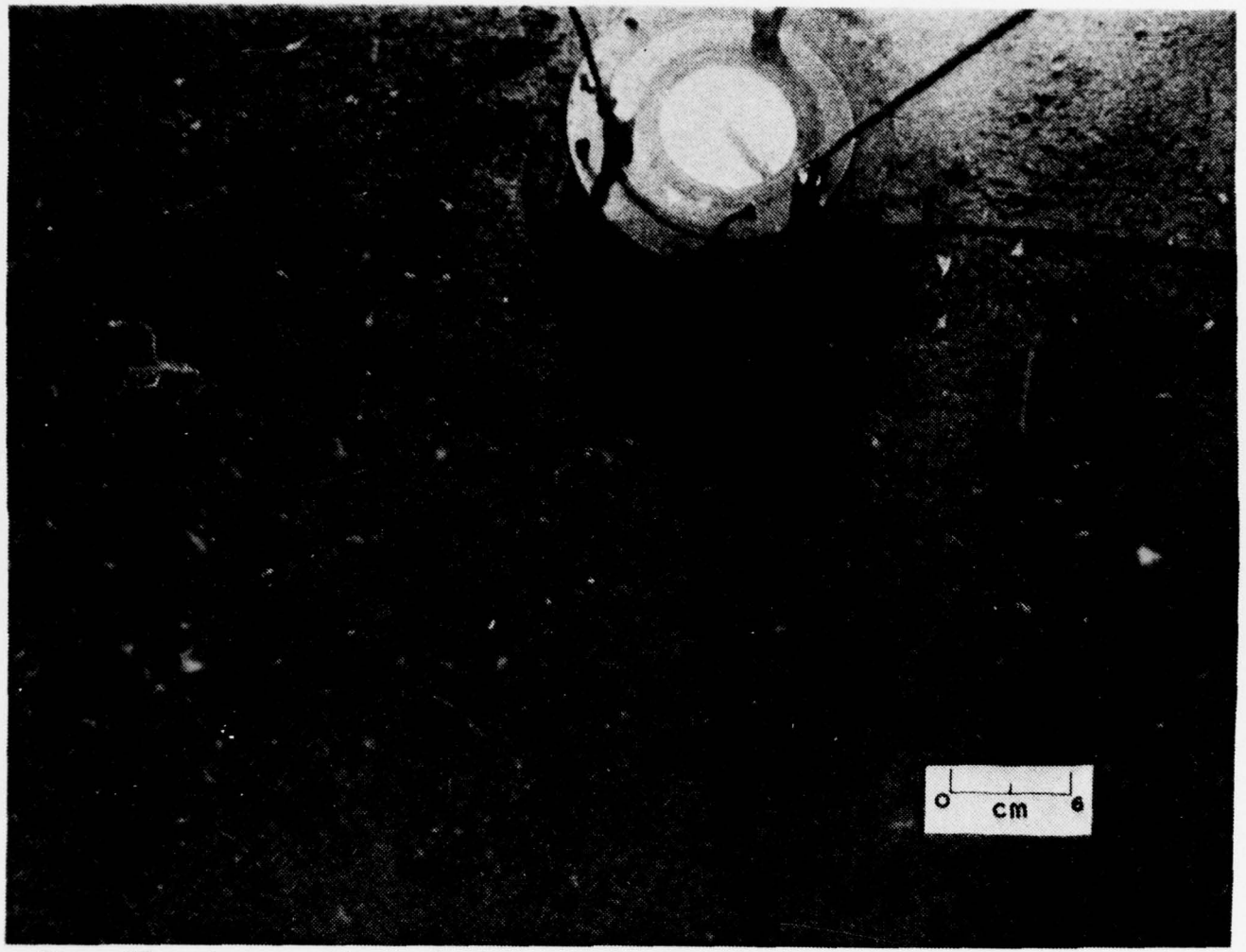


Fig. 77. Bottom Photograph Leg MN, 1346.3 hr, 660 m, Gastropods and unidentified organism protruding out of sediment

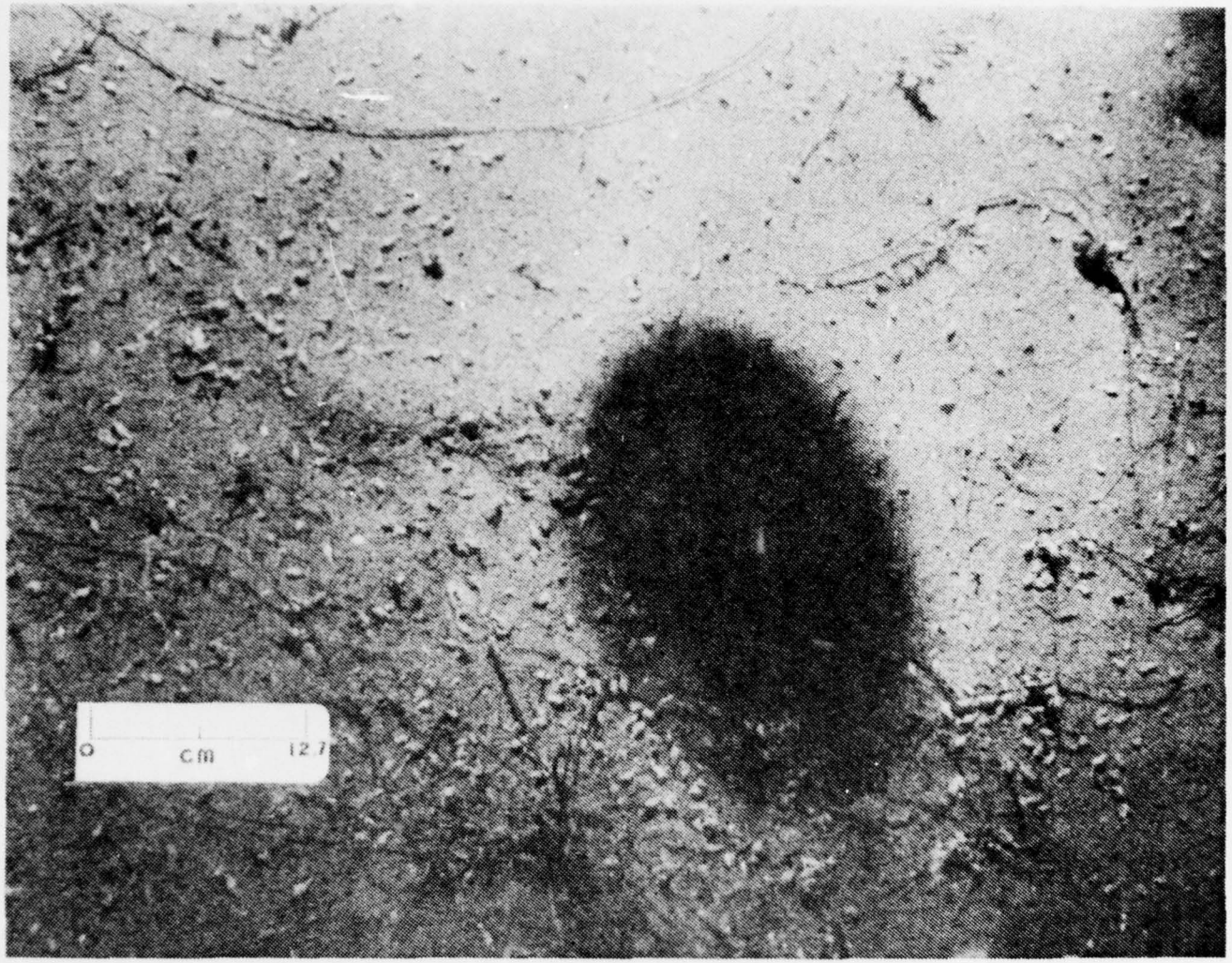


Fig. 78. Bottom Photograph Leg MN, 1350.2 hr, 660 m, High density of gastropods, surf grass debris, crab (lower right of shadow)

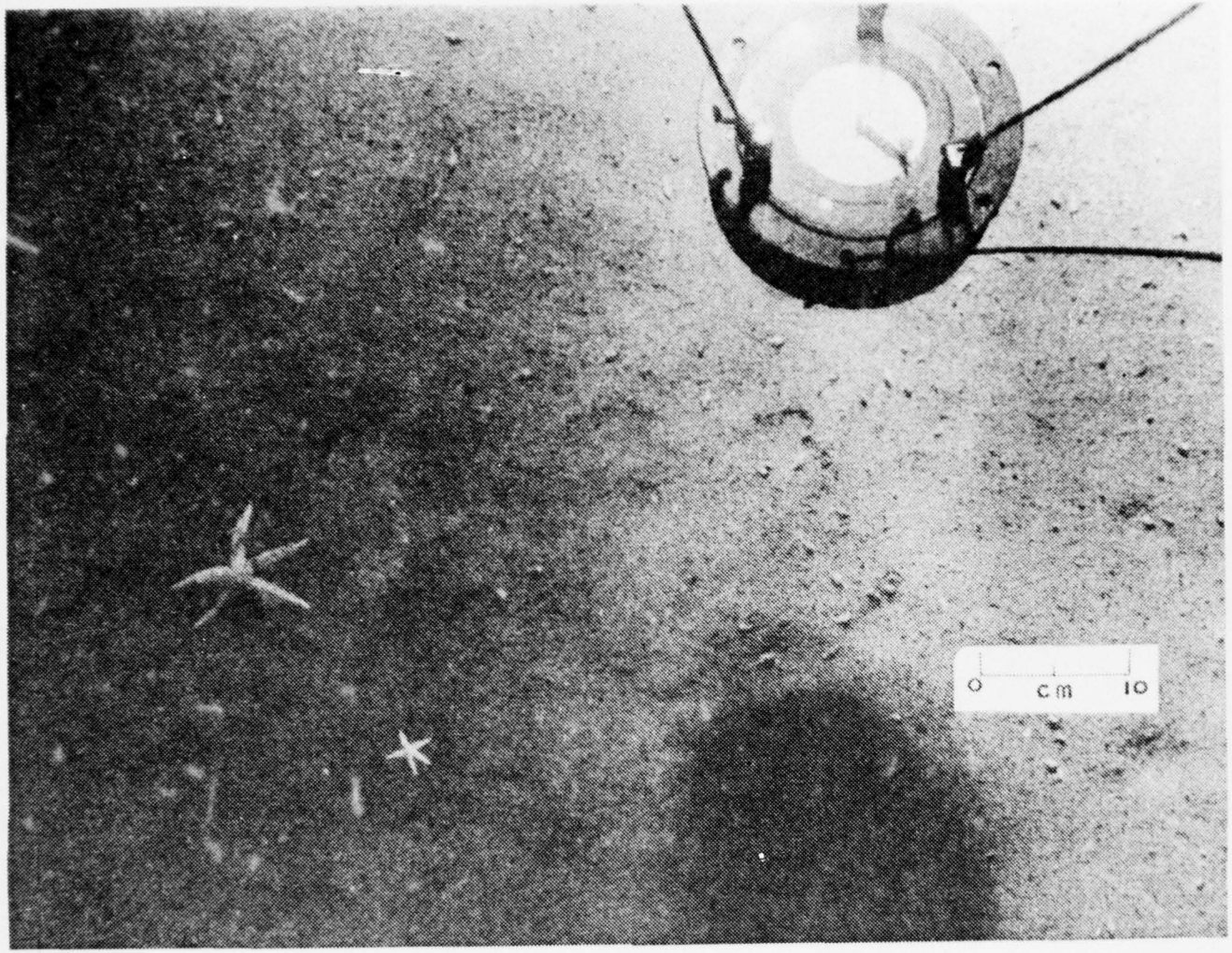


Fig. 79. Bottom Photograph Leg MN, 1352.2 hr, 660 m, Starfish and gastropods

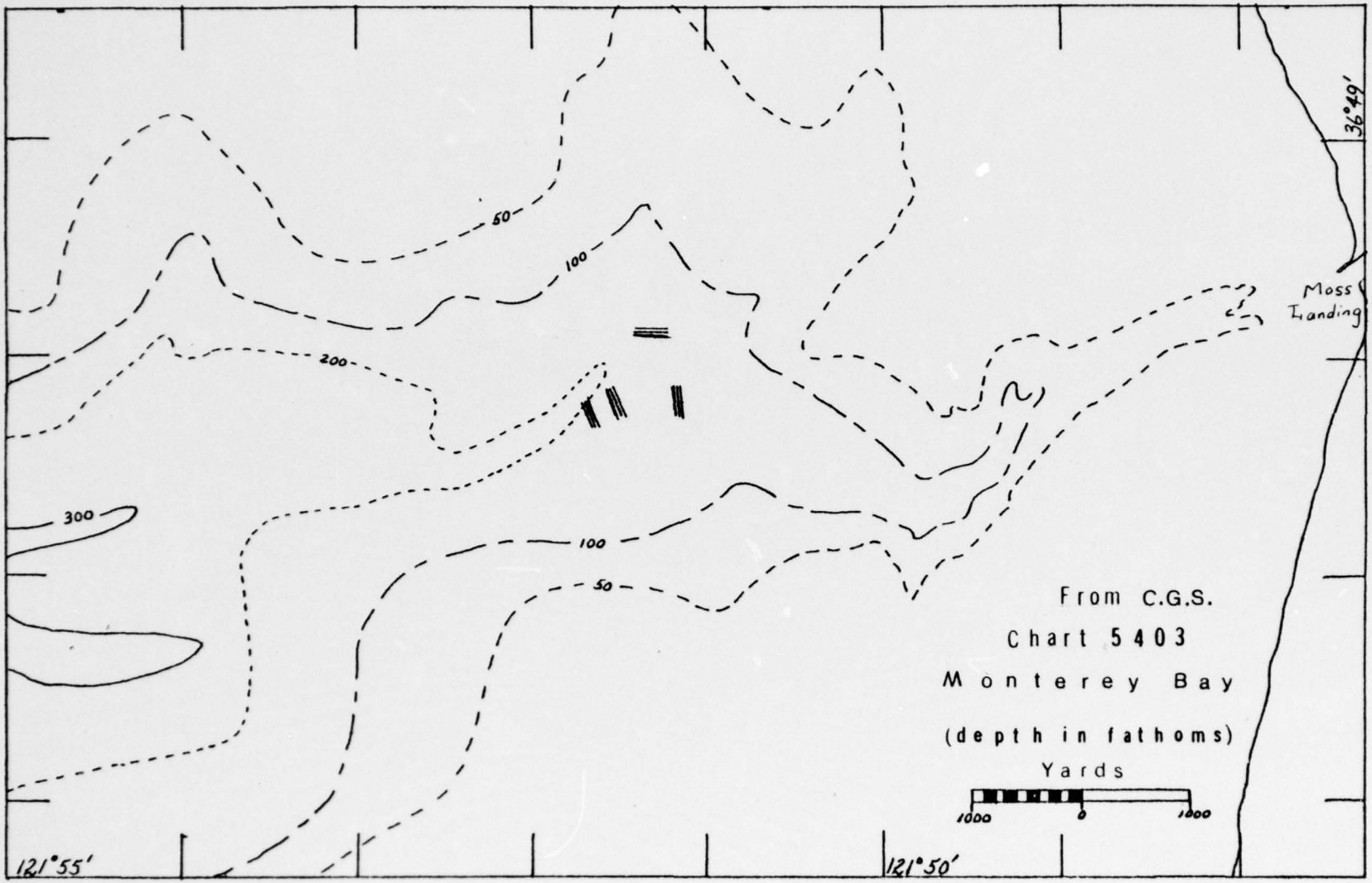


Fig. 80. Orientation of Ripple Mark Crests in Monterey Canyon

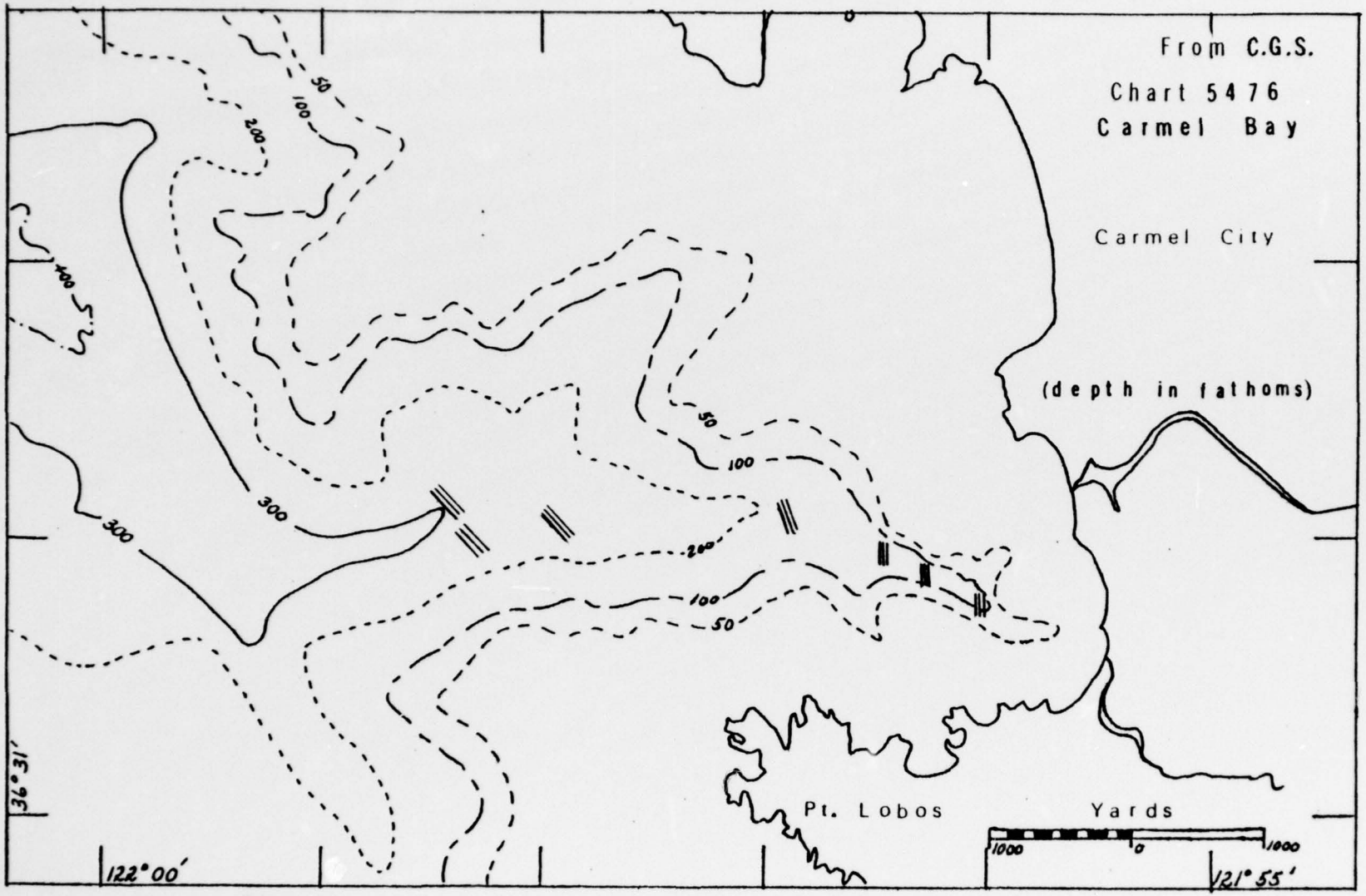


Fig. 81. Orientation of Ripple Mark Crests in Carmel Canyon

REFERENCES CITED

1. Akal, T. 1974. Acoustical characteristics of the sea floor: experimental techniques and some examples from the Mediterranean Sea, p. 447 to 480. In L. Hampton [ed.] Physics of sound in marine sediments. Plenum Press, New York.

2. Athearn, W.D. 1967. Estimation of relative grain size from sediment clouds, p. 177-185. In J.B. Hersy [ed.] Deep-sea photography. The John Hopkins Press, Baltimore, Md.

3. Carter, L.S. 1971. Recent marine sediments of Carmel Bay, California. M.S. Thesis, Naval Postgraduate School, Monterey, CA. 61 p.

4. Caster, W.A. 1969. Near bottom currents in Monterey Submarine Canyon and the adjacent shelf. M.S. Thesis, Naval Postgraduate School, Monterey, Ca. 204 p.

5. Dooley, J.J. 1968. An investigation of near bottom currents in the Monterey Submarine Canyon. M.S. Thesis, Naval Postgraduate School, Monterey, Ca. 58 p.

6. EG&G. 1960. Preliminary instruction manual series 8 and series 9 cameras and light sources. Edgerton, Germeshausen and Grier, Inc., Report No. B-2128, Boston.

7. Galliher, E.W. 1932. Sediments of Monterey Bay, California. Ph.D. Dissertation, Stanford University, Stanford, Ca. 143 p.

8. Gatje, P.H., and D.D. Pizinger. 1965. Bottom current measurements in the head of Monterey Submarine Canyon. M.S. Thesis, Naval Postgraduate School, Monterey. Ca. 61 p.

9. Greene, H.G. Geology of Monterey Bay, Ca. Ph.D. Thesis, Stanford University, Stanford, Ca. (in preparation)

10. Heezen, B.C., and C.D. Hollister. 1971. The face of the deep. Oxford University Press, Inc., New York. 659 p.

11. Hollister, J.E. 1975. Currents in Monterey Submarine Canyon. M.S. Thesis, Naval Postgraduate School, Monterey, Ca. 86 p.

12. Laughton, A.S. 1963. Microtopography, p. 437-472. In M.N. Hill [ed.] The sea: Vol. 3. Interscience Publishers, New York.

13. Martin, B.D., and K.O. Emery. 1967. Geology of Monterey Canyon, California. American Assoc. Petroleum Geologists Bull. 51 (11): 2281-2304.

14. Njus, I.J. 1968. An investigation of environmental factors affecting the near bottom currents in the Monterey Submarine Canyon. M.S. Thesis, Naval Postgraduate School, Monterey, Ca. 80 p.

15. Russel, F.S., and C.M. Yonge. 1963. The seas. Rev. ed. Frederick Warne and Co. LTD., New York. 376 p.

16. Shepard, F.R., and R.F. Dill. 1966. Submarine canyons and other sea valleys. 2nd ed. Rand McNally and Co., Chicago. 381 p.

17. Shepard, F.R., N.F. Marshall, and P.A. McLoughlin. 1974. Currents in submarine canyons. Deep-Sea Research 21: 691-706.

18. Shipek, C.J. 1966. Photo analysis of sea floor micro-relief. U.S. Navy Electronics Lab, Research Rep. No. 1374. 70 p.

19. Wallin, S.R. 1969. The sediments in the head of the Carmel Submarine Canyon. M.S. Thesis, Naval Postgraduate School, Monterey, Ca. 98 p.

INITIAL DISTRIBUTION LIST

		No. Copies
1.	Defense Documentation Center Cameron Station Alexandria, VA 22314	2
2.	Library, Code 0212 Naval Postgraduate School Monterey, CA 93940	2
3.	Department of Oceanography, Code 58 Naval Postgraduate School Monterey, CA 93940	3
4.	Oceanographer of the Navy Hoffman Building No. 2 200 Stovall Street Alexandria, VA 22332	1
5.	Office of Naval Research Code 410 NORDA, NSTL Bay St. Louis, MI 39520	1
6.	Dr. Robert E. Stevenson Scientific Liaison Office, ONR Scripps Institute of Oceanography La Jolla, CA 92073	1
7.	Library, Code 3330 Naval Oceanographic Office Washington, D.C. 20373	1
8.	SIO Library University of California, San Diego P.O. Box 2367 La Jolla, CA 92037	1
9.	Department of Oceanography Library University of Washington Seattle, WA 98105	1
10.	Department of Oceanography Library Oregon State University Corvallis, OR 97331	1
11.	Commanding Officer Fleet Numerical Weather Central Monterey, CA 93940	1

No. Copies

12. Commanding Officer — 1
Naval Environmental Prediction Research Facility
Monterey, CA 93940

13. Department of the Navy — 1
Commander Oceanographic System Pacific
Box 1390
FPO San Francisco, CA 96610

14. Director — 1
Naval Oceanography and Meteorology
Bay St. Louis, MI 39520

15. Library — 1
Hopkins Marine Station
Pacific Grove, CA 93950

16. R/V ACANIA — 1
Naval Postgraduate School
Monterey, CA 93940

17. Dr. P. Wilde — 1
Lawrence Berkeley Laboratory
Energy and Environmental Division
University of California
Berkeley, CA 94720

18. H.G. Greene — 1
United States Geological Survey
Marine Geology Branch
345 Middlefield Road
Menlo Park, CA 94025

19. Dr. Gary B. Griggs — 1
Division of National Science
Applied Sciences Building
University of California
Santa Cruz, CA 95064

20. Commander — 1
Patrol Wings Pacific
NAS Moffett Field, CA 94035
Attn: Flag Administrative Unit

21. Eric Anderson — 1
Moss Landing Marine Laboratories
Moss Landing, CA 95039

No. Copies

22. Dr. Robert S. Andrews
Naval Postgraduate School
Monterey, CA 93940
2

23. Dr. Stevens P. Tucker
Naval Postgraduate School
Monterey, CA 93940
2

24. LT John A. Jensen
P.O. Box 65
Cornwall, NY 12518
2